RELIABILITY BASED SAFETY LEVEL EVALUATION OF TURKISH
TYPE PRECAST PRESTRESSED CONCRETE BRIDGE GIRDERS
DESIGNED IN ACCORDANCE WITH THE LOAD AND RESISTANCE
FACTOR DESIGN METHOD

A THESIS SUBMITTED TO
THE GRADUATE SCHOOL OF NATURAL AND APPLIED SCIENCES
OF
MIDDLE EAST TECHNICAL UNIVERSITY

BY
OKTAY ARGINHAN

IN PARTIAL FULFILLMENT OF THE REQUIREMENTS
FOR
THE DEGREE OF MASTER OF SCIENCE
IN
CIVIL ENGINEERING

DECEMBER 2010

Approval of the thesis:

RELIABILITY BASED SAFETY LEVEL EVALUATION OF TURKISH TYPE PRECAST PRESTRESSED CONCRETE BRIDGE GIRDERS DESIGNED IN ACCORDANCE WITH THE LOAD AND RESISTANCE FACTOR DESING METHOD

submitted by **OKTAY ARGINHAN** in partial fulfillment of the requirements for the degree of **Master of Science in Civil Engineering Department, Middle East Technical University** by,

Prof. Dr Canan Özgen
Dean, Graduate School of **Natural and Applied Sciences**   _____

Prof. Dr. Güney Özcebe
Head of Department, **Civil Engineering**   _____

Assist. Prof. Dr. Alp Caner
Supervisor, **Civil Engineering Dept., METU**   _____

Prof. Dr. M. Semih Yücemen
Co-Supervisor, **Civil Engineering Dept., METU**   _____

Examining Committee Members:

Assist. Prof. Dr Ayşegül Askan Gündoğan
Civil Engineering Dept., METU   _____

Assist. Prof. Dr. Alp Caner
Civil Engineering Dept., METU   _____

Prof. Dr. M. Semih Yücemen
Civil Engineering Dept., METU   _____

Assist. Prof. Dr Afşin Sarıtaş
Civil Engineering Dept., METU   _____

Yeşim Esat
General Directorate of Highways of Turkey   _____

Date: _____

I hereby declare that all information in this document has been obtained and presented in accordance with academic rules and ethical conduct. I also declare that, as required by these rules and conduct, I have fully cited and referenced all material and results that are not original to this work.

Name, Last name: Oktay Argınhan

Signature   :

ABSTRACT

RELIABILITY BASED SAFETY LEVEL EVALUATION OF TURKISH
TYPE PRECAST PRESTRESSED CONCRETE BRIDGE GIRDERS
DESIGNED IN ACCORDANCE WITH THE LOAD AND RESISTANCE
FACTOR DESING METHOD

Argınhan, Oktay

M.S., Department of Civil Engineering

Supervisor: Assist. Prof. Dr. Alp Caner

Co-Supervisor: Prof. Dr. M. Semih Yücemen

December 2010, 137 pages

The main aim of the present study is to evaluate the safety level of Turkish type precast prestressed concrete bridge girders designed according to American Association of State Highway and Transportation Officials Load and Resistance Factor Design (AASHTO LRFD) based on reliability theory. Span lengths varying from 25 m to 40 m are considered. Two types of design truck loading models are taken into account: H30S24-current design live load of Turkey and HL93-design live load model of AASHTO LRFD. The statistical parameters of both load and resistance components are estimated from local data and published data in the literature. The bias factors and coefficient of variation of live load are estimated by extrapolation of cumulative distribution functions of maximum span moments of truck survey data (Axle Weight Studies) that is gathered from the Division of Transportation and Cost Studies of the General Directorate of Highways of Turkey. The uncertainties associated

with C40 class concrete and prestressing strands are evaluated by the test data of local manufacturers. The girders are designed according to the requirements of both Service III and Strength I limit states. The required number of strands is calculated and compared.

Increasing research in the field of bridge evaluation based on structural reliability justifies the consideration of reliability index as the primary measure of safety of bridges. The reliability indexes are calculated by different methods for both Strength I and Service III limit states. The reliability level of typical girders of Turkey is compared with those of others countries. Different load and resistance factors are intended to achieve the selected target reliability levels. For the studied cases, a set of load factors corresponding to different levels of reliability index is suggested for the two models of truck design loads. Analysis with Turkish type truck models results in higher reliability index compared to the USA type truck model for the investigated span lengths

Keywords: Reliability Analysis, Reliability Index, Bridge Live Load Models, Prestressed Precast Bridge Girders, Target Reliability Level, Bridges of Turkey.

ÖZ

YÜK VE DAYANIM KATSAYILARI TASARIM YÖNTEMİNE GÖRE TASARLANMIŞ, TÜRKİYE'DE KULLANILAN PREFABRİK ÖNGERMELİ KÖPRÜ KİRİŞLERİNİN GÜVENİRLİK DÜZEYLERİNİN DEĞERLENDİRMESİ

Argınhan, Oktay

Yüksek Lisans, İnşaat Mühendisliği Bölümü

Tez Yöneticisi: Yrd. Doç. Dr. Alp Caner

Ortak Tez Yöneticisi: Prof. Dr. M. Semih Yücemen

Aralık 2010, 137 sayfa

Bu tez çalışmasında, AASHTO LRFD şartnamesine göre tasarlanmış, Türkiye'de kullanılan öngermeli prefabrik köprü kirişlerinin güvenirlik seviyesi değerlendirilmiştir. 25m'den 40m'ye kadar açıklığa sahip köprüler göz önünde tutulmuştur. Yük ve dayanımın istatistiksel parametreleri, yerel verilerden ve uluslararası çalışmalardan elde edilmiştir. İki tip tasarım kamyonu yük modeli hesaba katılmıştır; H30S24 - Türkiye'de tasarımda kullanılan tasarım kamyon yüklemesi ve HL93-AASHTO LRFD de belirtilen tasarım kamyonu yüklemesi. Karayolları Genel Müdürlüğü, Ulaşım ve Maliyet Etütleri şubesinden alınan dingil ağırlığı etüt verileri ile hesaplanan orta açıklık maksimum momentleri kullanılarak birikimli dağılım işlevi Gumbel olasılık kâğıdına çizilmiştir ve bu dağılımlar daha uzun periyotlara extrapole edilerek tasarım kamyon yükü istatistiksel parametreleri belirlenmiştir. Yerel üreticilerden alınan test verileri kullanılarak C40 beton sınıfı ve öngerme

halatının dayanımlarına ilişkin istatistiksel parametreler belirlenmiştir. Öngerilmeli kirişler, servis ve mukavemet sınır durumları düşünülerek tasarlanmış ve gerekli öngerilme halat sayıları belirlenerek her iki sınır durumu için karşılaştırılmıştır.

Yapısal güvenirlik esasına dayalı köprü değerlendirme alanında yapılan çalışmalar, güvenirlik indeksinin köprü yapı emniyetinin temel ölçüsü olduğunu doğrulamaktadır. Bu çalışmada, farklı metodlar kullanılarak hem servis hem de mukavemet sınır durumları için güvenirlik indeksi hesaplanmıştır ve karşılaştırılmıştır. Türkiye'deki belirsizliklere göre tasarlanan tipik öngerilmeli köprü kirişlerinin güvenirlik seviyesi diğer ülkelerin belirsizlikleri ve tasarım şartnameleri ile karşılaştırılmıştır. Belirlenen hedef güvenirlik seviyelerine göre farklı yük ve dayanım katsayıları elde edilmiştir.

Anahtar Kelimeler: Güvenirlik Analizi, Güvenirlik İndeksi, Köprü Hareketli Yük Modelleri, Öngermeli Prefabrik Köprü Kirişleri, Hedef Güvenirlik Seviyesi, Türkiye'deki Köprüler.

To My Parents,

ACKNOWLEDGMENTS

TABLE OF CONTENTS

LIST OF TABLES

LIST OF FIGURES

LIST OF SYMBOLS

AASHTO	American Association of State Highway and Transportation Officials
A_{ps}	Area of Prestressing Steel
A_s	Area of Mild Steel Tension Reinforcement
A'_s	Area of Compression Reinforcement
b	Width of Compression Flange
b_w	Web Width of Beam
b_n	Nominal Precast Beam Width
CDF	Cumulative Distribution Function
COV	Coefficient of Variation
c	Depth of Neutral Axis
D	Dead Load
D_A	Dead Load due to Asphalt
DC	Dead Load of Structural and Non-structural Components
DW	Dead Load of Wearing Surface and Utilities
D_{sta}	Maximum Static Deflection
D_{dyn}	Dynamic Deflection
d_b	Distance from Extreme Compression Fiber to the Centroid of the Prestressing Strand
d_s	Distance from Extreme Compression Fiber to the Centroid of Non-prestressed Tensile Reinforcement
d'_s	Distance from Extreme Compression Fiber to the

	Centroid of Nonprestressed Compression Rein.
d_{pn}	Nominal Effective Depth
e_c	Strand Eccentricity
E_p	Modulus of Elasticity of Prestressing Steel
E_{ct}	Modulus of Elasticity of Concrete at Transfer or Time of Load Application.
E_B	Modulus of Elasticity of Beam Material
E_F	Modulus of Elasticity of Deck Material
f_b	Bottom Fiber Tensile Stress
f_c'	Compressive Stress of Deck Concrete
f_s	Yield Strength of Tension Reinforcement
f_s'	Stress in Mild Steel Compression Reinforcement at Nominal Flexural Resistance
f_{pi}	Prestressing Steel Stress Immediately prior to Transfer
f_{ps}	Average Stress in Prestressing Steel
f_{pu}	Tensile strength of Prestressing Steel
f_c'	Specified 28-day Concrete Strength of Precast Beam
f_{cgp}	Concrete Stress at the Center of Gravity of Prestressing Tendons due to the Prestressing Force Immediately after Transfer
LRFD	Load and Resistance Factor Design
LL	Vehicular Live Load
L	Span Length
GDF	Girder Distribution Factor
GP	Gumbel Probability Paper
K_g	Longitudinal Stiffness Parameter
IM	Impact factor

I	Moment of Inertia of Beam
h_f	Depth of Compression Flange
H	Average Annual Ambient Relative Humidity
NCHRP	National Cooperative Highway Research Program
NP	Normal Probability Paper
$\overline{N}$	Mean Correction Factor
M	Span Moment
M_g	Unfactored Bending Moment due to Beam Self-Weight
M_s	Unfactored Bending Moment due to Slab and Haunch Weights
M_{ws}	Unfactored Bending Moment due to Barrier Weights
M_{LT}	Unfactored Bending Moment due to Truck Load
M_{LL}	Unfactored Bending Moment due to Lane Load
P_{pe}	Total Prestressing Force
P_F	Probability of Failure
R	Flexural resistance capacity
S	Spacing of Beams
S_b	Section Modulus for the Extreme Bottom Fiber of the Non-composite Precast Beam
S_{bc}	Composite Section Modulus for the Extreme Bottom Fiber of the Non-composite Precast Beam
t_s	Depth of Concrete Slab
β	Reliability Index
ϕ	Resistance Factor
ϕ^{-1}	Inverse Standard Normal Distribution Function
η	Reduced Variate
μ	Mean Value,

σ		Standard Deviation,
λ		Location Parameter of Gumbel Distribution
δ		Scale Parameter of Gumbel Distribution
β_1		Stress Factor of Compression Block
γ_h		Correction Factor for Relative Humidity of Ambient Air
γ_{st}		Correction Factor for Specified Concrete Strength at Time of Prestress Transfer to the Concrete Member
Δ		Prediction Error
Δf_{pES}		Sum of all Losses or Gains due to Elastic Shortening or Extension at the Time of Application of Prestress
Δf_{pLT}		Losses due to Long Term Shrinkage and Creep of Concrete and Relaxation of the Steel
Δf_{pR}		Estimate of relaxation loss

CHAPTER 1

INTRODUCTION

Highway bridges have a crucial role in the modern transportation system. Therefore, the safety of design and overall quality of construction is ensured by certain design specifications. All over the world, there are many specifications that the bridge engineers can utilize, whereas some counties have their own bridge design specifications such as American Association of State Highway and Transportation Officials Load and Resistance Factor Design (AASHTO LRFD) [1] code in United States, Eurocode in Europe, some developing countries such as Turkey use modified versions of these specifications.

The current design practice in Turkey is using a modified version of AASHTO Load Factor Design (LFD) specification in design of bridges. AASHTO LFD [23] has been used since 1971 for the design of bridges in US. In 1993, AASHTO adopted the Load and Resistance Factor Design (LRFD) specifications for bridge design to eliminate gaps and inconsistencies in AASHTO LFD and increase the uniformity of the margin of safety across various structure types. LFD specification was calibrated based on judgment and experience, whereas LRFD specifications were developed based on probability based calibration process considering uncertainty of load and resistance parameters. By the new alternative code (LRFD), live load models, impact factors, lateral distribution factors, load combinations and design of fatigue were modified. Both specifications have been utilized for bridge design until today. However, AASHTO organization made a decision to cease the

support and update of LFD design specification. Bridge engineers worldwide are shifting their attention from LFD to LRFD specification. Also, General Directorate of Highways of Turkey is seriously considering to use a modified version of the AASHTO LRFD in the design of Turkish bridges.

AASHTO LRFD Bridge Design Specification has been prepared according to the conditions and needs of bridges of America. Therefore, safety level of bridges of Turkey designed by AASHTO LRFD should be checked. Thus, this study aims to investigate and determine the safety level of a part of AASHTO LRFD and suggest load and resistance factors to achieve the target safety level. In this study, the prestressed precast concrete bridge girders, which are the most common bridge types constructed on highways of Turkey, are considered for span ranges of 25 m to 40 m. In addition, this study only focuses on the strength I and service III limit states and flexural resistance at midspan.

The most preferred bridge safety measure is currently based on reliability methods. The reliability index, β, has been used by many code-writing groups throughout the world to express structural risk. β includes different sources of uncertainties involved in the estimation of resistance and load effects. The target reliability level is chosen to provide the required safety of structure during calibration of design codes. Target reliability levels are determined based on cost-safety analysis. In order to achieve higher safety levels, the resistance should be increased. Therefore, higher reliability levels lead to an increase in the cost of structural projects. Therefore, providing a balance between cost and risk is a very crucial part of the reliability analysis. β is usually within the range of 2 to 4, and it shows variation for different structural applications. For instance, β is taken as 3.5 for the calibration of the Strength I Limit State in AASHTO LRFD specifications [1].

1.1 OBJECTIVES

This study aims to focus on reliability based safety level evaluation of Turkish type precast prestressed concrete bridge girders designed in accordance with the load and resistance factor design method.

Here mainly the procedure outlined in the calibration report of AASHTO LRFD done by Nowak [12] is followed. Consistent with Nowak's study firstly, the statistical parameters (bias factor, coefficient of variation and probability distribution) of load and resistance components are estimated. Load parameters are live load, dead load, impact factor, girder distribution factor, and resistance parameters are compressive strength of concrete, tensile strength of prestressing strand, dimensions. Some of them are estimated by statistical data assessed in Turkey, whereas others for which no local data is available are determined from the calibration report of AASHTO LRFD and international research.

Live load is the most important load component of highway bridges, since it directly affects the safety level of bridges. Truck loads are highly site specific. Therefore, many countries need to evaluate their standards and current design practice on the basis of live load model considering the country's own conditions and characteristics. For this purpose, in order to evaluate the statistical parameters of bridge live loads of Turkey, truck survey data provided by General Directorate of Highways of Turkey is used. Statistical analysis is carried out for both design live load models, H30S24 and HL93, for comparison. H30S24 is the current design truck model in Turkey and HL93 is the live load model of current AASHTO LRFD code.

This study also aims to assess the uncertainties associated with the resistance of prestressed precast concrete girders constructed in Turkey. The statistical parameters of compressive strength of concrete used in girders as well as those

of prestressing strands are estimated according to the design and construction conditions of Turkey. For this purpose, the test results of manufacturers were collected. It is to be noted that resistance is calculated according to AASHTO LRFD code for both design live load models.

Deterministic analysis is done for strength and service limit states to determine required number of prestressing strands for comparison and to carry out the reliability analysis. The reliability indexes are calculated for both live load models considering 25 m to 40 m span length for typical bridge cross-sections of Turkey. Differences between the reliability level of service and strength limit states are presented. It is aimed to estimate different load and resistance factors to achieve different safety levels.

1.2 SCOPE

The rest of the thesis is organized as follows:

Chapter 2 presents the results of the literature survey on reliability analysis of bridge girders. The calibration report of AASHTO LRFD and its update report are summarized. The reliability levels of different codes such as Spanish Norma, Eurocode, Chinese code, Hong Kong code and AASHTO LRFD code are introduced.

H30S24 and HL93 live load models are explained in Chapter 3. The 75 year maximum live load effect and maximum two lane live load effects are estimated by extrapolation of truck survey data. Finally, application and statistical parameters of girder distribution factor and impact factor according to AASHTO LRFD are presented.

In Chapter 4, calculation of nominal flexural resistance according to AASHTO LRFD Code is introduced. The bottom tensile stress check in service limit state is explained. Then, the uncertainties of resistance parameters are estimated considering the conditions in Turkey.

Chapter 5 displays the dimensions of typical prestressed precast concrete girders based on span length. This chapter also contains the drawings of the bridge cross sections of each span length, which indicate the spacing between girders.

In Chapter 6, the reliability analysis is carried out by various methods. The reliability level of girders designed by AASHTO LRFD code using both H30S24 and HL93 live load models is estimated for service and strength limit states. The comparison is done with the reliability levels of other design codes. The target reliability levels in AASHTO LRFD code and Eurocode are discussed. Finally, various load and resistance factors are tried to achieve different target reliability levels.

Chapter 7 concludes the thesis and summarizes the main results of the study.

CHAPTER 2

LITERATURE SURVEY / BACKGROUND

2.1 REVIEW OF LITERATURE

This study is carried out by the procedures described in National Cooperative Highway Research Program (NCHRP) Report 368 [12], "Calibration of LRFD Bridge Design Code" considering the case of Turkey. This report is a basis for code calibration procedures for bridge designs. Most of the researches used statistical parameters and assumptions described in this report to compare their design codes based on the reliability index.

In the past, AASHTO Standard 1992 was used to design highway bridges in the US. This code does not provide a consistent and uniform safety level. Therefore, a new code was intended to be developed based on reliability methods to provide uniform safety levels for various spans and bridge types. To further explain the development of the new code, Nowak et al. [12] aimed to present the procedures used in the calibration of a load and resistance factor design bridge code for ultimate strength limit state of different types of bridges in NRCHP Report 368, "Calibration of LRFD Bridge Design Code". In addition, the new code aims to establish a new live load model. In that report, the newly developed live load is compared with the old one, HS20. [23]

In the current AASHTO LRFD code, HL93 truck model is used in designs. This live load consists of lane load and truck load. The only difference from

the previously used load model, HS20, is the lane load that is applied with truck load. Both design models, HL93 and HS20, have the same axle spacing and weight. The live load model is investigated by the available statistical data. In that report, the weight-in-motion (WIM) database created by Ontario Ministry of Transportation in 1975 is used. [12]
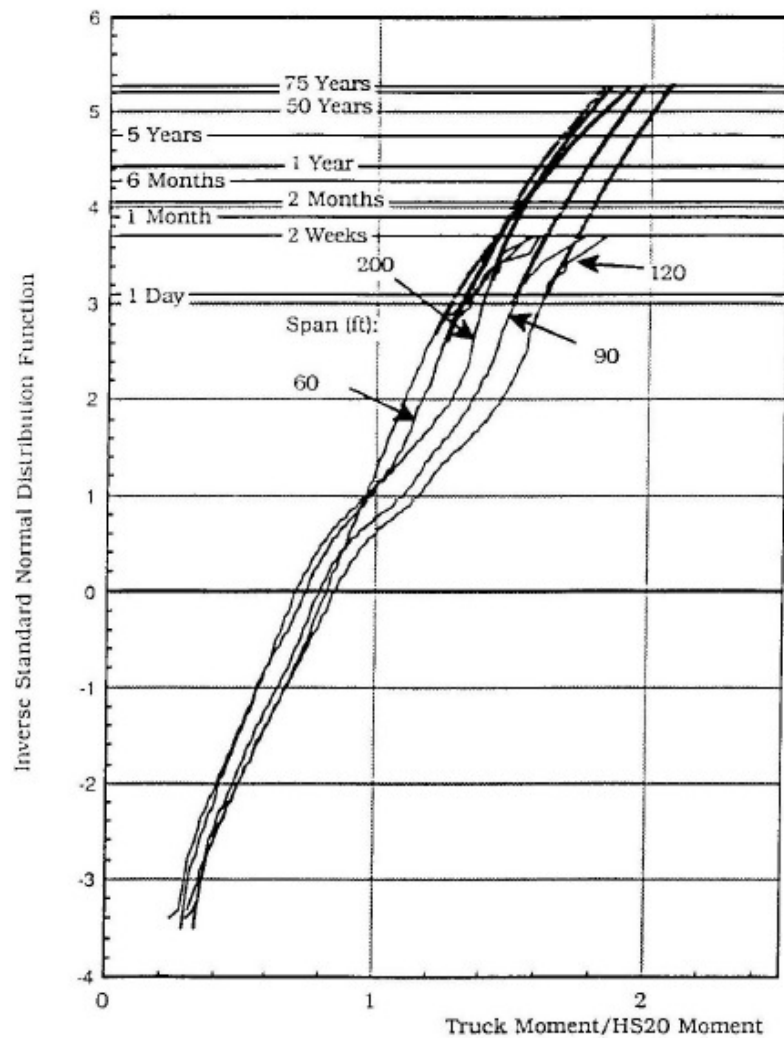
Figure 2-1 Extrapolated Moment Ratios Obtained from Truck Survey Data [12]

The inverse standard normal distribution was plotted using moments and shears calculated by each surveyed truck, and the mean 75 year maximum live load

7

was estimated by extrapolation of data for various span lengths. Extrapolated cumulative distribution functions (CDF) of various span lengths are shown in Figure 2-1 for only maximum span moments. Figure 2-2 highlights that the new live load model, HL93, provides a uniform bias for different span lengths in comparison with the past one, HS20. In Figure 2-2, M(75) denotes to 75 year mean maximum moment and M(HL93) and M(HS20) are the maximum design span moments due to each design truck. In this report, information on dynamic factor and girder distribution factor is also presented in a comprehensive way. The details are explained in CHAPTER 3. [12]
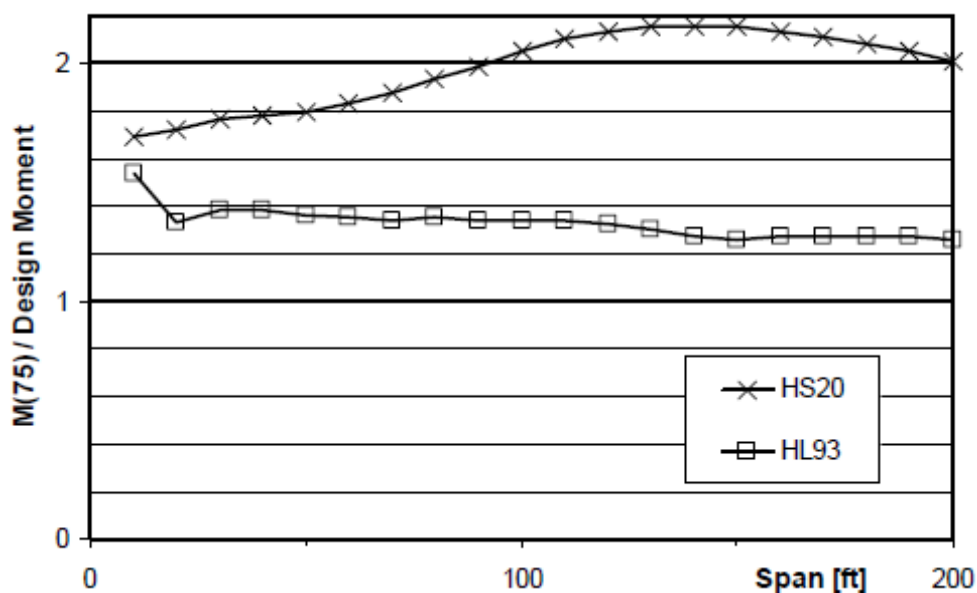
Figure 2-2 Bias Factor for Simple Span Moment: Ratio of M(75) / M(HL93) and M(75) / M(HS20) [13]

In the calibration report, resistance is taken as the product of three factors: material (strength), fabrication (dimensions) and professional (actual to theoretical behavior). Statistical parameters of resistance are estimated by the existing literature and special studies for different girder bridges (steel,

reinforced concrete and prestressed concrete). Resistance is taken as a lognormal variate. [12]

The reliability index is calculated by using the Mean Value First Order Second Moment (MVFOSM) method together with Rackwitz and Fiessler algorithm in the calibration report. The reliability indexes are calculated for bridge girders designed by AASHTO (standard 1992) specification by using the following design equation,

$$\phi R > 1.3D + 2.17(1+I)L \qquad (2\text{-}1)$$

where R is resistance, ϕ is resistance factor, D is dead load, I is impact factor, and L is live load. The calculated reliability index by this past code is shown in Figure 2-3 for various span lengths and girder spacing.
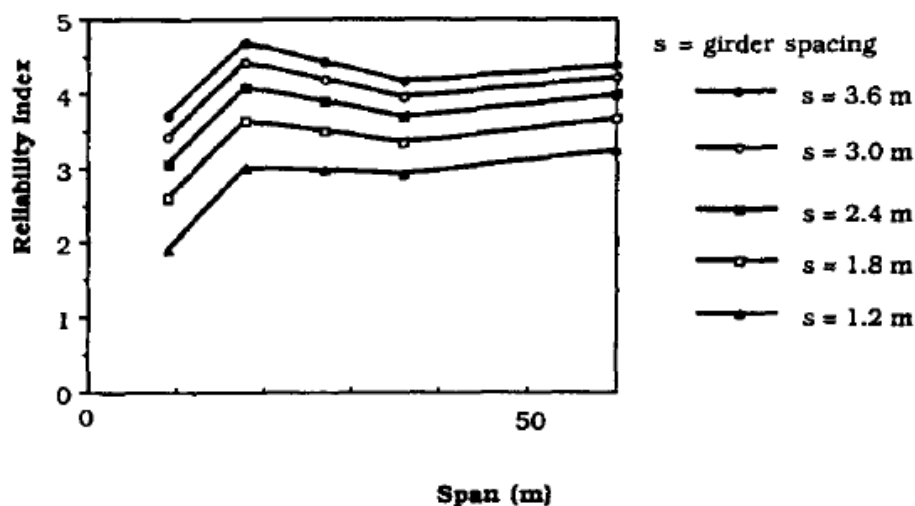
Figure 2-3 Reliability Indexes for Prestressed Concrete Girders-Span Moments; AASHTO (Standard 1992) [12]

9

The reliability index calculated by the previous AASHTO specifications (Standard 1992) is not uniform and changes considerably by the spacing between girders. Thus, the load and resistance factors are calibrated to achieve a uniform safety level for all spans. In the calibration report, various load and resistance factors were tried to be taken up to the target reliability level, as displayed in Figure 2-4. In calibration of AASHTO LRFD Specifications, the target reliability level is taken as 3.5. Therefore, after calibration, the design equation becomes

$$\phi R > 1.25D + 1.5D_A + 1.75(1+I)L \qquad (2\text{-}2)$$

where, R is resistance, ϕ is resistance factor (1.0 for moment and prestressed concrete girders), D is dead load, D_A is the dead load due to asphalt, I is impact factor and L is live load.

By the new code (current) the dead load has been divided into two different load components: weight of structural components and weight of wearing surface. Dead load due to the asphalt has higher load factor because it involves higher uncertainty. Another revision in the new code is the formulation of girder distribution factor. The new expression minimizes the reliability index changes due to girder spacing. As indicated in Figure 2-4, the new load and resistance factors provide a uniform reliability level throughout a wide spectrum of spans.
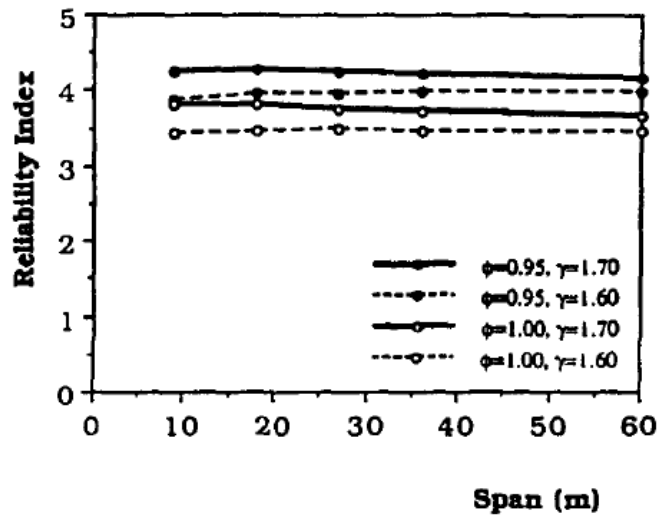
Figure 2-4 Reliability Indexes for Prestressed Concrete Girders-Span
Moments; Proposed LRFD Code (Current AASHTO LRFD) [12]

Another report [13] was published in 2007 to update the previously presented
report, NCHRP Report 368. This report summarizes the report of calibration of
LRFD bridge design code and presents procedures for collecting data. What
lacked in the previous report is explained. Indeed, in the previous report, the
reliability indexes were calculated by an iterative procedure (Rackwitz and
Fiessler). In this method, the non-normal variables are approximated to
equivalent normal variables by satisfying certain requirements. However, this
report suggests Monte Carlo Simulation technique to calculate the reliability
index because this procedure eliminates the need to approximate the
distribution. [13]

In updating the calibration report, the reliability index of girders of the 124
bridges designed by AASHTO LRFD Specifications is estimated by Monte
Carlo simulation. Figure 2-5 shows the reliability indexes of all types of
bridges: Prestressed concrete boxes (1-45), "California" prestressed concrete
boxes (46-51), prestressed concrete I-Beams (51-85), reinforced concrete slabs

(86-95) and steel welded plate girders (95 -124). The numbers in parenthesis refers to bridges mentioned in the report [13] . In addition, Figure 2-6 shows the reliability indexes of prestressed concrete girders. As seen in Figure 2-6, reliability indexes of prestressed concrete I beams are between 3.93 and 3.44. It is stated that the concrete bridges have higher reliability indexes than the steel bridges, and the reliability index decreases as the span length increases. It is also explained that an increase in dead load to live load ratio also results in an increase in the reliability indexes.
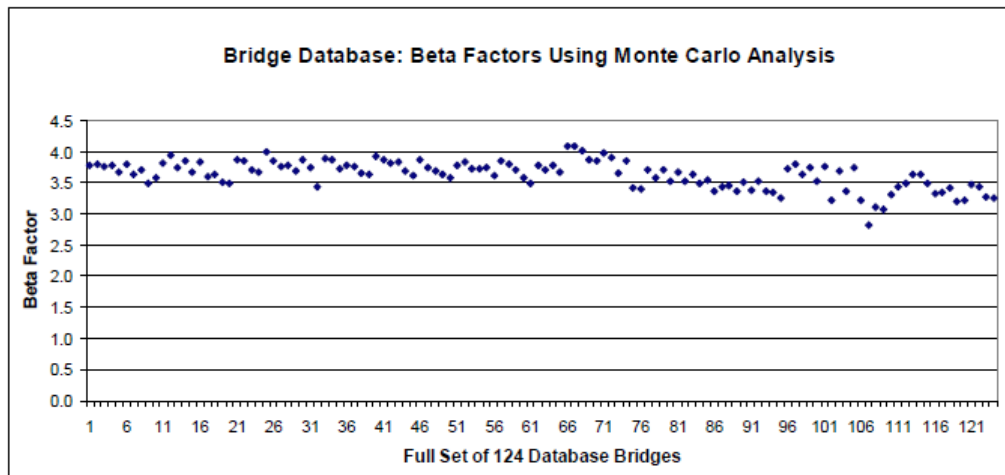
Figure 2-5 Monte Carlo Results for All Bridges [13]
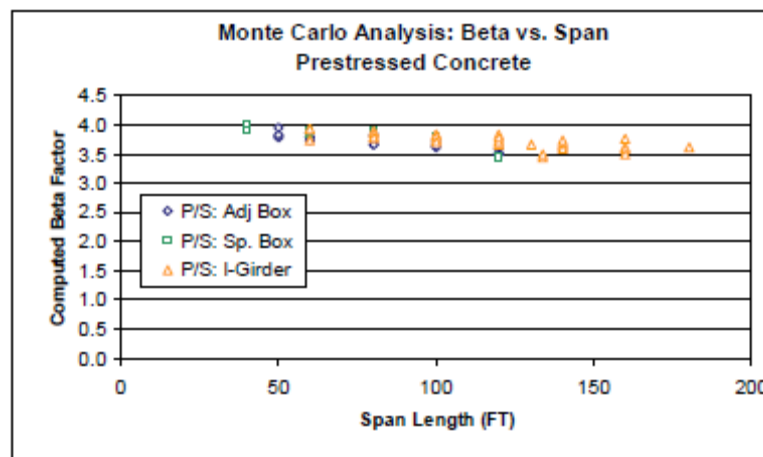
Figure 2-6 Beta Factors for Various Types of P/S Concrete Girders [13]

Another study carried out by Nowak et al. [3] compares the reliability level of girders designed by Spanish Norma, Eurocode and AASHTO LRFD code. Typical precast girders used in Spain are considered. The statistical parameters used in the study are generally based on the previously explained calibration report. In reliability analysis, statistical parameters of Spanish truck survey and Ontario truck survey (used in calibration of AASHTO LRFD) are considered. Extrapolated CDF of Spanish truck data is displayed in Figure 2-7. It is stated that the cumulative distribution function (CDF) of moments is assumed to follow an extreme type I (Gumbel) distribution, but it is approximated to normal distribution; in particular this applies to the upper tail of CDF. Bias factor for both truck data is shown in Figure 2-8. An iterative procedure is used estimating the reliability index as described by Rackwitz and Fiessler. Reliability analysis is done for both Ontario and Spanish truck data as shown in Figure 2-9 and Figure 2-10. The reliability indexes calculated based on Spanish truck data are higher than those calculated based on Ontario truck data. The results show that Eurocode is the most conservative one and AASHTO LRFD is the most permissive code, and AASHTO LRFD provides the most uniform safety level. [3]
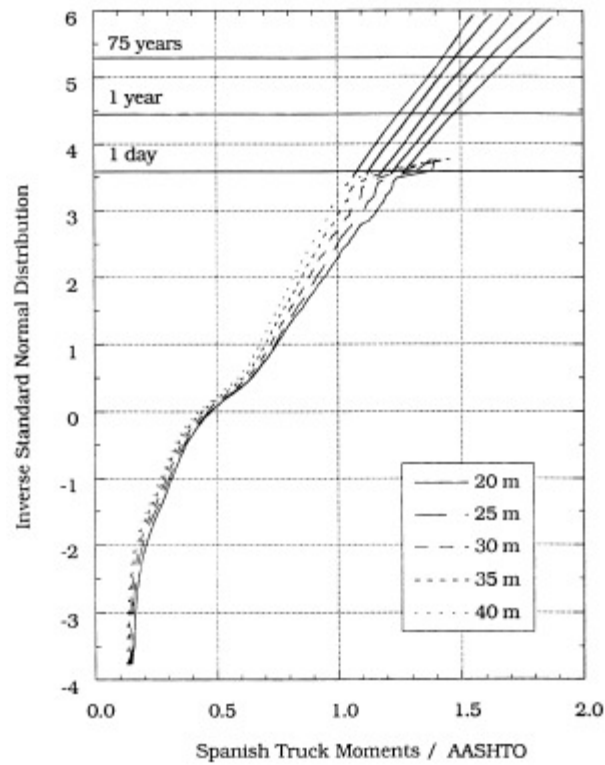
Figure 2-7 Moment Ratios Obtained from Spanish Truck Survey [3]
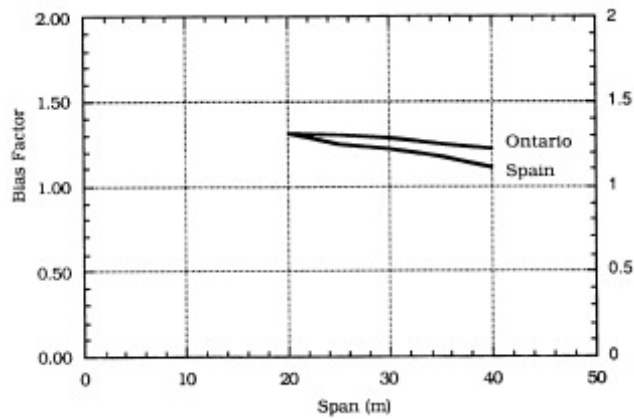
Figure 2-8 Bias Factors for the Moment per Girder (including Dynamic load Factor, DLF) for the Ontario Truck Data and Spanish Truck Data, with the Nominal Moment Corresponding to AASHTO LRFD [3]
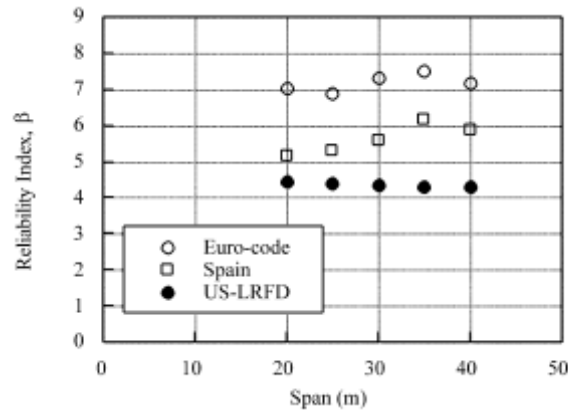
Figure 2-9 Reliability Indexes for Ontario Truck Traffic [3]
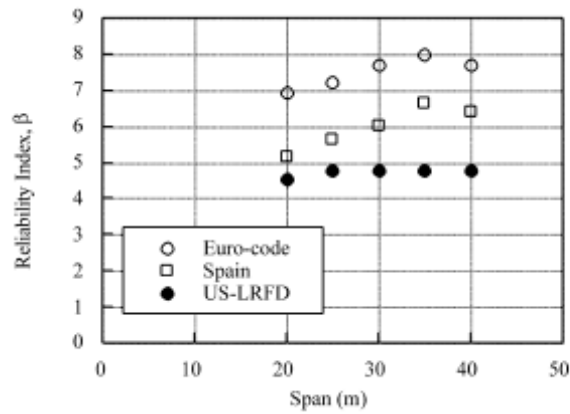
Figure 2-10 Reliability Indexes for Spanish Truck Traffic [3]

In another work, Du and Au et al. [17] carried out deterministic and reliability based analyses of prestressed concrete bridge girders to compare the Chinese, Hong Kong and AASHTO LRFD codes. Firstly, deterministic analysis is carried out to find moments due to dead load and live load for four typical prestressed concrete girders having span lengths varying between 25 m to 40 m. The required number of prestressing strands is calculated for girders designed by three codes considering strength and service limit states, as shown in Figure 2-11. In service limit state, the allowable concrete tensile stress is taken as zero for all three design codes for ease of comparison. This results in a

15

higher number of strands. As Figure 2-11 indicates, the service limit state governs both Chinese and AASHTO LRFD codes. However, for Hong Kong code, service limit state governs only the longer spans. The required number of strands according to Chinese code is slightly more than that needed by the AASHTO LRFD code, but the required number of strands needed by Hong Kong code is significantly more than that needed by other codes. [17]
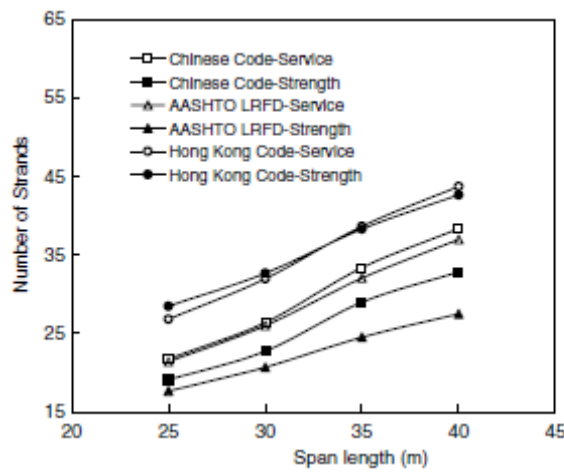
Figure 2-11 Number of 12.7 mm Strands per Girder Required for Strength and Service Limit States [17]

In that research, the reliability indexes are calculated by the same statistical parameters and procedures described in the calibration report of AASHTO LRFD [12]. The reliability index is calculated by using the Mean Value First Order Second Moment (MVFOSM) method together with Rackwitz and Fiessler algorithm. The estimated reliability indexes are plotted in Figure 2-12 and Figure 2-13 for strength and service limit states, respectively. The reliability index calculated for flexural capacity at the strength limit state in the Hong Kong code is lower than that of the AASHTO LRFD and Chinese codes due to the high live load moment for the strength limit state in the Hong Kong code. The reliability index based on service limit state requirements is higher than that for the strength limit state that is about 43-65% for AASHTO LRFD

16

code, 83-103% for Hong Kong code, and 23-30% for Chinese code. The reliability indexes of service limit state are fairly close to one another for all of the three codes. [17]
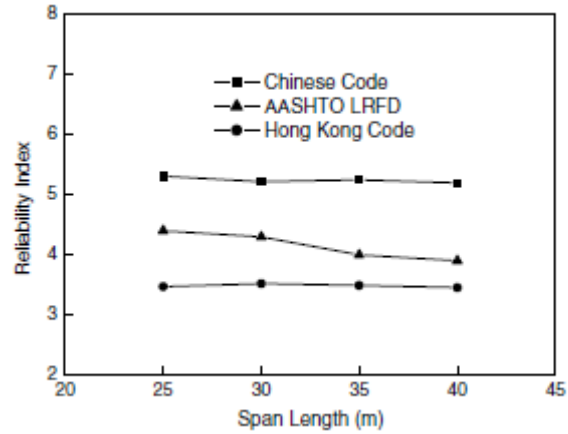
Figure 2-12 Reliability Indexes for Flexural Capacity Based on the Requirements of the Strength Limit State in the Three Codes [17]
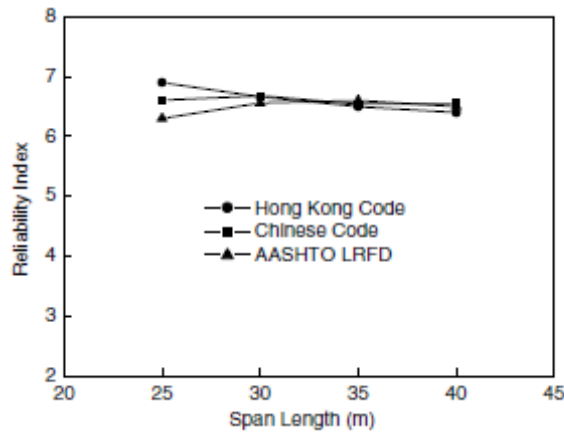
Figure 2-13 Reliability Indexes for Flexural Capacity Based on the Requirements of the Service Limit State in the Three Codes [17]

17

CHAPTER 3

STATISTICS OF LOAD

3.1 DESIGN LIMIT STATES AND LOAD COMBINATIONS

The following limit states are specified in AASHTO LRFD Specifications (AASHTO LRFD 3.4.1) to design components and connections of a bridge [1];

- Strength I – Basic load combination relating to the normal vehicular use of the bridge without wind.

- Strength II – Load combination relating to the use of the bridge by owner-specified special design vehicles, evaluation permit vehicles, or both without wind.

- Strength III – Load combination relating to the bridge exposed to wind velocity exceeding 55 mph.

- Strength IV – Load combination relating to very high dead load to live load force effect ratios.

- Strength V – Load combination relating to normal vehicular use of the bridge with wind of 55 mph velocity.

- Extreme Event I – load combination including earthquake.

- Extreme Event II – load combination relating to ice load, collision by vessels and vehicles, and certain hydraulic events with a reduced live load other than that which is part of the vehicular collision load.

- Service I – Load combination relating to the normal operational use of the bridge with a 55 mph wind and all loads taken at their nominal values.

- Service II – load combination intended to control yielding of steel structures and slip of slip-critical connections due to vehicular live load.

- Service III – Load combination for longitudinal analysis relating to tension in prestressed concrete superstructures with the objective of crack control and to principal tension in the webs of segmental concrete girders.

- Service IV – Load combination relating only to tension in prestressed concrete columns with the objective of crack control.

- Fatigue – fatigue and fracture load combination relating to repetitive gravitational vehicular live load and dynamic responses under a single design truck.

The design of prestressed beams usually needs to be checked against the requirements of Service I, Service III and Strength I limit states [2]. Service I checks the compression stress, and Service III checks the tensile stress in prestressed concrete component at the critical section and critical top or bottom fiber. Strength I is used to estimate the ultimate strength. In designing prestressed beam, typically Service III governs and controls the design in terms of the determining number of prestressing steel for a selected cross-section. In

a typical prestressed bridge girder design, industry accepted span to depth ratios are used to select the depth of girder and corresponding shelf cross-section. The cracking at bridge girders is the most unwanted situation since the bridge girders cannot be protected adequately from environmental conditions. Typically, cracking of concrete is controlled by limiting the tension stress of concrete fibers.

The reliability analysis of prestressed concrete girders is carried out for the Strength I Limit state   that is set to ensure that bridge itself or its elements will have certain strength and stability to resist the specified statistically significant gravity load combination that a bridge could be subjected during its economic life. Reliability analysis for Service III limit state is also evaluated to ensure that bridge will continue to maintain a certain level of durability and passenger comfort under statistically determined gravity loads and load combinations while in use.

According to AASHTO LRFD Bridge Design Specifications [1], the load combination for Strength I limit state for multi-girder simple span bridge superstructure can be computed from the below relationship:

$$Q = 1.25 \cdot DC + 1.50 \cdot DW + 1.75 \cdot LL \cdot (1 + IM) \cdot GDF \qquad \text{(3-1)}$$

Load combination for Service III limit state is expressed below

$$Q = DC + DW + 0.8 \cdot LL \cdot (1 + IM) \cdot GDF \qquad \text{(3-2)}$$

where DC is dead load of structural and non structural components, DW is dead load of wearing surface and utilities, LL is vehicular live load, IM is the impact factor, and GDF is the girder distribution factor. In this section, live

load including truck load, lane load, impact factor and girder distribution factor and dead load will be identified, and related uncertainties due to these load components will be assessed.

3.2 DEAD LOAD

The dead load consists of four components:

D_1 - Weight of factory made elements (steel and precast beams)

D_2 - Weight of cast-in-place concrete (deck)

D_3 - Weight of wearing surface (asphalt)

D_4 - Weight of miscellaneous (railing, luminaries).

In strength I limit state, the load factor for weight of factory prepared elements, D_1, and cast-in-place concrete components, D_2, are set to 1.25, and the load factor for wearing surface, D_3, and miscellaneous items, D_4, are set to 1.5.

In this study, statistical parameters of dead load components are taken from Nowak's study [13]. All dead load variables are considered to be normally distributed. The wearing surface, i.e. the asphalt layer, has the highest uncertainty among the dead load components. For miscellaneous components, the bias factor and coefficient of variation can vary, but in this study, these values are taken as 1.05 and 0.10, respectively to stay on the conservative side. Mean bias factor is the ratio of the mean of true value to nominal value. (Increase in the bias factor and coefficient of variation for load components typically results in lower reliability indexes.)

Table 3-1 Statistical Parameters of Dead Load from Nowak et al. [12]

Dead Load Component	Bias Factor	Coefficient of Variation
Factory Made Members,D_1	1.03	0.08
Cast-in-place,D_2	1.05	0.1
Wearing Surface,D_3	1	0.25
Miscellaneous,D_4	1.03~1.05	0.08~0.10

3.3 LIVE LOAD

3.3.1 Live Load Models

In this section, live load model of AASHTO LRFD, HL-93, and the live load model of Turkey, H30-S24 will be introduced, and the span moment due to both HL-93 and H30-S24 loading will be presented.

3.3.1.1 HL-93 Loading

The live load model of AASHTO LRFD Bridge Design specifications consists of a combination of

- Design truck or design tandem, and
- Design lane.

HL-93 truck model is used as the design truck. The weights and spacings of axles and wheels for the design truck are specified in Figure 3-1. The spacing between the two back axles is varied from 4.3 m to 9.0 m   to produce the maximum load effect. The width of loads for a single lane is assumed to occupy 3000 mm [1].

The design tandem consists of a pair of 110000 N axles spaced 1200 mm apart and the transverse spacing of wheels is taken as 1800 mm. Design lane load consists of a load of 9.3 N/mm uniformly distributed in the longitudinal direction, and it is assumed to be uniformly distributed over 3000 mm width.[1]

In order to obtain the extreme force effect, the effects of an axle sequence and the lane load are superposed. Extreme force effect is taken as the larger of the following:
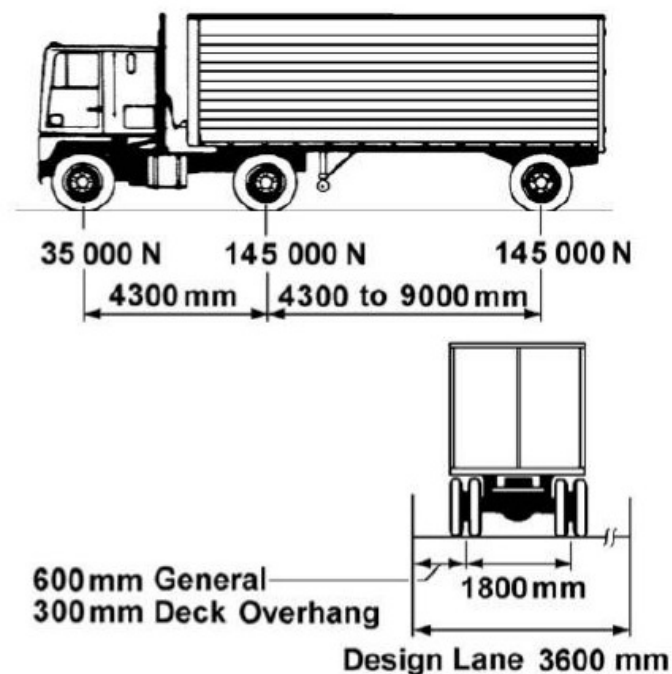
Figure 3-1 Characteristics of Design Truck, HL-93

    i.   the effect of one design truck with the variable axle spacing combined with the effect of the design lane load (as shown in Figure 3-2.a),

    ii.   the effect of the design tandem combined with the effect of the design lane load (as shown in Figure 3-2.b),

iii.   to maximize both negative moment and reaction at interior piers between points of contra flexure under a uniform load on all spans, 90 percent of the effect of two design trucks spaced at a minimum of 15000 mm between the lead axle of one truck and rear axle of other truck, combined with 90 percent of the effect of the design lane load, is utilized. The distance between the 145000 N axles of each truck is taken as 4300 mm. (It is noted, in this study, that the continuous spans are not included.) (as shown in Figure 3-2.c)[1]
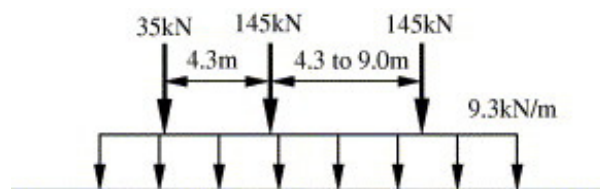
a. Tuck and Uniform Load
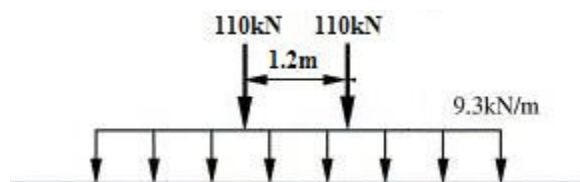
b. Tandem and Uniform Load
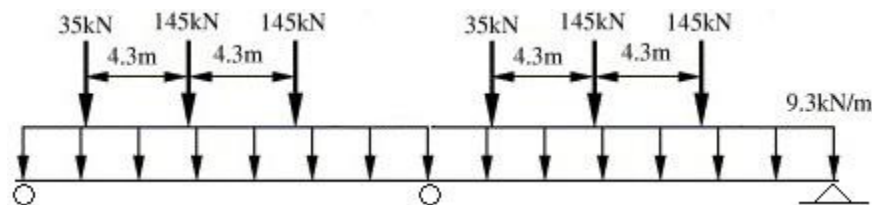
c. Alternative Load for Negative Moment (reduced to 90%)

Figure 3-2 Design Live Load in AASHTO LRFD,HL-93

24

3.3.1.2 H30-S24 Loading

The live load model consisting of design truck load and design lane load with concentrated load is specified in the Technical Specifications for Roads and Bridges in Turkey [14]. H30-S24 is specified as a design truck, the weights and spacings of axles and wheels for the design truck are depicted in Figure 3-3. Gross weight of H30-S24 truck is 600 kN. Concentrated loads are usually combined with design lane load to develop maximum moment and shear effect along the superstructure. Similar to HL-93 truck, effective load width for a single lane can be assumed as 3000 mm. Extreme force effect is taken as the larger of the following:

i. The maximum effect of one design truck (as shown in Figure 3-4.a),

ii. The maximum effect of the design lane load combined with concentrated load (as shown in Figure 3-4.b).
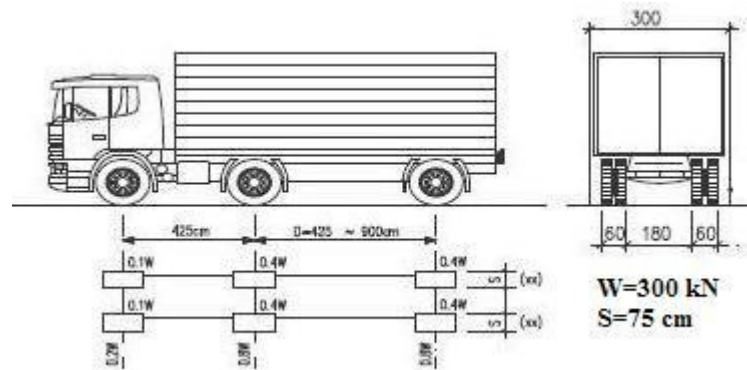
Figure 3-3 Characteristics of Design Truck, H30-S24
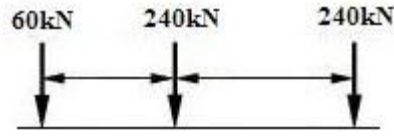
a. Only Truck Load
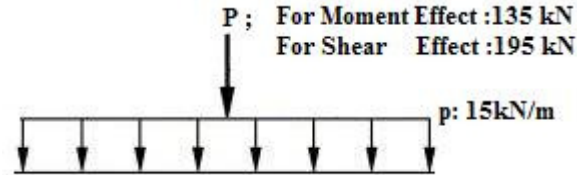
b. Lane and Concentrated Load

Figure 3-4 Design Live Load in Turkey, H30-S24 [14]

3.3.1.3 Maximum Span Moments due to HL-93 and H30-S24

The maximum mid-span moments were calculated by determining the optimum position of the truck model on the span that will develop the maximum load effect on the mid-span. Results for HL-93 and H30-S24 are tabulated and shown in Table 3-2 and Table 3-3, respectively. HL-93 will mean the load effect per maximum of truck load with lane load and tandem load, and H30-S24 will mean the load effect per maximum of only truck load and tandem with lane load, throughout this thesis. As the results indicate, tandem loads do not result in the maximum span moments. Moreover, the maximum span moment due to H30-S24 is approximately 10% higher due to HL-93. However, the difference in maximum moment decreases as the span length increases. This decrease is caused by the additional lane load with truck loading in HL-93. Figure 3-5 indicates the difference between both loadings.

Table 3-2 Maximum Span Moment due to HL-93

Span Length(m)	Truck + Lane Load	Tandem + Lane Load	Mmax (kN.m)
	M (kN.m)	M (kN.m)	
25	2375.00	2049.84	2375.00
30	3100.76	2647.53	3100.76
35	3884.09	3303.74	3884.09
40	4725.72	4017.28	4725.72

Table 3-3 Maximum Span Moment due to H30-S24

Span Length(m)	Only Truck Loading	Tandem + Lane Load	Mmax (kN.m)
	M (kN.m)	M (kN.m)	
25	2748.30	2015.63	2748.30
30	3421.50	2700.00	3421.50
35	4095.21	3478.13	4095.21
40	4769.25	4350.00	4769.25
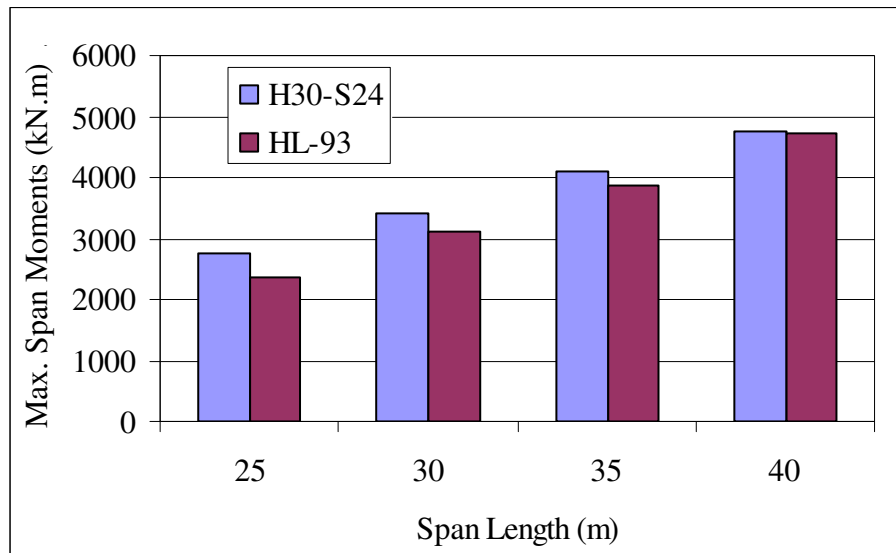
Figure 3-5 Comparison of Maximum Span Moments due to HL93 and H30S24

Corresponding to Different Span Length

27

3.3.2 Evaluation of Truck Survey Data

The truck survey data was gathered from the Turkish General Directorate of Highways to evaluate the statistical parameters of live load in Turkey. This survey data was examined and the suspicious measurements (i.e. measurements with possible errors) were deleted to carry out more accurate statistical analysis. The maximum span moments due to surveyed trucks were calculated in this chapter.

3.3.2.1 Truck Survey Data

In Turkey, truck-survey programs have been carried out by the General Directorate of Highways. Division of Transportation and Cost Studies under the Department of Strategy Development is responsible for carrying out site measurements and collecting data. Site measurements are done at any selected station of highways throughout the year. These measurements are referred to as "Axle Weight Studies". Every year, this study is conducted at over 40 stations and covers a total of nearly 15000 vehicles.

Department of Strategy Development works on this data and on other transportation surveys to produce statistical information about the highways of Turkey. Results of these surveys assist the experts in making decisions about the future of highways and planning and managing the facilities. After the evaluation of data obtained from the traffic survey, reports are published every year.

Axle Weight Studies are carried out on highways. The officials locate a selected station on the highways. They control the vehicles by stopping them randomly. It is similar to traffic police controls. Not only the heavy trucks but also the buses, vans, empty trucks, trailers are stopped, and measurements are

taken. Name and kilometers of location, weight of each axle, type of truck axle, type and model of vehicles are recorded during these site studies.

In order to examine the statistical parameters of live load on bridges in Turkey, Axle Weight Studies were carried out by the Division of Transportation and Cost Studies. A survey on trucks provides data belonging to years 1997-2006, and a part of this data is presented in Table 3-4.

Notations are used to classify the vehicles according to axle types. A list of notations used in this survey is presented in Table 3-5. In this table, 15 different notations are shown. The notation which is in parentheses has the same axle configuration with the other, but has different tire numbers. One of the example notations is illustrated in Figure 3-6. Each number indicates the axles. That is, "1" indicates that there is one tire on each side, and "2" indicates that there are two tires on each side. A point in notation is used for dividing front axles from back axles. The numbers that are to the left of the point are the front axles of vehicle, and followings are the back axles. The types of vehicles are noted at the truck survey. These types are shown in Table 3-6.

Table 3-4 Partial Sample Data for Axle Weight Measurements (BABAESKİ-
LÜLEBURGAZ Direction) [24]

SNO	YON	TCIN	NETAG	ISHAD	TMAR	TTIP	TMOD	YCIN	GELY	GITY	KM	DTIP	D1	D2	D3	D4	D5	D6
1	1	2	8890	16110	MERCEDES	2523	04	1	39	59	93	1.22	2.30	4.20	0.00	0.00	0.00	0.00
2	1	1	6025	33	MITSUBISHI	POWERS	06	30	39	59	120	1.2	0.00	0.00	0.00	0.00	0.00	0.00
3	1	2	3900	4600	IVECO	80-12	01	5	39	39	23	1.2	1.70	3.60	0.00	0.00	0.00	0.00
4	1	2	11000	22000	BMC	PRO822	00	2	39	6	618	11.22	2.80	4.10	6.90	4.90	0.00	0.00
5	1	2	5100	6540	MAN	12.163	04	6	39	59	93	1.22	1.40	1.60	1.50	0.00	0.00	0.00
6	1	2	3140	219	ISUZU	NKR 66	05	6	22	59	139	1.2	0.90	2.10	0.00	0.00	0.00	0.00
7	1	2	8120	17380	FORD	2520	97	1	59	39	123	1.22	1.40	2.00	1.10	0.00	0.00	0.00
8	1	2	3110	390	ISUZU	NKR 66	99	6	22	39	84	1.2	1.10	1.90	0.00	0.00	0.00	0.00
9	1	2	4027	3673	MITSUBISHI	659	04	9	39	39	23	1.2	1.50	1.90	0.00	0.00	0.00	0.00
10	1	1	5920	27	OTOKAR	N 145	06	10	39	59	120	1.2	0.00	0.00	0.00	0.00	0.00	0.00
11	1	1	6551	31	ISUZU	TURKUAZ	05	2	22	59	181	1.2	0.00	0.00	0.00	0.00	0.00	0.00
12	1	2	1730	1150	KIA	K 2500	04	4	39	39	62	1.2	0.60	0.90	0.00	0.00	0.00	0.00
13	1	3	14200	28050	MAN	19-422	99	1	39	39	23	1.2+222	2.90	2.80	0.00	2.60	1.90	0.00
14	1	2	7950	17550	FORD	2520	92	1	22	39	71	1.22	1.70	1.70	1.40	0.00	0.00	0.00
15	1	2	9510	16490	FARGO	26-200	95	6	39	34	181	1.22	3.00	6.10	5.00	0.00	0.00	0.00
16	1	2	4110	2890	MITSUBISHI	FE 449	92	6	39	34	209	1.2	1.10	1.80	0.00	0.00	0.00	0.00
17	1	1	13700	46	MITSIBUSHI	MS 827	01	22	22	34	236	1.2	0.00	0.00	0.00	0.00	0.00	0.00
18	1	3	14400	24600	MERCEDES	1840	05	1	39	59	93	1.2+111	2.80	2.80	0.00	1.90	1.80	0.00
19	1	2	10050	21950	FORD	3227	05	1	39	59	120	11.22	1.30	1.30	3.30	0.00	0.00	0.00
20	1	2	3627	3878	ISUZU	NPR 66	00	9	39	39	23	1.2	1.50	4.20	0.00	0.00	0.00	0.00
21	1	2	8577	16423	MERCEDES	2523	04	1	39	59	93	1.22	2.50	2.60	1.70	0.00	0.00	0.00
22	1	1	13570	46	MERCEDES	0403	03	26	39	34	209	1.2	0.00	0.00	0.00	0.00	0.00	0.00
23	1	2	3627	3873	ISUZU	NPR 66	00	9	39	39	23	1.2	1.40	4.40	0.00	0.00	0.00	0.00
24	1	2	8538	16462	MERCEDES	2521	94	9	22	41	328	1.22	2.70	3.50	3.40	0.00	0.00	0.00
25	1	2	7586	17414	FORD	2517	90	6	39	34	181	1.22	2.70	6.00	4.50	0.00	0.00	0.00
26	1	2	2250	950	IVECO	35-9	01	9	39	34	181	1.2	1.20	1.40	0.00	0.00	0.00	0.00
27	1	2	2125	1378	IVECO	35-10	01	9	39	39	62	1.2	0.90	1.40	0.00	0.00	0.00	0.00
28	1	1	6490	27	OTOKAR	N 145-S	04	14	39	59	93	1.2	0.00	0.00	0.00	0.00	0.00	0.00
29	1	2	8640	16360	BMC	200-26	02	1	59	59	96	1.22	1.70	3.40	0.00	0.00	0.00	0.00
30	1	2	12850	19000	BMC	PRO 827	03	2	59	39	89	11.22	4.20	2.70	7.70	5.30	0.00	0.00
31	1	2	10800	21200	FARGO	32-26	04	4	39	39	62	11.22	3.60	5.00	9.10	7.00	0.00	0.00
32	1	2	8400	16600	BMC	200-264	98	9	59	39	89	1.22	2.60	3.40	1.90	0.00	0.00	0.00
33	1	2	8040	16949	FORD	2520	03	1	39	59	120	1.22	1.70	3.40	0.00	0.00	0.00	0.00
34	1	2	13250	12235	IVECO	330-30	96	4	39	39	23	1.22	3.10	3.20	3.00	0.00	0.00	0.00
35	1	2	12110	13900	IVECO	330-30	93	4	39	39	23	1.22	3.60	5.70	5.30	0.00	0.00	0.00
36	1	3	14700	32600	MERCEDES	1840	05	1	39	39	23	1.2+111	2.80	2.90	0.00	2.00	1.60	0.00
37	1	2	13250	12235	IVECO	330-30	95	4	39	39	23	1.22	2.50	2.80	2.90	0.00	0.00	0.00
38	1	2	10000	15000	MERCEDES	2500	98	4	39	39	93	1.22	3.90	7.90	6.10	0.00	0.00	0.00
39	1	2	10150	21700	MERCEDES	3228	05	1	39	59	71	11.22	2.10	0.00	3.70	0.00	0.00	0.00
40	1	2	1225	4775	MITSUBISHI	AE 449	97	1	39	39	23	1.2	2.10	1.80	1.80	0.00	0.00	0.00
41	1	2	9000	16000	FORD	2217	89	1	22	39	139	1.22	1.90	1.50	1.10	0.00	0.00	0.00
42	1	3	15100	28710	MERCEDES	1840	04	1	22	39	159	1.2+111	2.70	2.40	0.00	1.80	1.65	0.00
43	1	2	6950	14050	FORD	2014	89	4	39	39	93	1.21	2.00	7.10	2.30	0.00	0.00	0.00
44	1	2	8990	16010	BMC	PRO 620	00	1	22	39	68	1.22	2.40	2.20	1.80	0.00	0.00	0.00
45	1	2	12540	13460	MERCEDES	3028	04	4	39	39	23	1.22	3.20	5.20	5.00	0.00	0.00	0.00
46	1	2	3100	3900	MITSUBISHI	449	97	1	22	39	68	1.2	0.80	1.40	0.00	0.00	0.00	0.00
47	1	2	12010	19990	BMC	PRO 822	02	5	39	39	23	11.22	3.80	0.00	5.50	3.50	0.00	0.00
48	1	1	5600	29	OTOKAR	145,5	04	10	39	59	120	1.2	0.00	0.00	0.00	0.00	0.00	0.00
49	1	2	6900	17030	BMC FATİH	145-22	88	2	59	39	99	1.22	2.90	6.60	4.60	0.00	0.00	0.00
50	1	1	4300	23	IVECO	M 23	97	2	39	39	23	1.2	0.00	0.00	0.00	0.00	0.00	0.00
51	1	2	10500	21500	FORD	32-20	06	2	39	6	618	11.22	4.10	0.00	8.20	6.20	0.00	0.00
52	1	3	15110	25100	MERCEDES	1840	04	5	59	34	153	1.2+111	3.30	5.60	2.90	2.90	2.90	0.00
53	1	3	15050	28050	MAN	26-321	78	1	59	34	196	1.2+22	2.50	2.10	2.20	1.20	0.00	0.00
54	1	2	4160	3340	MITSUBISHI	659	98	1	39	39	23	1.2	0.90	1.30	0.00	0.00	0.00	0.00
55	1	2	1950	1250	KIA	K 2500	05	9	22	59	139	1.2	0.60	0.70	0.00	0.00	0.00	0.00
56	1	2	6800	16300	MERCEDES	1517	01	1	22	39	84	1.22	1.80	4.10	3.40	0.00	0.00	0.00
57	1	3	14100	28200	DAF	85-400	95	2	22	59	127	1.2+111	3.30	6.60	4.80	4.70	4.20	0.00
58	1	2	5525	16975	VOLVO	F 10	91	9	39	39	23	1.22	1.50	4.60	4.60	0.00	0.00	0.00
59	1	1	6025	33	MITSUBISHI	POWERP	06	20	39	59	93	1.2	0.00	0.00	0.00	0.00	0.00	0.00
60	1	1	6000	30	MERCEDES		05	28	39	59	93	1.2	0.00	0.00	0.00	0.00	0.00	0.00
61	1	2	9000	23000	SCANIA	94-GB	01	2	39	26	500	11.22	2.40	2.80	6.20	5.80	0.00	0.00
62	1	2	7490	15610	MERCEDES	15-17	04	1	39	59	120	1.22	1.30	3.20	0.00	0.00	0.00	0.00
63	1	2	10320	15180	MERCEDES	25 17	91	1	22	39	71	1.22	2.20	2.20	1.40	0.00	0.00	0.00
64	1	2	2920	580	MITSIBUSHI	639	05	5	59	59	67	1.2	1.00	1.50	0.00	0.00	0.00	0.00
65	1	2	12050	19950	FARGO	AS 32	05	4	22	39	84	11.22	3.00	3.40	5.90	4.90	0.00	0.00
66	1	2	6000	9000	MERCEDES	1517	05	9	59	39	68	1.2	1.90	2.40	0.00	0.00	0.00	0.00
67	1	2	2900	500	MERCEDES		06	1	900	34	250	1.1	0.90	1.20	0.00	0.00	0.00	0.00
68	1	2	5480	6000	FARGO	AS 32	05	1	59	39	34	11.22	1.00	1.80	0.50	0.30	0.00	0.00
69	1	2	9350	15650	DODGE	AS 950	97	4	39	39	23	1.22	1.90	2.80	2.30	0.00	0.00	0.00
70	1	2	9965	15035	MERCEDES	2523	06	1	39	59	93	1.22	2.30	2.40	1.90	0.00	0.00	0.00
71	1	2	5060	7040	ISUZU	NOR 30	04	1	22	59	139	1.21	1.20	1.30	0.50	0.00	0.00	0.00
72	1	2	2301	5399	MITSUBISHI	FE659	00	9	39	39	23	1.2	1.30	3.10	0.00	0.00	0.00	0.00
73	1	1	6551	31	ISIZU TURZ	31	04	14	22	59	139	1.2	0.00	0.00	0.00	0.00	0.00	0.00
74	1	2	2300	950	DODGE	200	97	9	39	39	23	1.1	0.90	1.30	0.00	0.00	0.00	0.00

Table 3-5 Notation of Axle Types
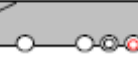
1.1		1.2+2	
1.2		1.2+21	
1.21		1.2+11 (1.2+22)	
1.22		1.22+11 (1.22+22)	
1.121 (1.122)		1.2+111	
11.21		1.2+122 (1.2+222)	
11.22		1.22+111 (1.22+222)	

1 1 . 1 2 1

↑ ↑   ↑ ↑ ↑

1st 2nd 3rd 4th 5th Axle

1 : one tire on each side

2 : two tires on each side

Figure 3-6 Example of Axle Type Notation

Table 3-6 Vehicle Type

Type No	Type Name
1	Truck
2	Truck + Trailer
3	Wrecker
4	Wrecker + Half Trailer
5	Bus

3.3.2.2 The Span Moments due to Surveyed Trucks

The last two years of measurements of a ten-year data covering axle weight measurements was used to carry out statistical evaluations. Manufacturers design more efficient vehicles using new technologies in order to better respond to the increasing demand. Vehicle configurations and load carrying capacities have changed over the years. Therefore, to reflect today's vehicle configurations, the past survey results were ignored, but only truck measurements of the years 2005 and 2006 were considered in this study.
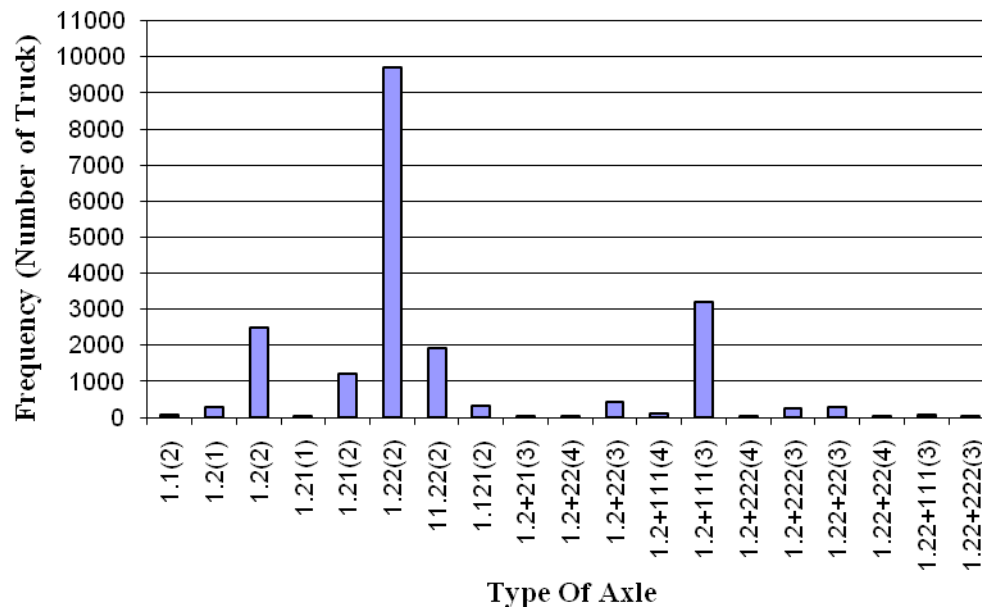
Figure 3-7 Histogram of Vehicles according to Axle Types

Data covering the two years have more than 20.000 records of vehicles. Figure 3-7 shows the variation of vehicle numbers according to the axle types. Also, note that the numbers in parenthesis denote the type of vehicle as presented in

Table 3-6. The truck having three axles, "1.22" is observed to be the most common vehicle in the survey.

In this study, only trucks were considered in evaluating the live load models. "1.1", "1.2" and "1.21" type trucks were excluded from the calculations since they have lighter weights compared to other trucks; and also the wreckers, which are denoted as 3 and 4, were excluded from the analysis. The histogram of gross vehicular weight of the trucks considered in this study is shown in Figure 3-8. The maximum and minimum gross weights are 30.48 tons and 2.9 tons, respectively. The mean of the gross weights is 11 tons.
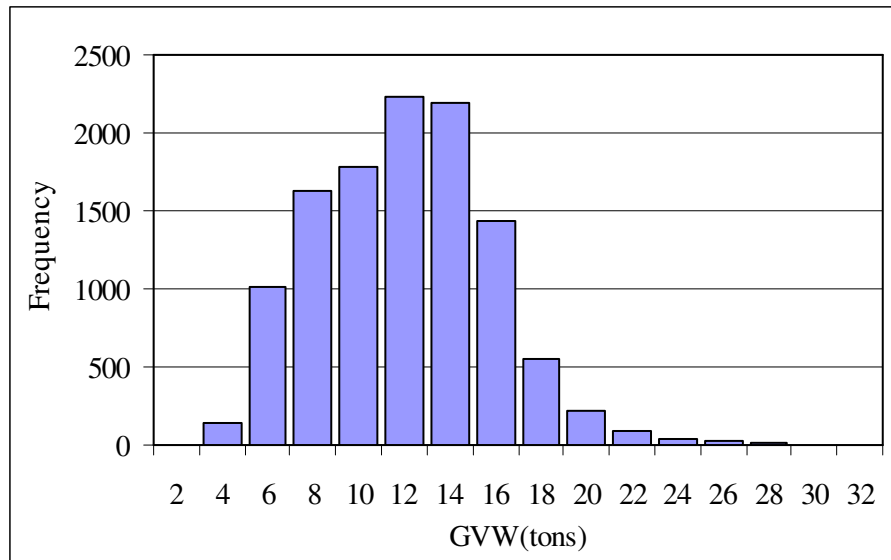
Figure 3-8 Histogram of Gross Vehicle Weights (GVW) of Surveyed Trucks

The aim in using axle weight studies is to evaluate the variation of truck loads on Turkish highways. This variation is described through span moments calculated for different span lengths. In order to calculate span moments based on truck survey data, the distances between each axle, in addition to axle weights, need to be known. Unfortunately, these distances have not been

measured in the axle weight studies. For this reason, these distances are assumed according to catalog search for each truck type. The truck catalogs of manufacturers are obtained from their web sites. The distances between axles are taken from these catalogs, and then the range of these distances is determined for each truck type as shown in Table 3-7 within parenthesis. Generally, the shortest distances from these ranges are assumed for the distances between axles for each truck type, and these distances are used for every truck of corresponding types. In some cases, the most common axle distance is taken. It should be noted that using the shortest axle distances results in high moments induced by truck passages over the spans.

Table 3-7 Assumed Truck Axle Distances

Truck Type	Distance between Each Axles (m)		
	D1-D2	D2-D3	D3-D4
1.21 and 1.22	3.80 $(3.60 \leq 5.00)$	1.35 $(1.15 \leq 1.40)$	-
11.22	1.70 $(1.70 \leq 1.95)$	2.80 $(2.80 \leq 3.40)$	-
1.121	3.80 $(3.80 \leq 5.00)$	1.35 $(1.15 \leq 1.40)$	1.35 $(1.15 \leq 1.40)$
Where, D: Axle (D1 is the front axle, D2 is the back axle)			

Axle weights of nearly 11000 trucks were used in moment calculations. For each truck, the bending moment was calculated by using assumed truck axle distances for each type (Table 3-7), and they were determined separately for the span lengths of which are 25 m, 30 m, 35 m, 40 m. The macro algorithm was developed at Excel to calculate each truck load effect. Maximum moments due to truck survey data were evaluated by moving the axle weight of each truck on simple beam model at 0.25 m increment. For each increment, the maximum moment was determined and stored. After all axles of each truck

passed through whole length of the span, the maximum moment due to this truck was calculated by taking the maximum of stored moments. Histograms of calculated surveyed tuck moment are plotted in Figure 3-9 to Figure 3-12.
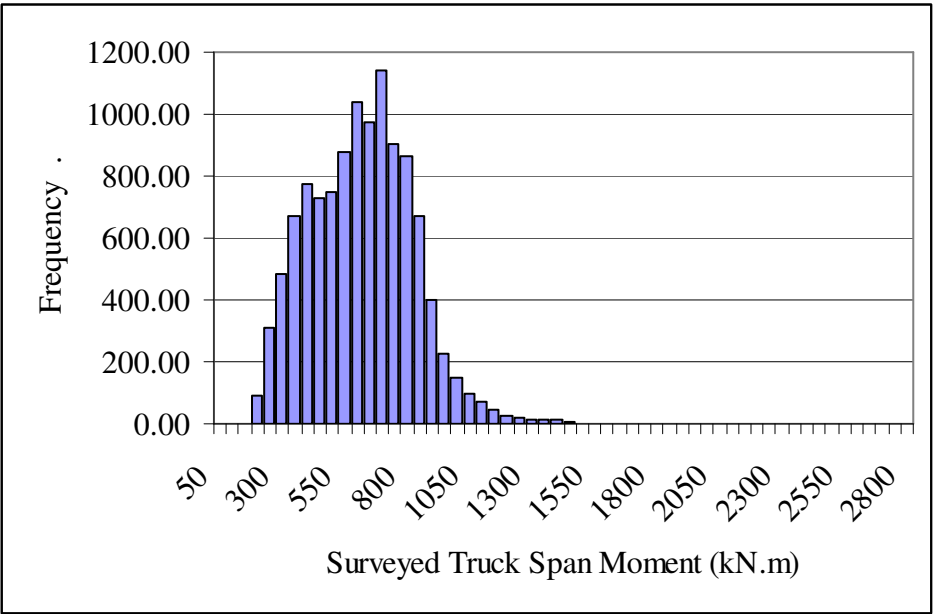
Figure 3-9 Histogram of Surveyed Truck Span Moments for 25 m Span Length
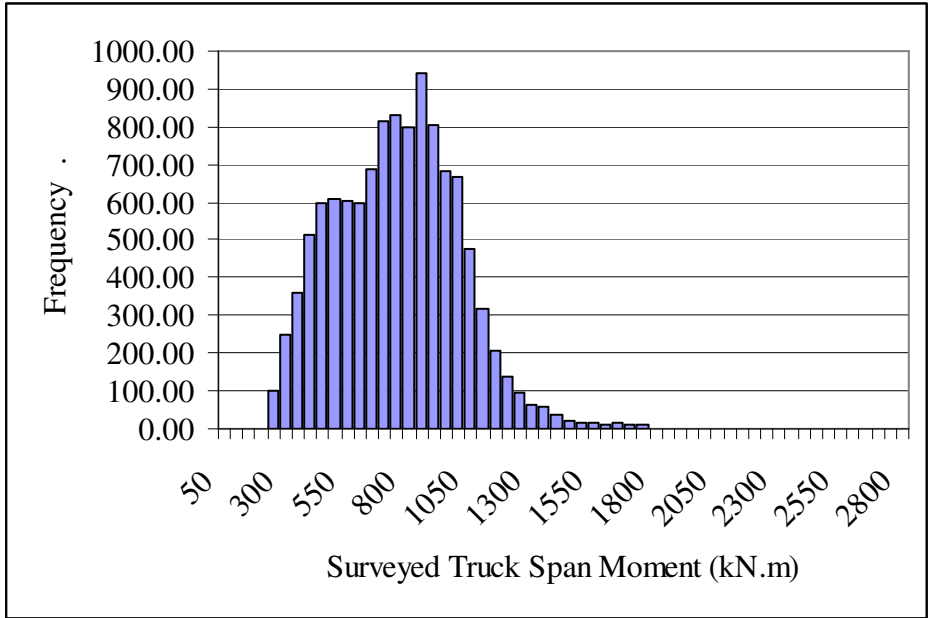
Figure 3-10 Histogram of Surveyed Truck Span Moments for 30 m Span Length

35
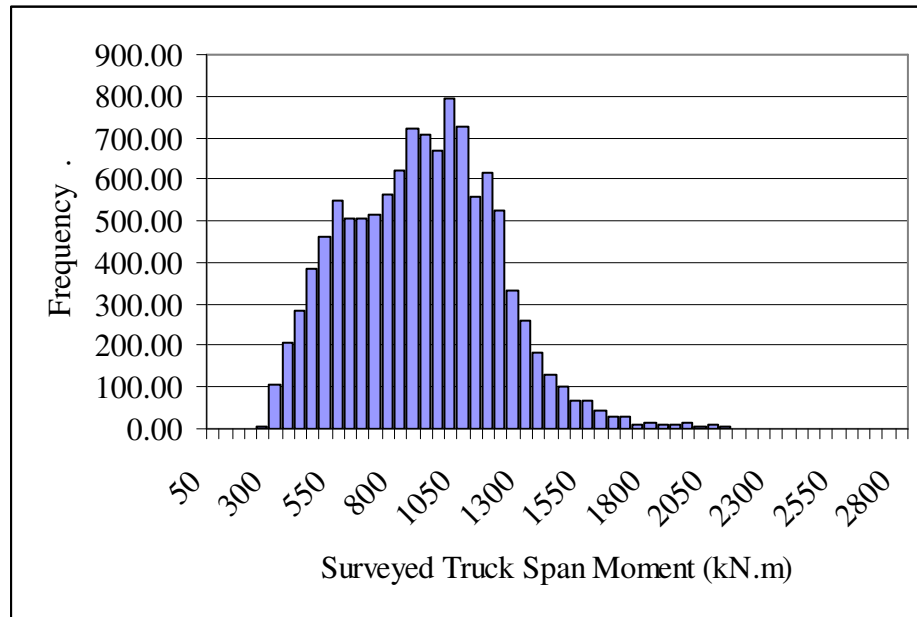
Figure 3-11 Histogram of Surveyed Truck Span Moments for 35 m Span
Length
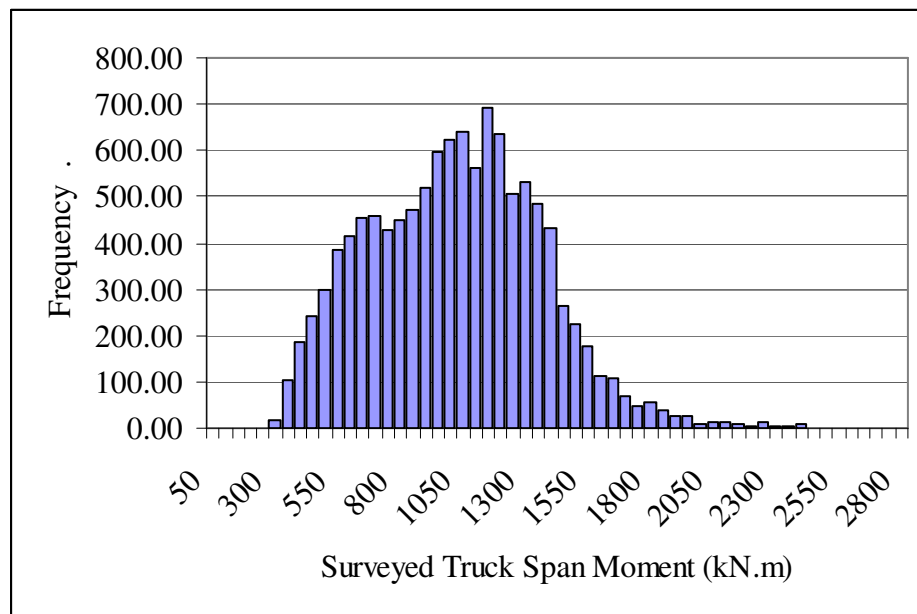
Figure 3-12 Histogram of Surveyed Truck Span Moments for 40 m Span
Length

36

3.3.2.3 Uncertainty Involved in the Truck Survey Data

Besides the inherent (aleatory) uncertainty evaluated previously, truck survey data contains some errors and lacks information that causes prediction (epistemic) uncertainties in the statistical evaluation of the data. These errors are listed as follows:

- calibration of the weight measuring devices
- typing errors while performing the truck survey
- typing errors while transferring the truck survey measurements to computer
- lack of axle distance

Some calibration errors may occur during field measurements. Calibration of weight measuring devices is a very crucial part of site measurements to determine the accurate weights.

Another type of error is the human error. While performing field measurements, the value that is read from a weight measuring device is sometimes typed on the paper incorrectly. In addition, some mistakes may be made during the coding of field measurements into a computer program. Data should be filtered from such errors to achieve more reliable statistical estimations. For this purpose, axle weight measurements are examined row by row visually to identify errors. The data considered to have typing errors are deleted.

As previously mentioned, the axle weight measurements do not include axle distances. These distances are assumed according to truck catalog searches. Using assumed axle distances instead of using actual axle distances introduces uncertainty into the span moment calculations.

Assuming shortest axle distances in moment calculations results in conservative moments. Therefore, in this study, the additional uncertainties related to the errors and assumptions previously mentioned are not taken into account.

3.3.3 Assessment of the Statistical Parameters of Live Load

Statistical parameters of surveyed trucks are evaluated using the concepts developed for extreme value theory. The main objective of this theory is to extend the available data observed in shorter periods to longer periods by extrapolation. In this study, maximum mean truck effects for longer time periods are estimated by using this theory and assumptions set for calibration of AASHTO LRFD [12].

Three different cases are evaluated to assess the statistical parameters to define the live load; these are (1) overall surveyed trucks moments, where the original truck survey data is kept except the suspicious ones (2) upper tail of cumulative distribution functions of overall surveyed truck moments and (3) extreme (maximum) surveyed truck moments. Overall surveyed truck moments are calculated by using a total of 11000 axle truck loads as explained in section 3.3.2. Cumulative distribution functions of this overall data are plotted on probability papers (Gumbel) to estimate the parameters of the probability distribution. The maximum mean moments of future time periods are determined by extrapolation of straight lines fitting to the curves. In the second case, extrapolation of only the straight lines fitting to upper tail of the curves is utilized. In the third case, statistical parameters of live load are estimated by utilizing only the extreme truck moment values that is the highest 10% values of overall surveyed truck moments. This corresponds to the values exceeding the 90-percentile value of the original data. The third case is more

representative of extreme truck loads in the data set. In the rest of this thesis we refer to these cases, respectively as *overall*, *upper tail*, and *extreme*.

3.3.3.1 Straight Lines Fitted to the CDFs of Surveyed Truck Moments

Cumulative distribution functions (CDFs) of overall surveyed truck moments are plotted on both normal and Gumbel probability papers to examine the goodness of fit of the data to these two probability distributions. After this point, the moments are expressed as the ratio of surveyed truck moments to corresponding design moments (maximum span moments are calculated according to AASHTO LRFD for each live load model; H30S24 and HL93, see Table 3-2 and Table 3-3).

Moment ratios of overall truck survey data are plotted on normal probability papers in Figure 3-13 and Figure 3-14 for H30S24 and HL93 loadings. The vertical scale in these figures is the inverse of the standard normal distribution function (ϕ), ISDN, denoted by z;

$$z = \phi^{-1}[F(M)] \tag{3-3}$$

where, M is the span moment, F(M) is the cumulative distribution function of the span moment, ϕ^{-1} is the inverse standard normal distribution function. The horizontal scale shows the moment ratio. The maximum moment ratio can also be read from the plots. Maximum values on the vertical scale shows the maximum moments for the corresponding span lengths. For all spans, maximum moment ratios are nearly 0.59 of H30S24 loading, but they vary between 0.6-0.7 for HL93 loading due to the effect of applying truck load with a lane load in HL93 loading.

The plots of truck survey data on normal probability paper are shown separately in Figure 3-15 to Figure 3-22 for each considered spans and live load models. As seen from these plots, the data does not show a good fit to the straight line, indicating that the distribution of span moments do not completely fit to the normal distribution. For this reason, moment ratios are plotted also on the Gumbel probability paper to check the validity of this probability distribution.

Gumbel probability paper is the standard starting point when limit distribution of data is not known. Another reason is that Gumbel probability paper has been used to analyze the extreme value problems in many practical cases. In Gumbel probability paper, vertical scale is the reduced variate, η, defined as [15]

$$\eta = -\ln[-\ln[F(M)]] \qquad (3\text{-}4)$$

where M is span moment, F(M) is the cumulative distribution function of moment ratios. Horizontal scale is again the moment ratio.

The moment ratios obtained from overall surveyed truck data are plotted on Gumbel probability paper, and the straight lines are fitted to resulting data points. These plots are shown in Figure 3-15 to Figure 3-22. As the plots indicate, plotted data on Gumbel paper fall on a nearly straight line in comparison with the plotted data on normal probability paper. Consequently, surveyed truck moments can be assumed to follow the Gumbel (extreme type I) distribution.

The straight lines fitted to the upper tail of overall surveyed truck moment ratios are presented in Figure 3-23 to Figure 3-26. The upper tails of CDFs are determined by assuming that it is %10 of highest moment ratios. Finally, the straight lines fitted to the extreme surveyed truck moment ratios are shown in

Figure 3-27 to Figure 3-30. For these two cases, the moment ratios are only plotted on Gumbel probability paper. The equations of straight lines are displayed on plots which are required for extrapolation to longer time periods. It is to be noted that the vertical axis is the reduced variate and there is one to one correspondence between the reduced variate and the cumulative distribution function (Eq. 3-4). Therefore, the extrapolation is actually carried out on CDF's.
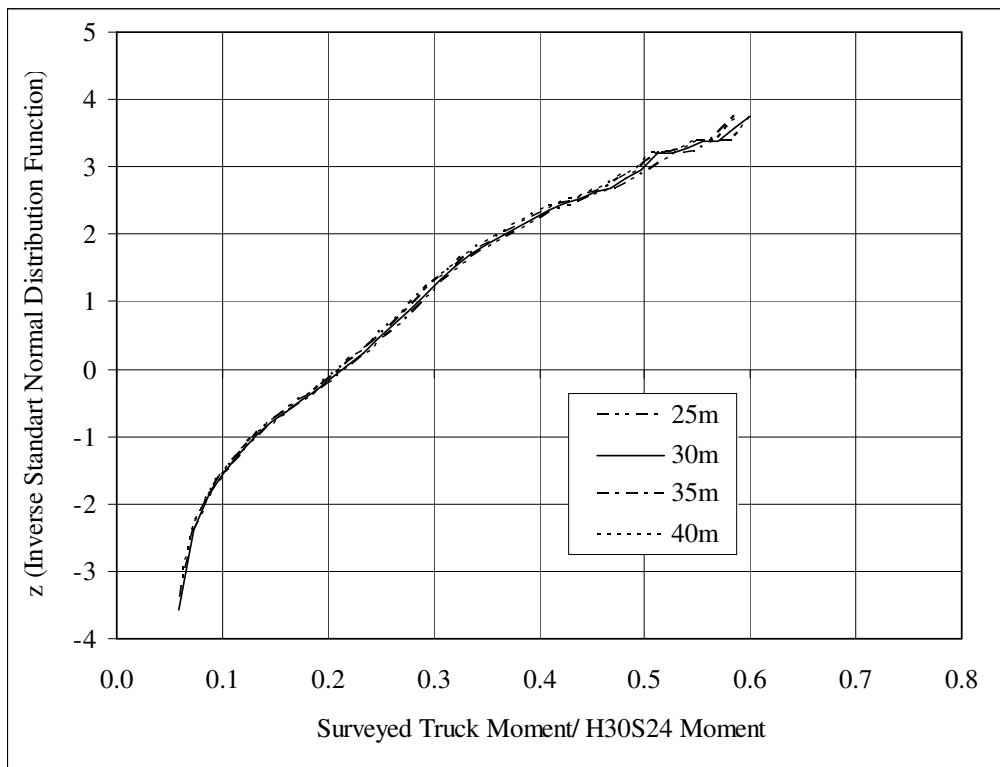
Figure 3-13 Plot of Moment Ratios Computed Based on Overall Truck Survey Data on Normal Probability Paper (H30S24)
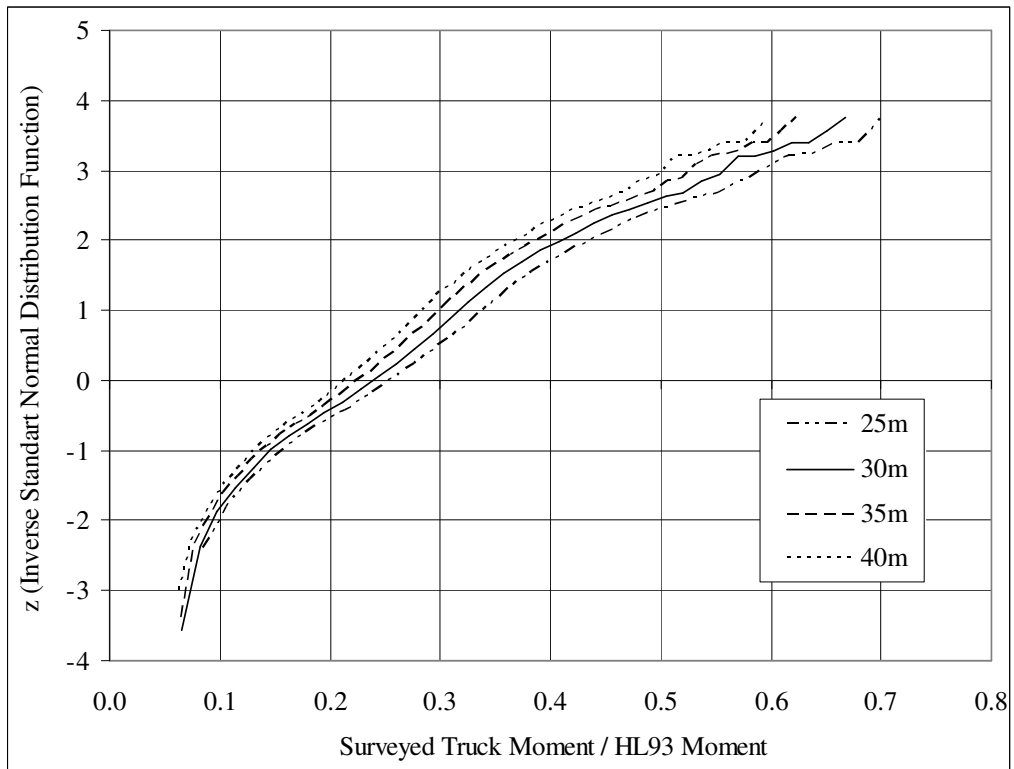
Figure 3-14 Plot of Moment Ratios Computed Based on Overall Truck Survey
Data on Normal Probability Paper (HL93)
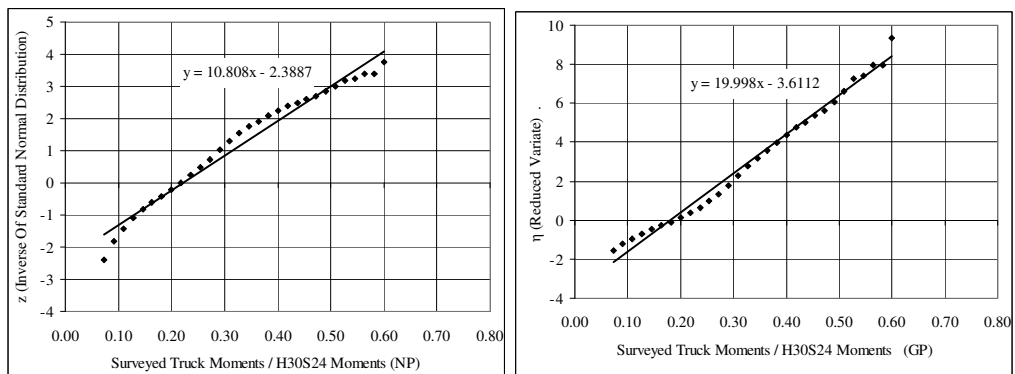
Figure 3-15 Straight Lines Fitted to Overall Moment Ratios on Normal (NP)
and Gumbel (GP) Probability Papers (H30S24-25 m span)
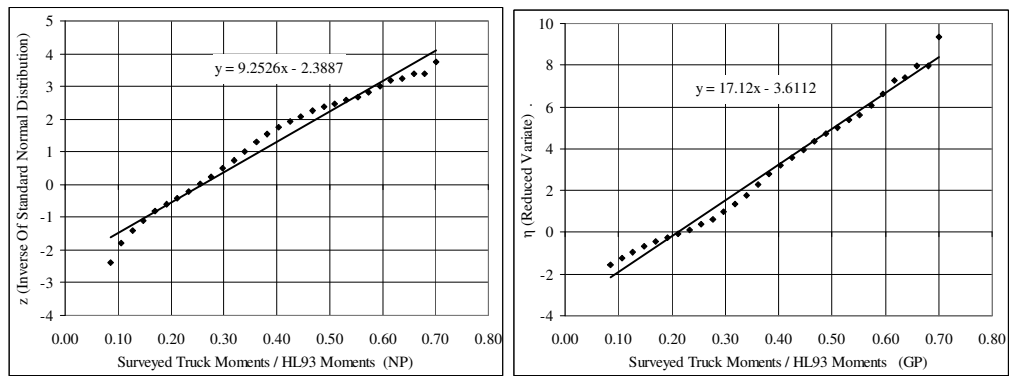
Figure 3-16 Straight Lines Fitted to Overall Moment Ratios on Normal (NP)
and Gumbel (GP) Probability Papers (HL93-25 m span)
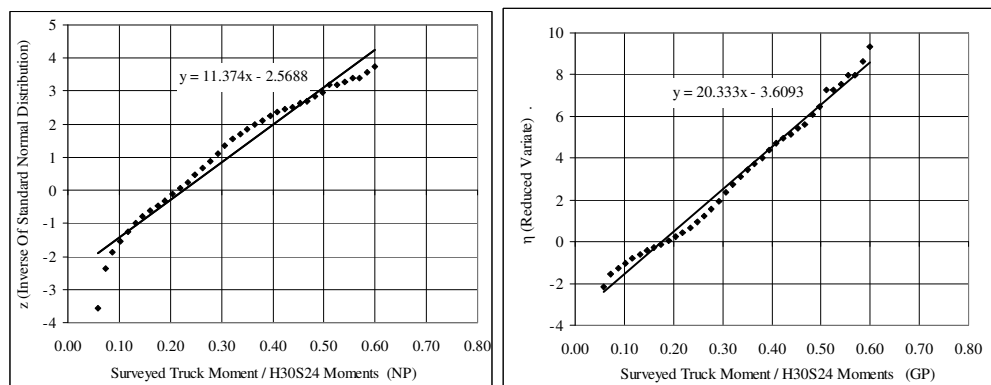
Figure 3-17 Straight Lines Fitted to Overall Moment Ratios on Normal (NP)
and Gumbel (GP) Probability Papers (H30S24-30 m span)
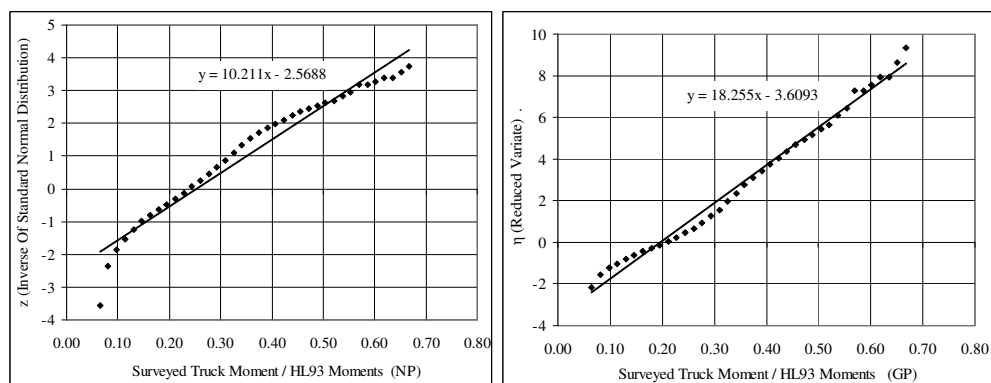
Figure 3-18 Straight Lines Fitted to Overall Moment Ratios on Normal (NP)
and Gumbel (GP) Probability Papers (HL93-30 m span)

43
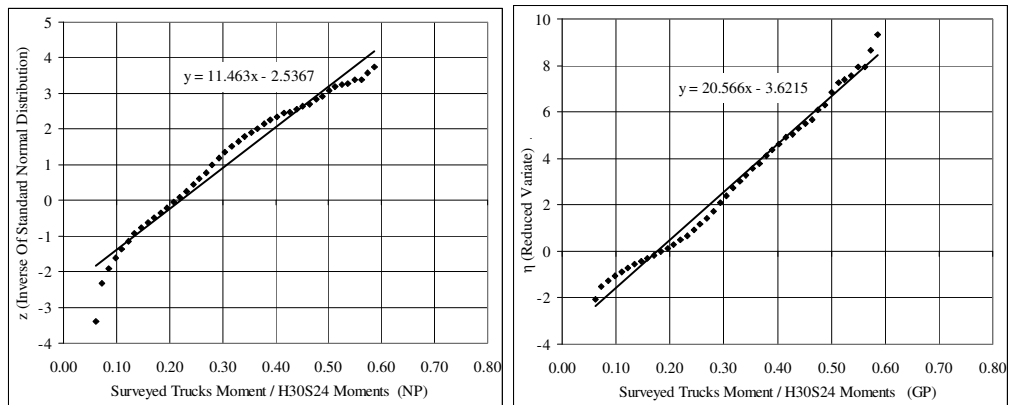
Figure 3-19 Straight Lines Fitted to Overall Moment Ratios on Normal (NP)
and Gumbel (GP) Probability Papers (H30S24-35 m span)
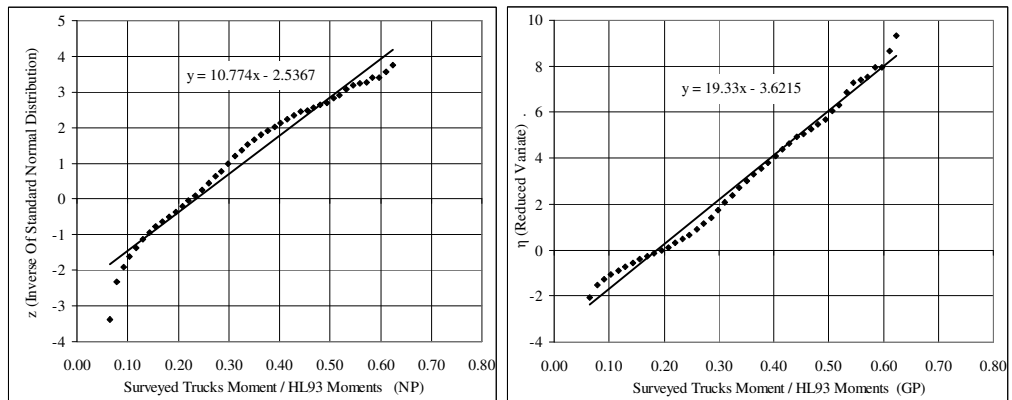
Figure 3-20 Straight Lines Fitted to Overall Moment Ratios on Normal (NP)
and Gumbel (GP) Probability Papers (HL93-35 m span)
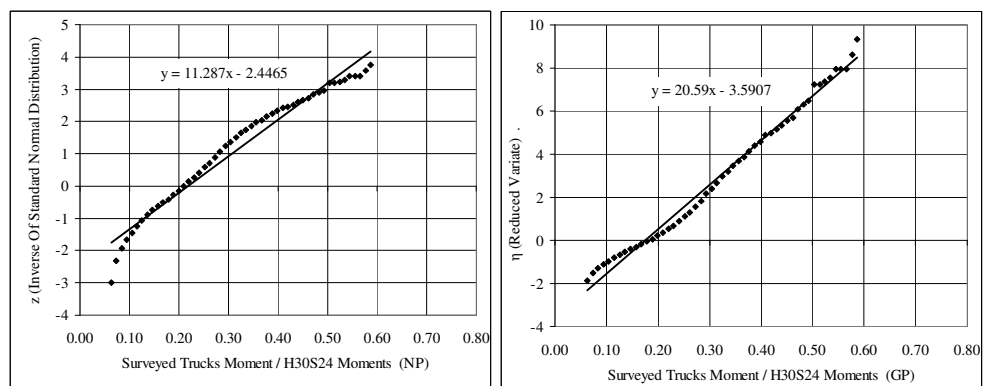
Figure 3-21 Straight Lines Fitted to Overall Moment Ratios on Normal (NP)
and Gumbel (GP) Probability Papers (H30S24-40 m span)

44
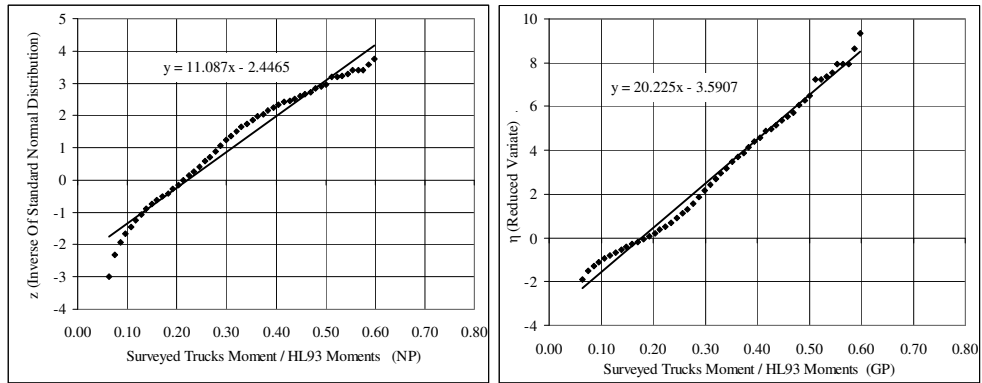
Figure 3-22 Straight Lines Fitted to Overall Moment Ratios on Normal (NP) and Gumbel (GP) Probability Papers (HL93-40 m span)
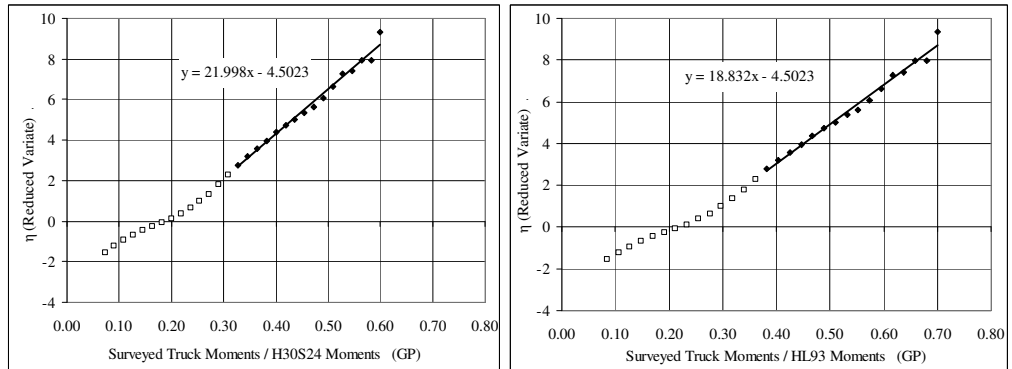
Figure 3-23 Straight Lines Fitted to the Upper Tail of Moment Ratios Plotted on Gumbel (GP) Probability Papers (25 m span)
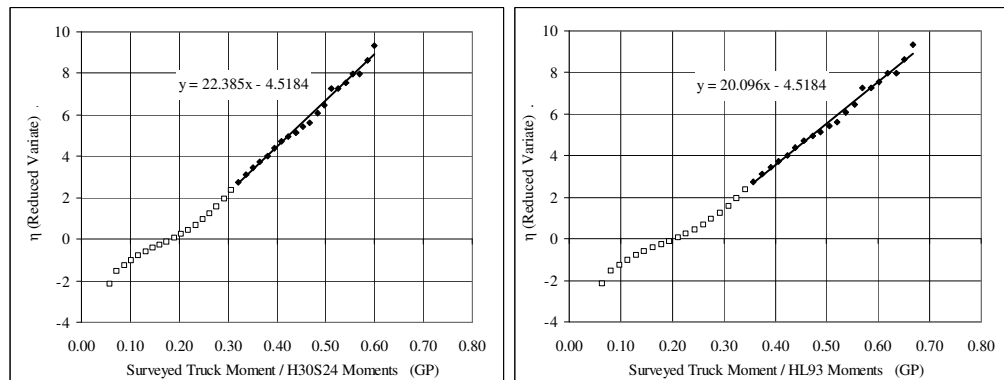
Figure 3-24 Straight Lines Fitted to the Upper Tail of Moment Ratios Plotted on Gumbel (GP) Probability Papers (30 m span)
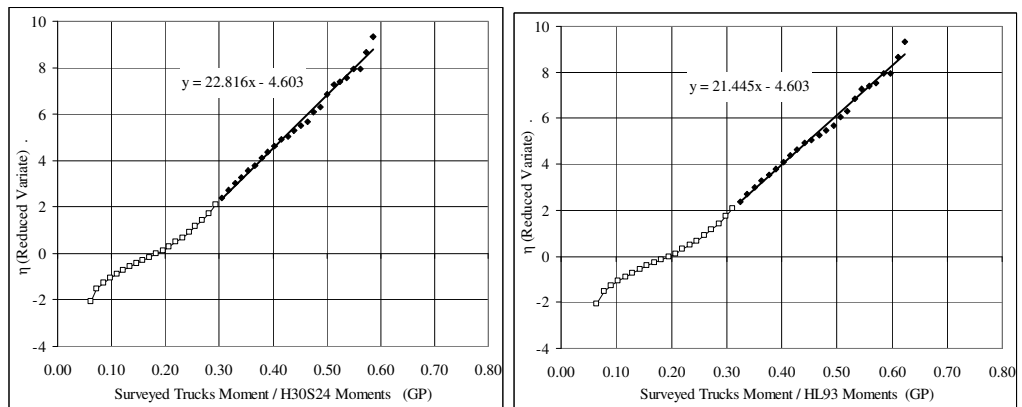
Figure 3-25 Straight Lines Fitted to the Upper Tail of Moment Ratios Plotted
on Gumbel (GP) Probability Papers (35 m span)
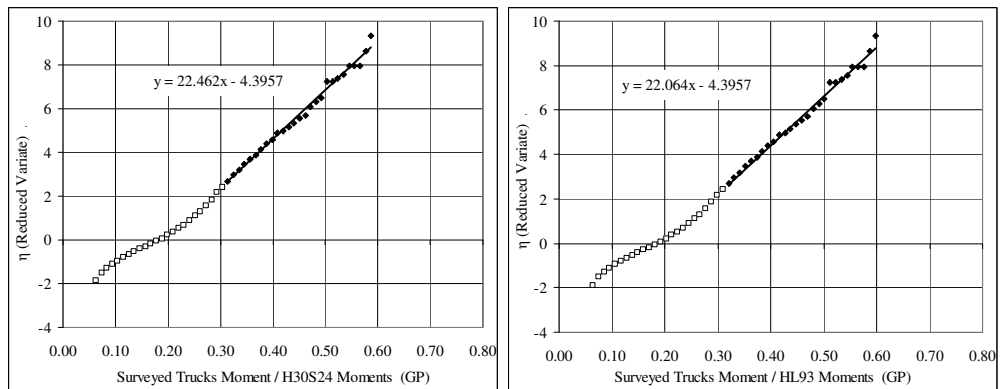
Figure 3-26 Straight Lines Fitted to the Upper Tail of Moment Ratios Plotted
on Gumbel (GP) Probability Papers (40 m span)
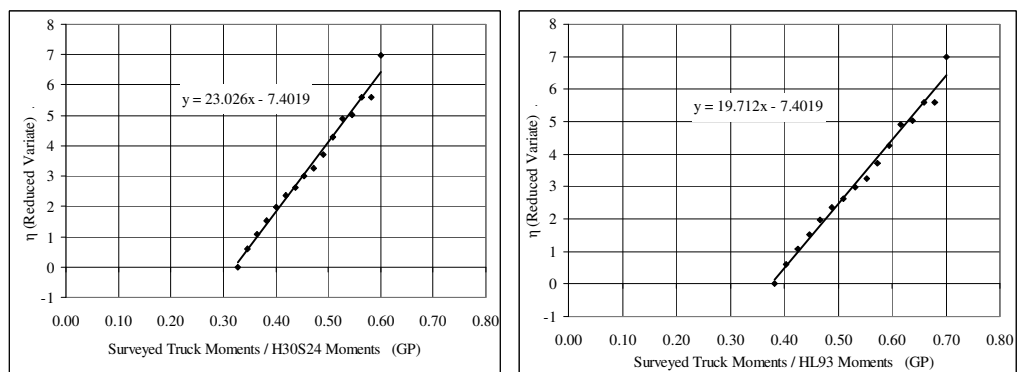
Figure 3-27 Straight Lines Fitted to Extreme Surveyed Truck Moments on
Gumbel (GP) Probability Papers (25 m span)

46
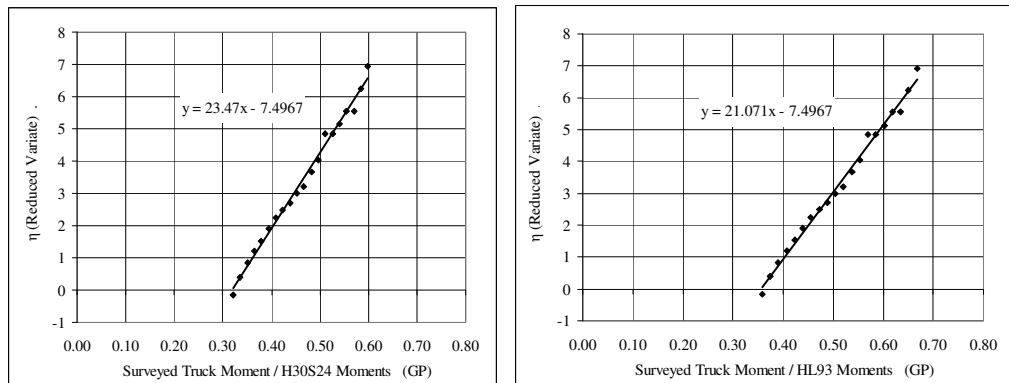
Figure 3-28 Straight Lines Fitted to Extreme Surveyed Truck Moments on
Gumbel (GP) Probability Papers (30 m span)
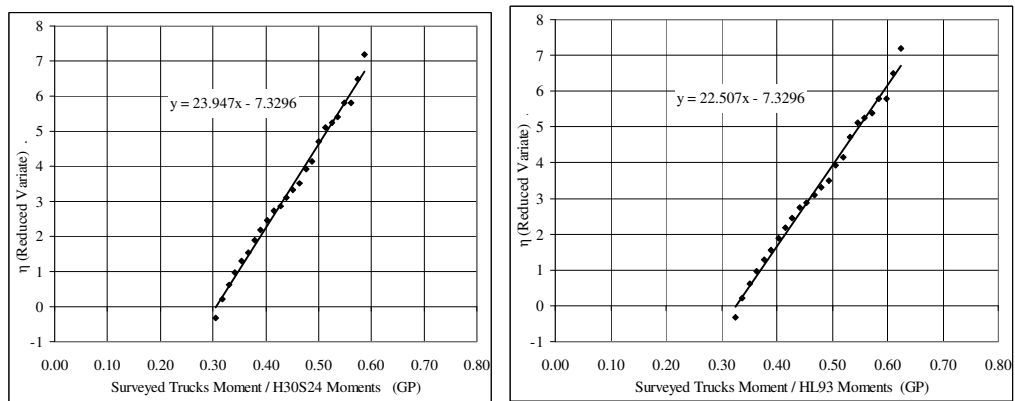
Figure 3-29 Straight Lines Fitted to Extreme Surveyed Truck Moments on
Gumbel (GP) Probability Papers (35 m span)
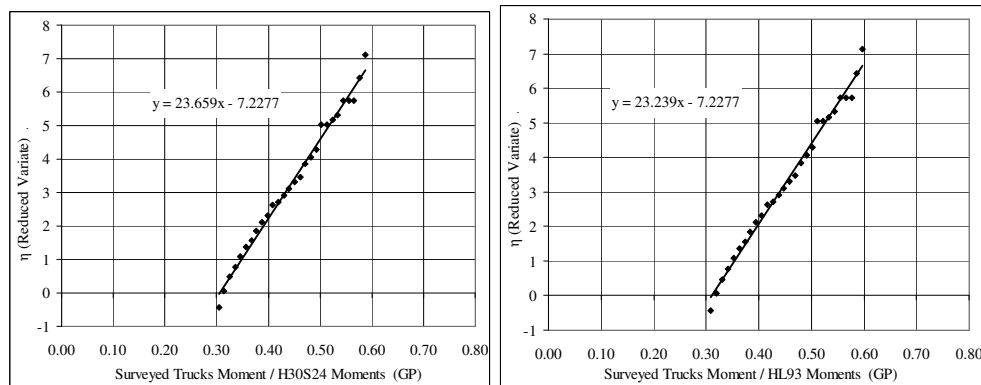
Figure 3-30 Straight Lines Fitted to Extreme Surveyed Truck Moments on
Gumbel (GP) Probability Papers (40 m span)

3.3.3.2 Mean Maximum Moments Predicted by Extrapolation

In the current AASHTO LRFD bridge design specification, the return period of maximum live load is taken as 75 years for live load equivalent to the design life of bridges, 75 years. For this reason, the expected maximum live load effect in a 75 year time period shall be determined. It is impossible to obtain future truck survey data for this time period. Thus, that is done by extrapolating the cumulative distribution functions to 75 years shown in Figures 3-15 to 3-30.

Extrapolations are carried out based on the procedure and assumptions of Nowak's study on the calibration of AASHTO LRFD [3]. It is assumed that truck survey data represents two weeks of heavy traffic on a bridge with average daily traffic of 1000 trucks. The extend of the CDFs of moment ratios shows the longer periods of time, e.g. 2 months, a year, 10 years, 50 years or 75 years. For example, there are 1950 two-week periods in 75 years. Therefore, the total number of trucks for 75 years can be calculated by multiplying the number of trucks corresponding to two-week time period, 1950, which is 1950x10000=20 million (10000 is the number of truck in two week time period). Therefore, the probability of occurrence of the heaviest truck in this population is $1/20000000 = 5 \times 10^{-8}$; this probability corresponds to z=5.33 ($\phi^{-1}[5 \cdot 10^{-8}] = 5.33$) on the vertical axis of the plots on the normal probability paper, η=16.81 ($-\ln[-\ln[5 \cdot 10^{-8}]] = 16.81$) on the vertical axis of the plots on Gumbel probability paper. It has also been observed that the change in volume of traffic computed based on this approach do not significantly change the probability parameter used in the extrapolation methods. For instance, a two times more truck traffic on bridge will result in (z=$\phi^{-1}[2.5 \cdot 10^{-8}] = 5.45$) in a 75 year time period that is only a 2% [(5.45/5.33-1)x100] increase in the probability parameter. Similar observations can also be made for the listed values of the z parameter shown in Table 3-8.

Other time periods like a month or a year can be evaluated in a similar way as explained above. The number of trucks, corresponding probabilities, inverse standard normal distribution values, and reduced variates are tabulated and shown in Table 3-8 for each time period. The number of trucks for each year in this table was taken from the calibration report of the AASHTO LRFD. As seen in this table, the number of trucks calculated in the previously explained way is rounded by Nowak [12].

Table 3-8 Number of Trucks vs. Time Period and Probability

Time Period T	Number of Trucks N	Probability 1/N	ISND z	Reduced Variate η
75 years	20,000,000	5.E-08	5.33	16.81
50 years	15,000,000	7.E-08	5.27	16.52
5 years	1,500,000	7.E-07	4.83	14.22
1 year	300,000	3.E-06	4.50	12.61
6 months	150,000	7.E-06	4.35	11.92
2 months	50,000	2.E-05	4.11	10.82
1 month	30,000	3.E-05	3.99	10.31
2 weeks	10,000	1.E-04	3.72	9.21
1 day	1,000	1.E-03	3.09	6.91

The mean maximum moment ratios corresponding to longer time periods are determined from the values listed in Table 3-8 by solving the equations of straight lines that presented in Figures 3-15 to 3-30. The calculated mean maximum moment ratios and the extrapolations are presented in the following tables and figures for all of the three cases.

Table 3-9 Mean Maximum Moment Ratios for H30-S24 (*Overall*)

Span (m)	Surveyed Truck Moment / H30-S24 Moment								
	1 day	2 weeks	1 month	2 months	6 months	1 year	5 years	50 years	75 years
25	0.53	0.64	0.70	0.72	0.78	0.81	0.89	1.01	1.02
30	0.52	0.63	0.68	0.71	0.76	0.80	0.88	0.99	1.00
35	0.51	0.62	0.68	0.70	0.76	0.79	0.87	0.98	0.99
40	0.51	0.62	0.68	0.70	0.75	0.79	0.87	0.98	0.99

Table 3-10 Mean Maximum Moment Ratios for HL-93 (*Overall*)

Span (m)	Surveyed Truck Moment / HL-93 Moment								
	1 day	2 weeks	1 month	2 months	6 months	1 year	5 years	50 years	75 years
25	0.61	0.75	0.81	0.84	0.91	0.95	1.04	1.18	1.19
30	0.58	0.70	0.76	0.79	0.85	0.89	0.98	1.10	1.12
35	0.54	0.66	0.72	0.75	0.80	0.84	0.92	1.04	1.06
40	0.52	0.63	0.69	0.71	0.77	0.80	0.88	0.99	1.01

Table 3-11 Mean Maximum Moment Ratios for H30-S24 (*Upper Tail*)

Span (m)	Surveyed Truck Moment / H30-S24 Moment								
	1 day	2 weeks	1 month	2 months	6 months	1 year	5 years	50 years	75 years
25	0.52	0.62	0.67	0.70	0.75	0.78	0.85	0.96	0.97
30	0.51	0.61	0.66	0.69	0.73	0.77	0.84	0.94	0.95
35	0.50	0.61	0.65	0.68	0.72	0.75	0.83	0.93	0.94
40	0.50	0.61	0.65	0.68	0.73	0.76	0.83	0.93	0.94

Table 3-12 Mean Maximum Moment Ratios for HL-93 (*Upper Tail*)

Span (m)	Surveyed Truck Moment / HL-93 Moment								
	1 day	2 weeks	1 month	2 months	6 months	1 year	5 years	50 years	75 years
25	0.61	0.73	0.79	0.81	0.87	0.91	0.99	1.12	1.13
30	0.57	0.68	0.74	0.76	0.82	0.85	0.93	1.05	1.06
35	0.54	0.64	0.70	0.72	0.77	0.80	0.88	0.99	1.00
40	0.51	0.62	0.67	0.69	0.74	0.77	0.84	0.95	0.96

Table 3-13 Mean Maximum Moment Ratios for H30-S24 (*Extreme*)

Span (m)	Surveyed Truck Moment / H30-S24 Moment								
	1 day	2 weeks	1 month	2 months	6 months	1 year	5 years	50 years	75 years
25	0.62	0.72	0.77	0.79	0.84	0.87	0.94	1.04	1.05
30	0.61	0.71	0.76	0.78	0.83	0.86	0.93	1.02	1.04
35	0.59	0.69	0.74	0.76	0.80	0.83	0.90	1.00	1.01
40	0.60	0.69	0.74	0.76	0.81	0.84	0.91	1.00	1.02

Table 3-14 Mean Maximum Moment Ratios for HL-93 (*Extreme*)

Span (m)	Surveyed Truck Moment / HL-93 Moment								
	1 day	2 weeks	1 month	2 months	6 months	1 year	5 years	50 years	75 years
25	0.73	0.84	0.90	0.92	0.98	1.02	1.10	1.21	1.23
30	0.68	0.79	0.85	0.87	0.92	0.95	1.03	1.14	1.15
35	0.63	0.73	0.78	0.81	0.86	0.89	0.96	1.06	1.07
40	0.61	0.71	0.75	0.78	0.82	0.85	0.92	1.02	1.03
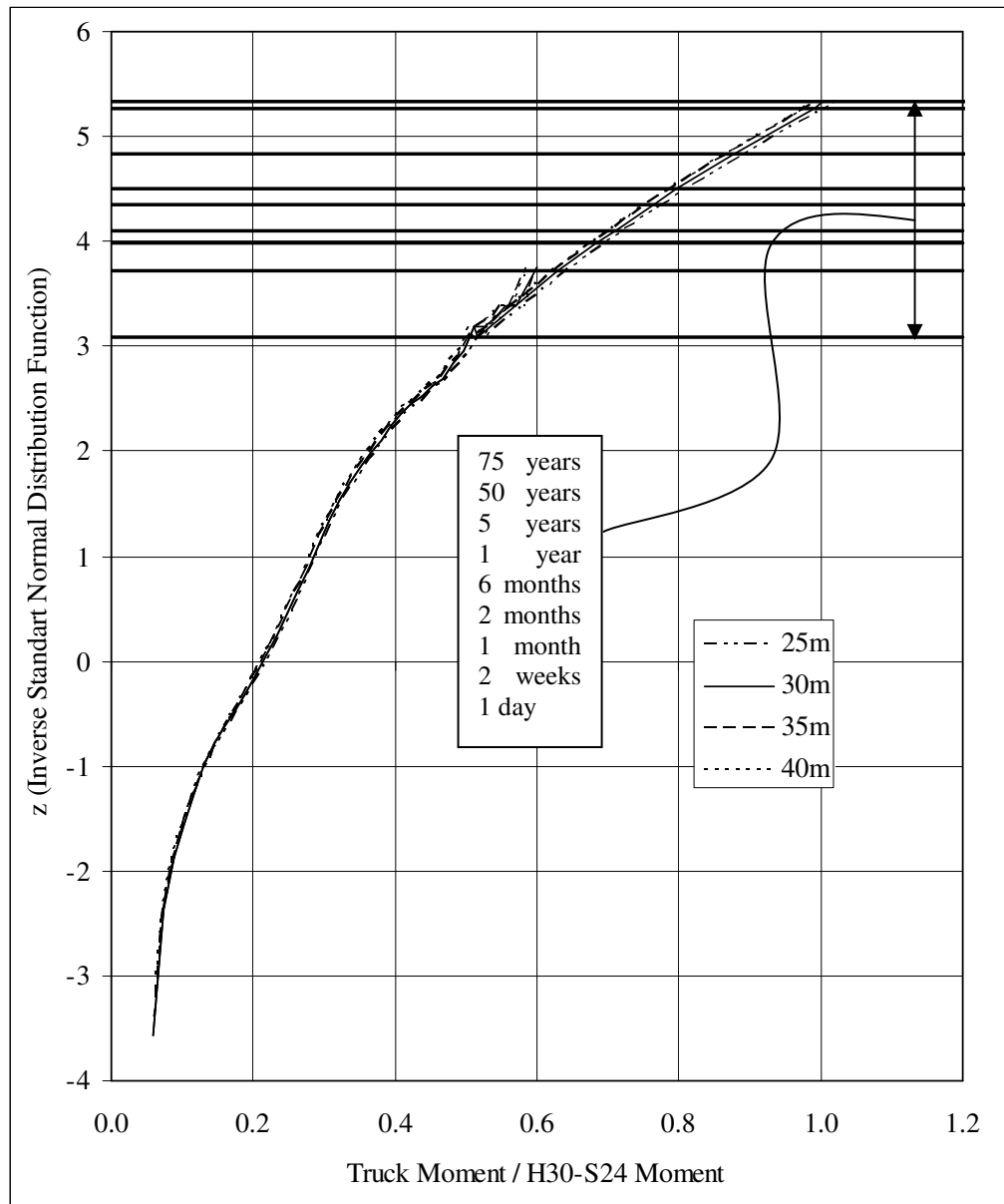
Figure 3-31 Extrapolated Moment Ratios for H30-S24 (*Overall*)
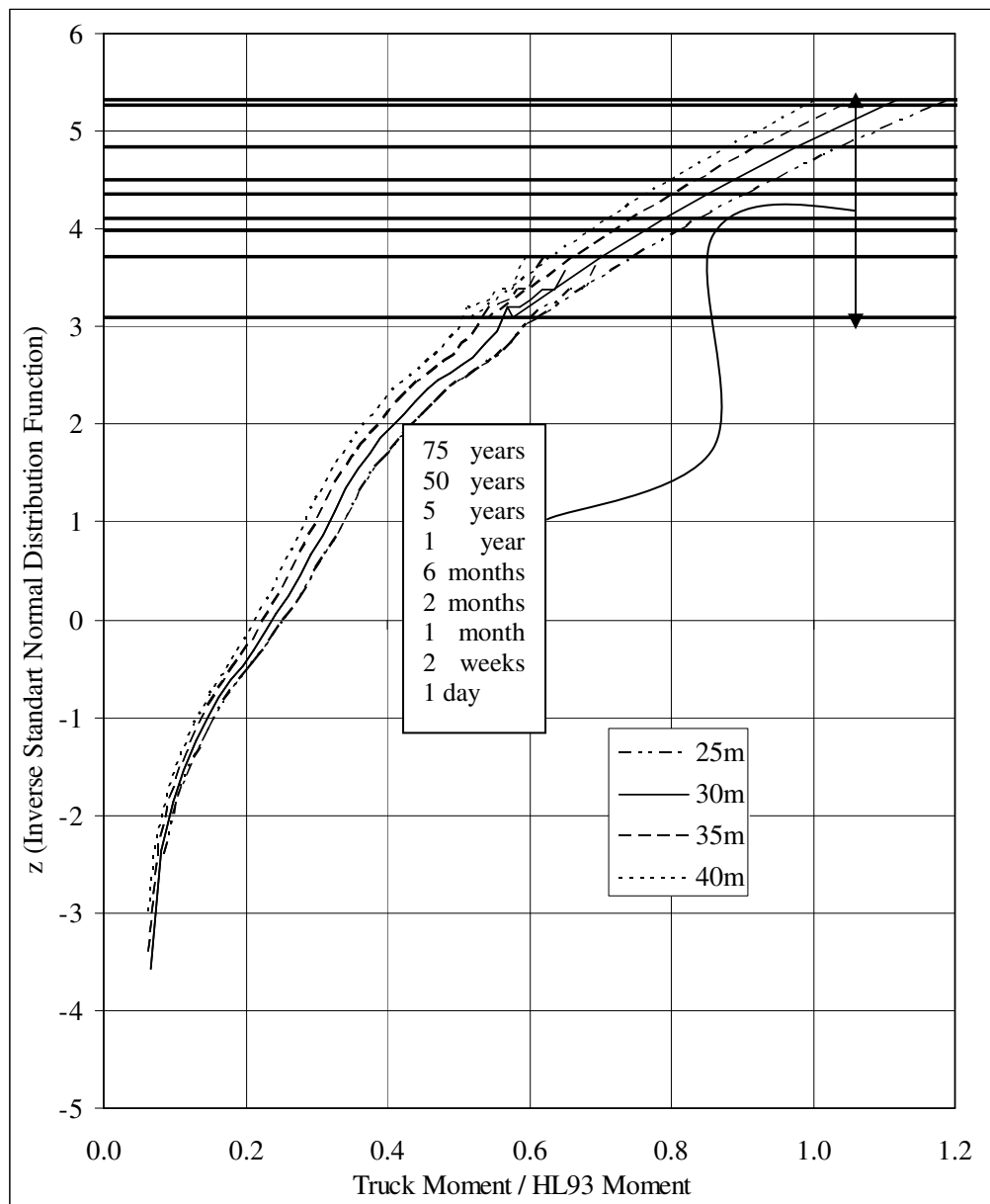
Figure 3-32 Extrapolated Moment Ratios for HL93 (*Overall*)

53
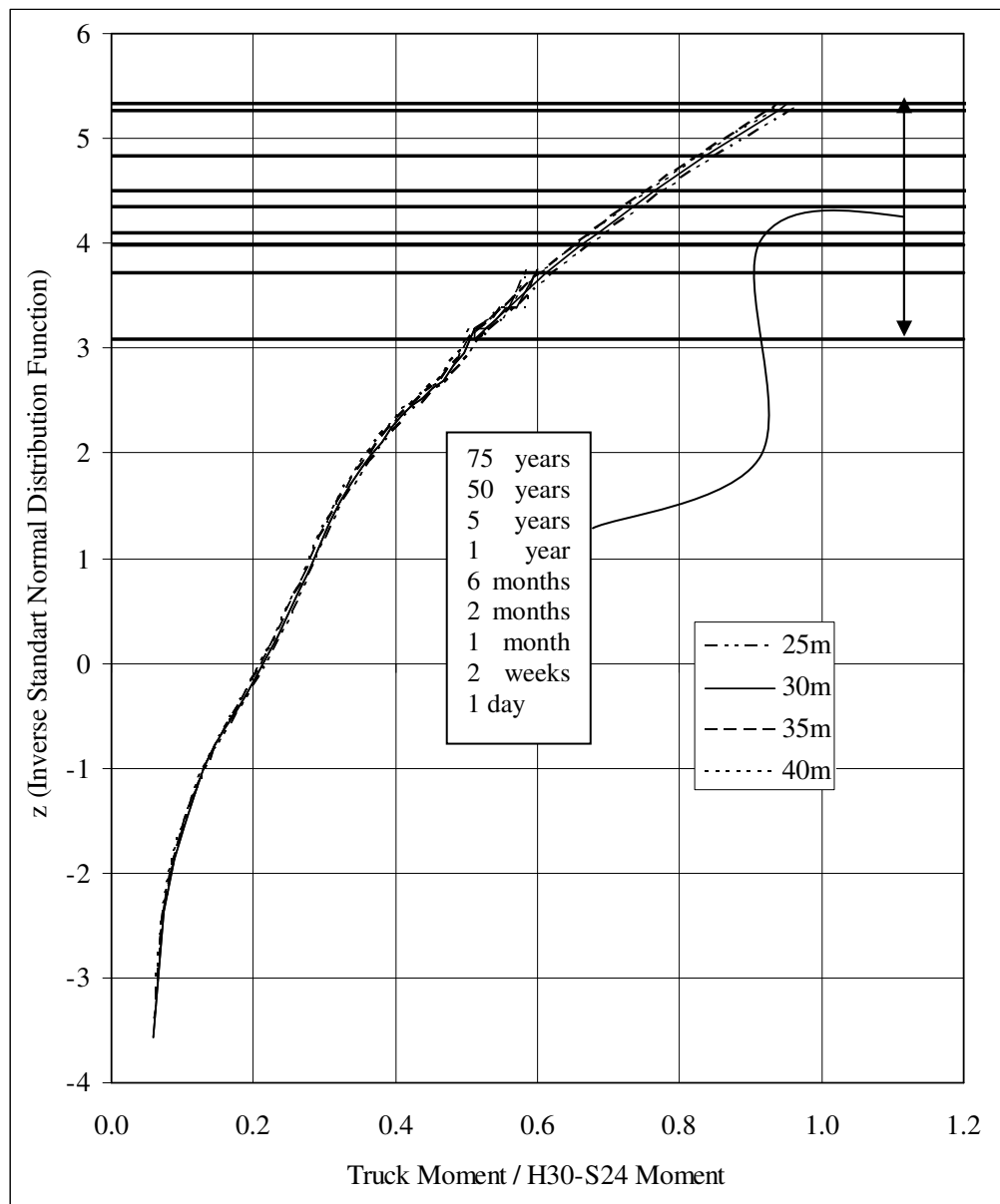
Figure 3-33 Extrapolated Moment Ratios for H30-S24 (*Upper Tail*)

54
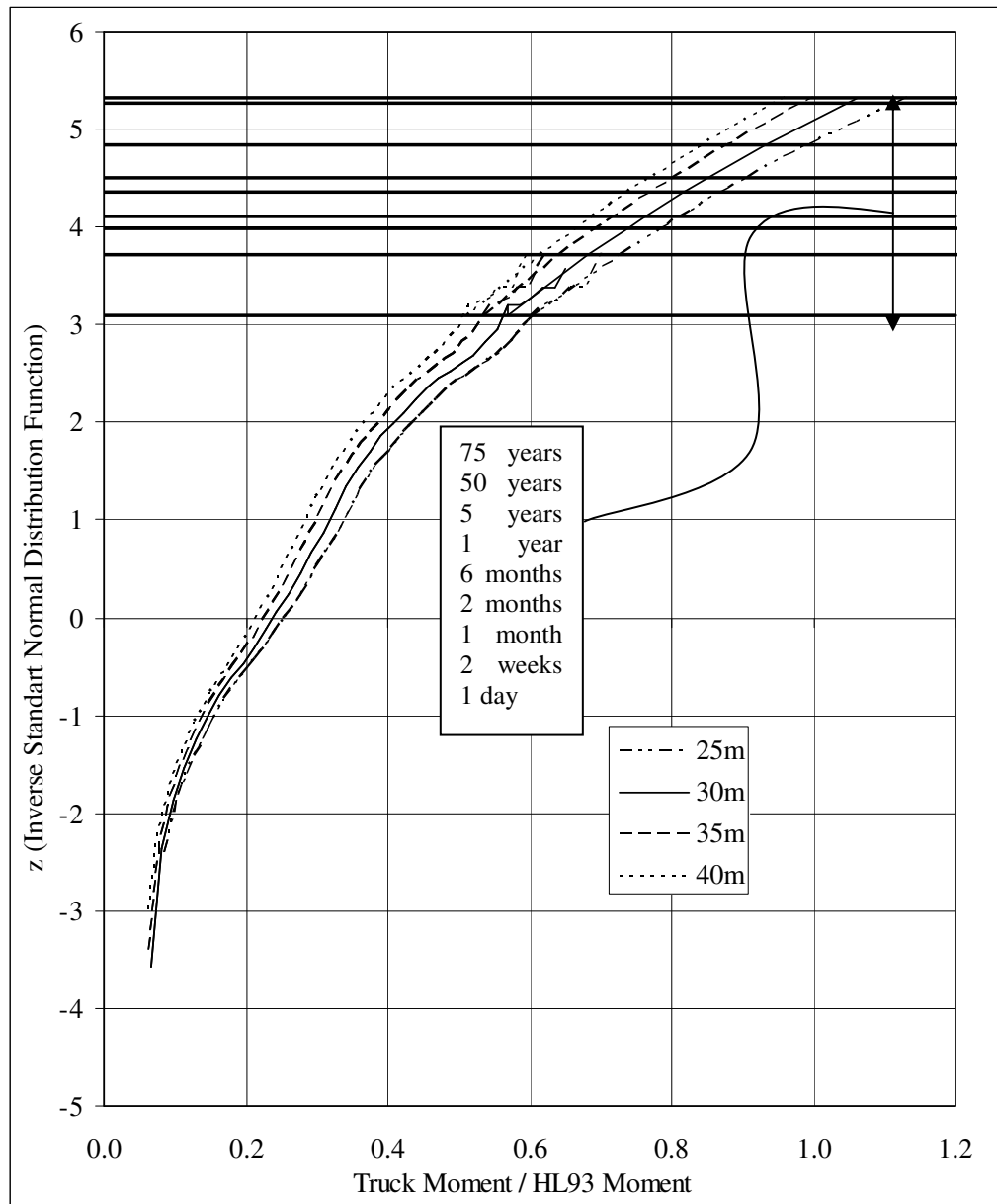
Figure 3-34 Extrapolated Moment Ratios for HL93 (*Upper Tail*)
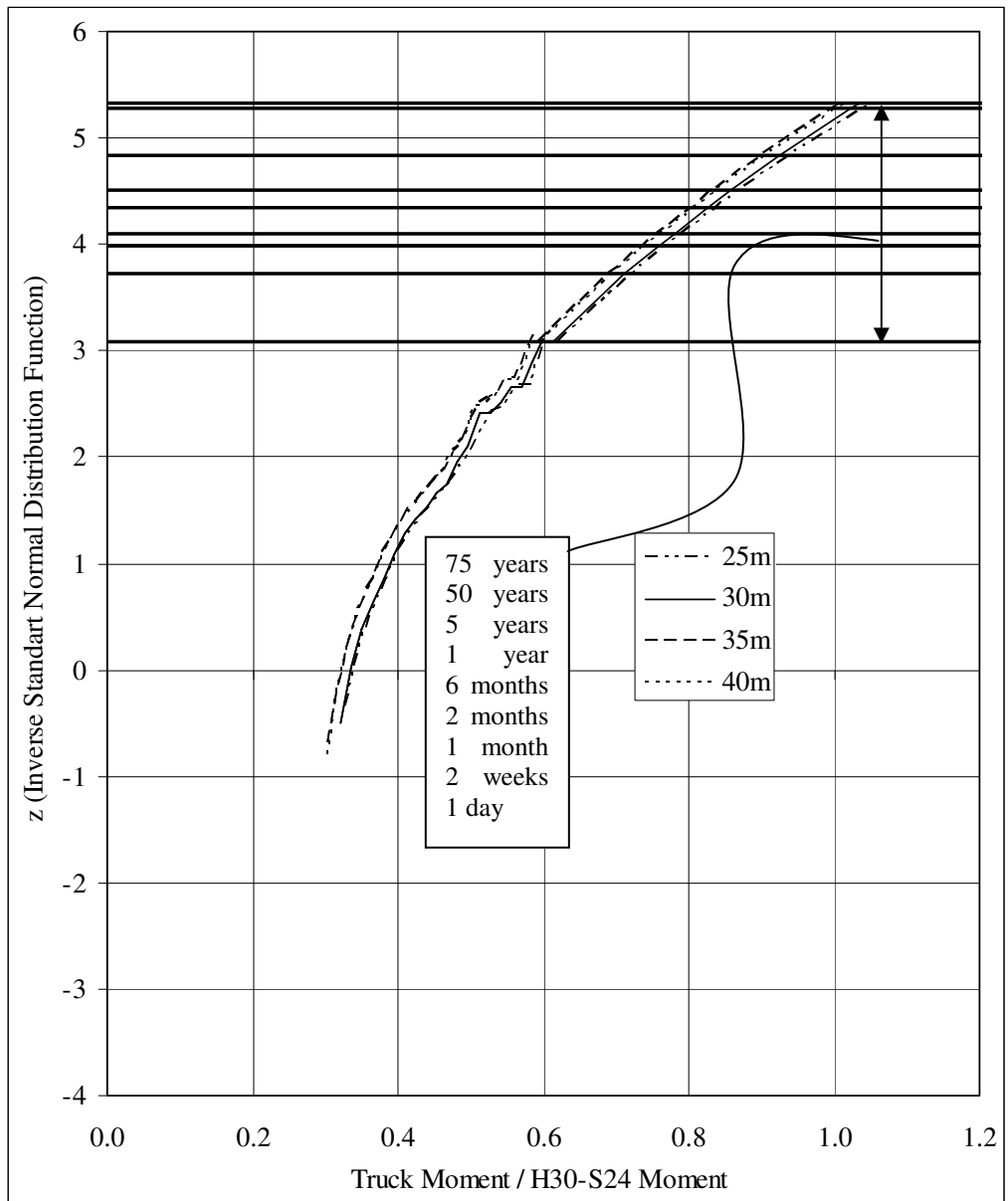
Figure 3-35 Extrapolated Moment Ratios for H30-S24 (*Extreme*)

56
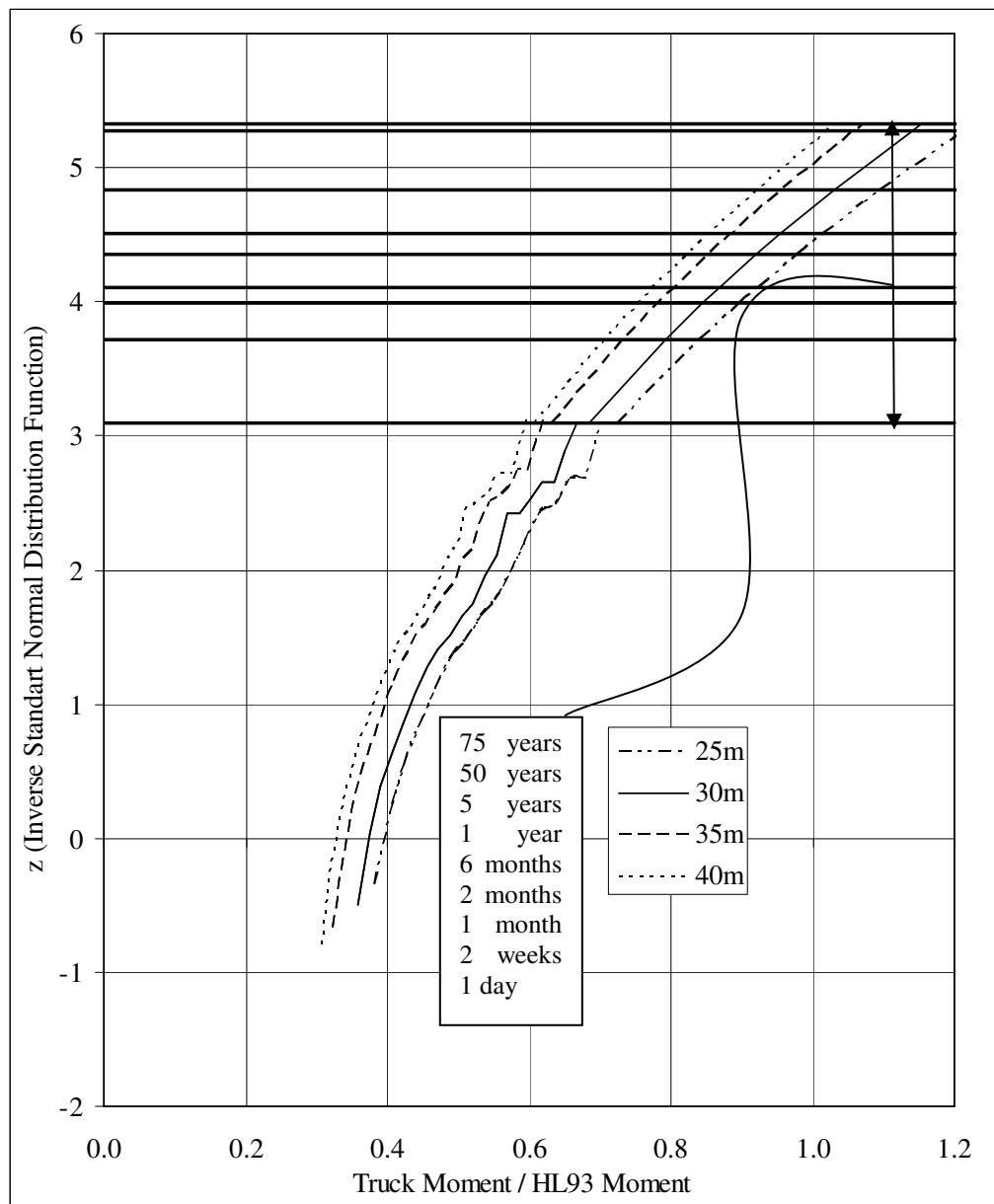
Figure 3-36 Extrapolated Moment Ratios for HL93 (*Extreme*)

3.3.3.3 Estimation of the Coefficient of Variation

The coefficients of variation for each of the three cases are calculated based on the data and by fitting straight lines to the data points plotted on Gumbel probability paper. Firstly, according to the basic statistical concepts, the coefficients of variation were estimated by using all calculated surveyed truck moment ratios by the following expressions:

$$\mu = \frac{\sum Mi}{N} \quad \text{and} \quad \sigma^2 = \frac{\sum(Mi-\mu)^2}{N-1} \Rightarrow COV = \frac{\sigma}{\mu} \tag{3-5}$$

where, μ is the mean value, σ is the standard deviation, COV is the coefficient of variation, Mi is the ith moment ratio , N is the total number of data. Calculated coefficients of variation are presented in Table 3-15. Due to the same truck survey data, the coefficient of variation is the same for each investigated case.

Table 3-15 Mean, Standard Deviation and Coefficient of Variation Values
Computed from the Whole Data for each Span

Span Length (m)	Surveyed Truck M./H30-S24 M.					Surveyed Truck M. / HL-93 M.				
	max	min	μ	σ	COV	max	min	μ	σ	COV
25	0.595	0.055	0.216	0.075	0.348	0.695	0.065	0.253	0.088	0.348
30	0.587	0.055	0.213	0.074	0.348	0.654	0.061	0.238	0.083	0.348
35	0.582	0.054	0.211	0.073	0.347	0.619	0.058	0.225	0.078	0.347
40	0.578	0.054	0.209	0.073	0.347	0.588	0.055	0.213	0.074	0.347

For Gumbel distribution, the coefficient of variation of live load is estimated from the straight lines fitted to the data points. The cumulative distribution function of the Gumbel distribution for maxima is given by [15]

$$y = F(x; \lambda, \delta) = \exp\left[-\exp\left[-\frac{x-\lambda}{\delta}\right]\right]; \quad -\infty < x < \infty \qquad (3\text{-}6)$$

where, λ and δ are the Gumbel distribution parameters. Then, the straight line equation that was fitted to the plotted points on Gumbel probability paper becomes [15]

$$\eta = h(y) = -\log\left[\log\left(\frac{1}{y}\right)\right] \rightarrow \quad \eta = \frac{x-\lambda}{\delta} \qquad (3\text{-}7)$$

The two parameters λ and δ can be estimated by setting $\eta = 0$ and $\eta = 1$, [15]

$$0 = x - \lambda \rightarrow x = \lambda \quad \text{and} \quad 1 = \frac{x-\lambda}{\delta} \rightarrow x = \lambda + \delta \qquad (3\text{-}8)$$

After fitting the straight line on Gumbel probability paper, the abscissas associated with ordinate values 0 and 1 of the reduced variate, η, give the values of λ and $\lambda + \delta$, respectively . After obtaining the values of λ and δ, the mean and variance of the Gumbel distribution can be calculated by the following expressions [15]:

$$\mu = \lambda + 0.5772\delta \quad \text{and} \quad \sigma^2 = \frac{\pi^2 \delta^2}{6} \qquad (3\text{-}9)$$

where, μ and σ are the mean and standard variation, respectively.

The coefficients of variation of the three different cases (namely overall, upper tail and extreme) are calculated based on the equations of straight lines fitting to the plotted points on the Gumbel probability paper. The results are presented in the following tables (Table 3-16 - Table 3-21).

Table 3-16 Parameters of Gumbel Distribution (*Overall*)

Span (m)	H30-S24		HL-93	
	λ	δ	λ	δ
25	0.181	0.050	0.211	0.058
30	0.178	0.049	0.198	0.055
35	0.176	0.049	0.187	0.052
40	0.174	0.049	0.178	0.049

Table 3-17 Mean, Standard Deviation and Coefficient of Variation of Moment Ratios (*Overall*) Estimated According to Gumbel Distribution

Span (m)	H30-S24			HL-93		
	μ	σ	COV	μ	σ	COV
25	0.209	0.064	0.306	0.245	0.075	0.306
30	0.206	0.063	0.306	0.229	0.070	0.306
35	0.204	0.062	0.305	0.217	0.066	0.305
40	0.202	0.062	0.308	0.206	0.063	0.308

Table 3-18 Parameters of Gumbel Distribution (*Upper Tail*)

Span (m)	H30-S24		HL-93	
	λ	δ	λ	δ
25	0.205	0.0455	0.239	0.053
30	0.202	0.0447	0.225	0.05
35	0.202	0.0438	0.215	0.047
40	0.196	0.0445	0.199	0.045

Table 3-19 Mean, Standard Deviation and Coefficient of Variation of Moment
Ratios (*Upper Tail*) Estimated According to Gumbel Distribution

Span (m)	H30-S24			HL-93		
	μ	σ	COV	μ	σ	COV
25	0.231	0.058	0.252	0.270	0.068	0.252
30	0.228	0.057	0.252	0.254	0.064	0.252
35	0.227	0.056	0.248	0.242	0.060	0.248
40	0.221	0.057	0.258	0.225	0.058	0.258

Table 3-20 Parameters of Gumbel Distribution (*Extreme*)

Span (m)	H30-S24		HL-93	
	λ	δ	λ	δ
25	0.321	0.0434	0.376	0.051
30	0.319	0.0426	0.356	0.047
35	0.306	0.0418	0.326	0.044
40	0.305	0.0423	0.311	0.043

Table 3-21 Mean, Standard Deviation and Coefficient of Variation of Moment Ratios (*Extreme*) Estimated According to Gumbel Distribution

Span (m)	H30-S24			HL-93		
	μ	σ	COV	μ	σ	COV
25	0.347	0.056	0.161	0.405	0.065	0.161
30	0.344	0.055	0.159	0.383	0.061	0.159
35	0.330	0.054	0.162	0.351	0.057	0.162
40	0.330	0.054	0.164	0.336	0.055	0.164

3.3.3.4 Comparison of the Different Extrapolation Cases

The mean maximum moments and coefficients of variation are calculated for three cases: overall original surveyed truck moments, upper tail (90 percentile and greater) of overall surveyed truck moments, and extreme surveyed truck moments. Calculations are carried out for both H30S24 and HL93 design truck loadings. The 75-year maximum mean moment ratios are plotted for H30S24 and HL93 loadings in Figure 3-37 and Figure 3-38, respectively, and coefficients of variation are shown in Figure 3-39. As the figures indicate, the mean moment ratios are higher and coefficient of variation is considerably lower for the case that the extrapolation is done from straight lines fitting to extreme surveyed truck moments. Extrapolation done by overall surveyed truck moments results in high coefficient of variation due to the fact that both maximum and minimum load effects are included. However, in reliability assessment, the load should be considered to be maximum to estimate the minimum safety level of design. Therefore, in this study, the statistical parameters of live load estimated by the extreme surveyed truck moment ratios are taken.
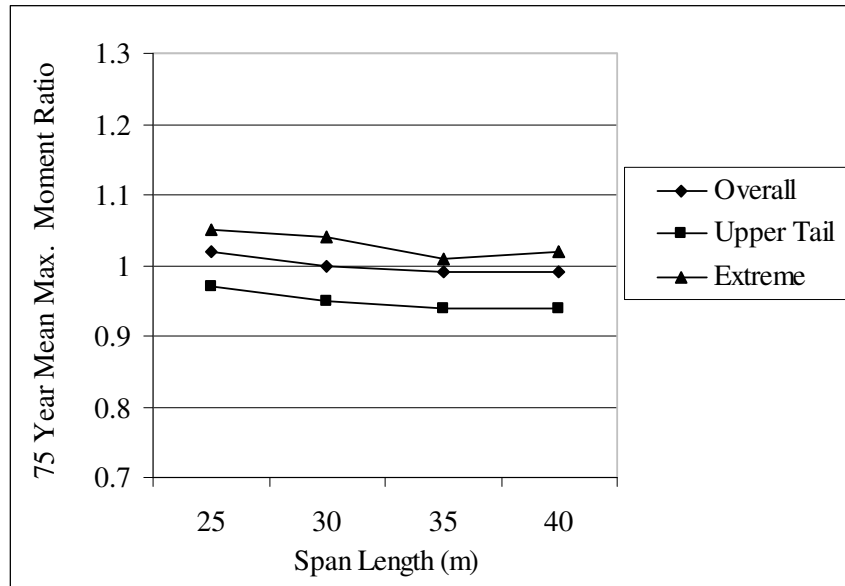
Figure 3-37 Variation of 75 year Mean Maximum Moment Ratio with Span Lengths According to Different Assumptions on Extrapolation of Data for H30S24
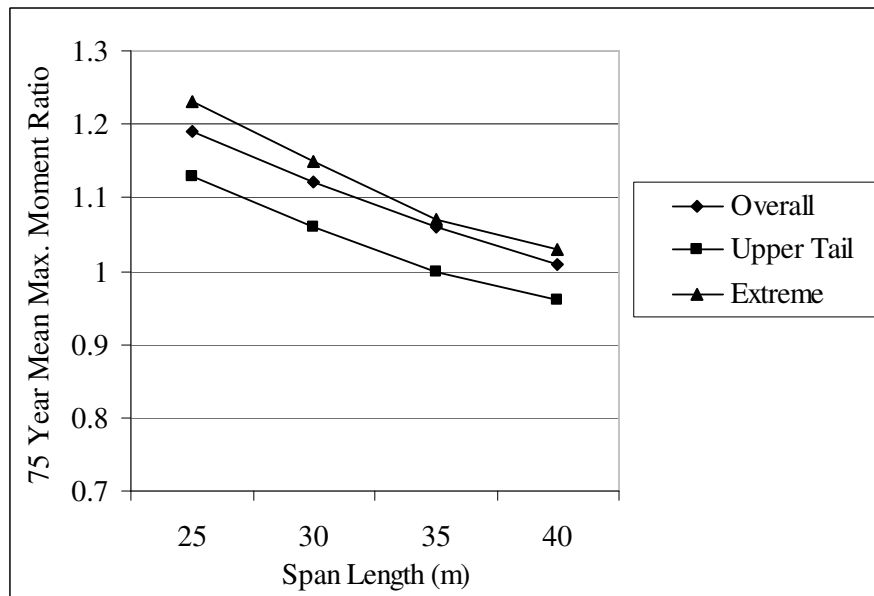
Figure 3-38 Variation of 75 year Mean Maximum Moment Ratio with Span Lengths According to Different Assumptions on Extrapolation of Data for HL93

63
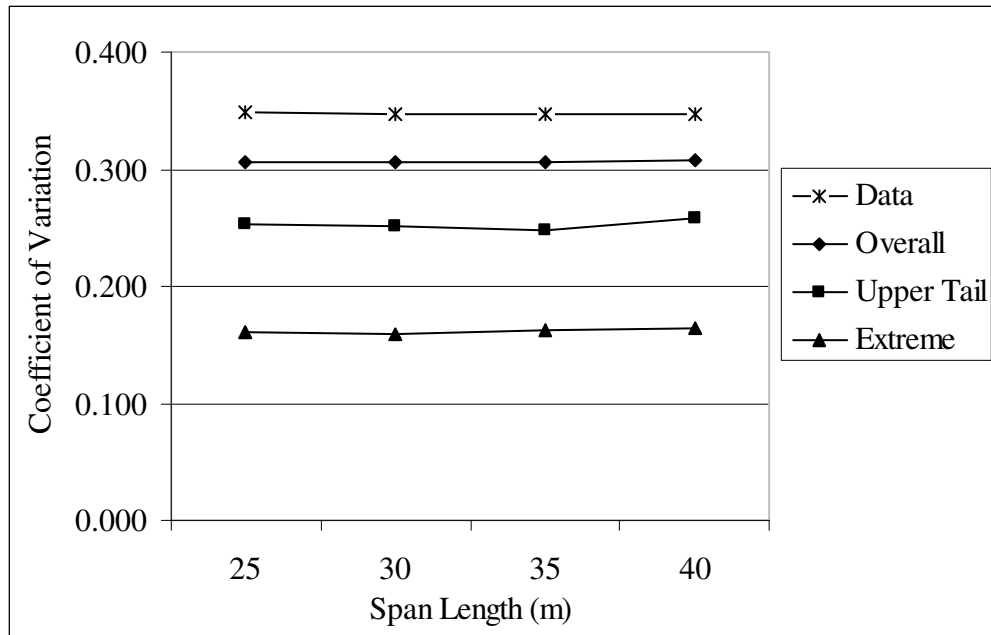
Figure 3-39 Comparison of the Coefficients of Variation Obtained from
Different Assumptions

Consequently, the coefficient of variation is taken as 0.165 for both loading type, and 75-year maximum mean moment ratio is taken as 1.0 and 1.12 (the average of the moment ratios of each span) for H30S24 and HL93 loadings, respectively. Nowak estimated the coefficient of variation of HL 93 live load as 0.12 [12]. The moment ratio is also denoted as the mean bias factor, which is the ratio of the mean value to nominal (design) value. Nowak et al. [13] assumes that 75- year maximum mean moment is the maximum load effect due to one truck being on a lane in a 75-year period, but in reliability analysis, multiple presence of trucks on a bridge should also be considered. Multiple presence of trucks means that two trucks are traveling side by side in two parallel lanes or back to back in a single lane. The following section deals with issue of multiple presence of trucks and estimation of the relevant their statistical parameters.

3.3.3.5 Consideration of Multiple Vehicles on Bridge

Nowak et al. [12] describes two types of multiple presence of vehicles. One is in the same lane; another is on the parallel lanes. In this study, multiple presence is evaluated based on the same assumptions used in the calibration of AASHTO LRFD. These assumptions are based on considerable degree of subjective judgment.[13]

3.3.3.5.1   Two Trucks in a Single Lane

It is assumed that approximately every 50th truck is followed from the behind by another truck with headway distance less than 100 ft (30 m) (20,000,000/50=400,000 trucks represent the mean maximum truck in a one-year period, see Table 3-8. Note that, 20,000,000 is the total number of truck in 75 year period), and about every 150th truck is followed from the behind by a partially correlated truck (20,000,000/150=150,000 trucks represent the mean maximum truck in a 6-month period), and about every 500th truck is followed from the behind by a fully correlated truck (20,000,000/500=40,000 trucks represent the mean maximum truck in a one-month period). Practically, fully correlated trucks mean that the trucks having the same axle configuration carry the same load and belong to the same owner. [13] The maximum surveyed truck moment is calculated by the following combination and configuration shown in Figure 3-40: [13]
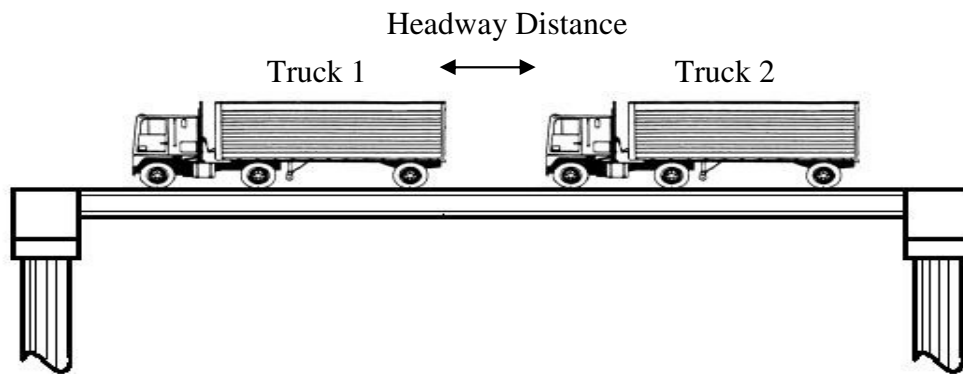
Figure 3-40 Sketch of Two Truck in Single Lane

a) Maximum 75 year Truck (Only one Truck)

b) Maximum 1 year truck (Truck 1) and average truck from survey (Truck 2),

c) Maximum 6 month truck (Truck 1) and maximum 1 day truck (Truck 2),

d) Maximum 1 month truck (Truck 1) and maximum 1 month truck (Truck 2).

The minimum headway distance is assumed to be 50 ft (15 m), which is conservative considering the braking distance [13]. Conservatively, in calculating the moment values for two trucks in one lane, the minimum distance headway is assumed to be the distance between load centers of two trucks. The moment ratios are calculated for these truck combinations, and presented in Table 3-22 and Table 3-23. As the results indicate, 75-year mean maximum moments govern for all cases. The one-lane maximum mean moment ratios are taken as 1.00 and 1.12 for H30S24 and HL93 loadings, respectively. Note that, these values are the average of the moment ratios.

Nowak et al. [12] estimated one-lane maximum mean moment ratio as between 1.23 and 1.36 for HL93.

Table 3-22 Maximum One Lane Truck Moment for H30S24 Loading

Span (m)	One Truck max 75 years	Two Trucks			Max One Lane Span Moment
		max 1 year and average	max 6 months and max 1 day	two max 1 month	
25	1.05	0.800	0.715	0.719	1.05
30	1.04	0.857	0.827	0.759	1.04
35	1.01	0.880	0.889	0.842	1.01
40	1.02	0.921	0.959	0.927	1.02

Table 3-23 Maximum One Lane Truck Moment for HL93 Loading

Span (m)	One Truck max 75 years	Two Trucks			Max One Lane Span Moment
		max 1 year and average	max 6 months and max 1 day	two max 1 month	
25	1.23	0.934	0.835	0.719	1.23
30	1.15	0.954	0.921	0.845	1.15
35	1.07	0.936	0.946	0.896	1.07
40	1.03	0.938	0.976	0.943	1.03

3.3.3.5.2   *Trucks in Two Parallel Lanes*

For two traffic lanes in the same direction, it is assumed that about every 15th truck is travelling on the bridge simultaneously with another truck in the adjacent lane and about every 150th truck with another truck that is partially correlated, and about every 450th truck is fully correlated. Therefore, the following combinations are considered: [13]

a) Maximum 75 year truck

b) Maximum 5 year truck and average truck from survey,

c) Maximum 6 month truck and maximum 1 day truck,

d) Maximum 2 month truck and maximum 2 month truck.

Nowak et al. [12] indicates that the side by side truck case equivalent to a two month truck pass in the design life of a bridge is governing the load case according to the results of simulations. In simulations, the trucks are placed 1.2 m (4 ft) apart. So, in this study, extrapolated two month truck moment ratios are assumed for the case of multiple presence of trucks in two parallel lanes. As indicated in Table 3-13 and Table 3-14, the two lane maximum mean moment ratios are taken as 0.78 and 0.86 (average of moment ratios) for H30S24 and HL93 loadings, respectively. Nowak et al. [12] estimated two-lane maximum mean moment ratio to lie between 1.08 and 1.15 for HL93.

3.4 DYNAMIC LOAD ALLOWANCE

The static effect of design truck or tandem is increased by the percentage specified in Table 3-24. In strength I and Service III Limit states, the dynamic load allowance factor (impact factor, IM) is taken as %33. This factor is not applied to lane load.

Table 3-24 Dynamic Load Allowance, IM (AASHTO LRFD Table 3.6.2.1-1)

Component	IM
Deck Joints – All Limit States	%75
All Other Component	
-Fatigue and Fracture Limit State	%15
-All Other Limit States	%33

Hwang and Nowak et al. [16] aimed to develop a procedure to calculate the dynamic load and to determine statistical parameters of the dynamic load to be used in the development of a reliability-based bridge design code. The study was carried out for different models developed for trucks, road surface (roughness), and the bridges.
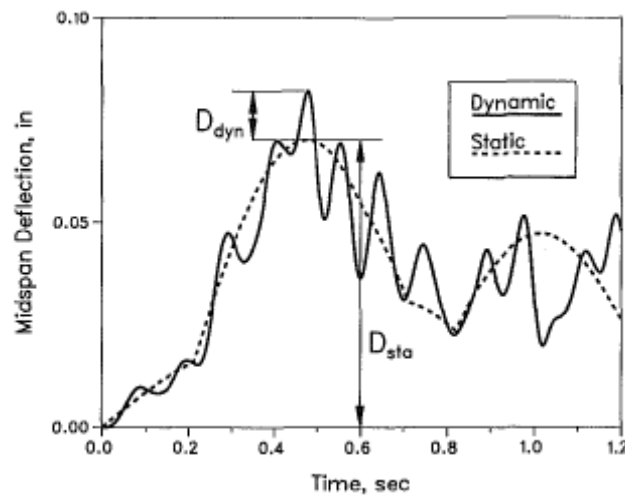
Figure 3-41 Maximum Static and Dynamic Deflections [16]

The dynamic load effect in a bridge is assessed in terms of the maximum static (D_{sta}) and dynamic deflections (D_{dyn}), as shown in Figure 3-41. The dynamic load factor is expressed as the maximum dynamic deflection divided by the maximum static deflection at mid-span. According to the research, the following results were obtained: [16]

- The dynamic load factor decreases as the gross vehicle weight increases.
- The dynamic and static live loads can be considered uncorrelated except for 30 m span bridges (low degree of correlation was observed).

- The dynamic load factor is higher for 30 and 12 m spans than 24 and 18 m spans. (see Table 3-25)
- The coefficient of variation ranges from 40% to 70% depending on the span length. (see Table 3-25)
- The dynamic load factors for two side-by-side trucks are lower than those for one truck (see Figure 3-42).
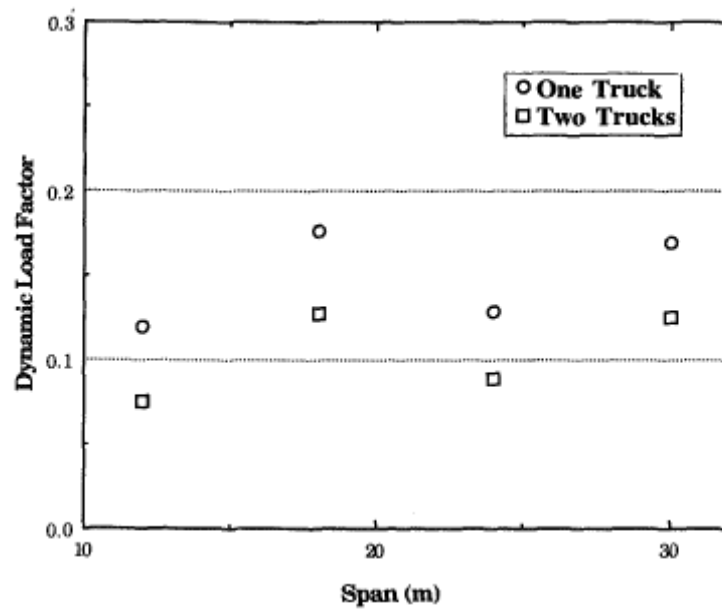
Figure 3-42 Dynamic Load Factors for One Truck and Two Trucks [16]

Table 3-25 Statistical Parameters of the Dynamic Load Factors (DLF) for Prestressed Concrete Girder Bridges [16]

Parameters	Span (m)			
	12	18	24	30
Dynamic deflection (mm)	0.36	0.35	0.66	1.60
Static deflection (mm)	1.7	3.8	5.5	12.2
Mean of DLF	0.21	0.09	0.12	0.13
Coefficient of variation of DLF	0.72	0.43	0.53	0.62

70

In a study on calibration of AASHTO LRFD, Nowak et al. [12] took the mean dynamic load as 0.10 for two trucks and 0.15 for one truck and the coefficient of variation as 0.8. In reliability analysis conducted in this study, these statistical parameters for the impact factor are used.

3.5 GIRDER DISTRIBUTION FACTOR

The design moment per lane is distributed to each interior girder by the following expression given in AASHTO LRFD Table 4.6.2.2.2b-1,

$$GDF = 0.06 + \left(\frac{S}{14}\right)^{0.4} \left(\frac{S}{L}\right)^{0.3} \left(\frac{K_g}{12.0Lt_s^3}\right)^{0.1} \text{, if one lane is loaded} \quad (3\text{-}10)$$

$$GDF = 0.075 + \left(\frac{S}{9.5}\right)^{0.6} \left(\frac{S}{L}\right)^{0.1} \left(\frac{K_g}{12.0Lt_s^3}\right)^{0.1} \text{, if two or more lanes are loaded}$$

$$(3\text{-}11)$$

where, GDF is the girder distribution factor, S is the spacing of beams (ft.), L span length of beam (ft.), K_g is the longitudinal stiffness parameter(in^4) and t_s is the depth of concrete slab (in.). The longitudinal stiffness can be expressed by (AASHTO LRFD 4.6.2.2.1-1)

$$K_g = n(I + Ae_g^2) \text{ and } n = \frac{E_B}{E_D} \quad (3\text{-}12)$$

where, E_B is the modulus of elasticity of beam material, E_F is the modulus of elasticity of deck material, I is the moment of inertia of beam (in^4) and e_g is the

distance between the centers of gravity of the basic beam and deck (in.). Note that, n is a non-dimensional coefficient.

In the calibrations of AASHTO LRFD by Nowak [13], the bias factor for girder distribution function is taken as 1.0 and coefficient of variation as 0.12. In this research work, GDF calculated according to AASHTO LRFD results in conservative values. In another research which compares the design codes, Spanish Norma, Eurocode, and AASHTO LRFD [3], the bias factor and coefficient of variation of GDF are taken as 0.93 and 0.12, respectively, and these statistical parameters of GDF are also used in this study.

3.6 SUMMARY OF STATISTICAL PARAMETERS OF LOAD

The probability distributions, coefficients of variation and mean bias factor values of the load parameters that are assessed in the previous sections are summarized in Table 3-26.

Table 3-26 Summary of Statistical Parameters of Load

Parameter	Description	Probability Distribution	Bias Factor	Coefficient of Variation
D1	Dead load- factory made members	Normal	1.03	0.080
D2	Dead load- cast in place members	Normal	1.05	0.100
D3	Dead load- wearing surface	Normal	1.00	0.250
D4	Dead load- miscellaneous	Normal	1.05	0.100
LL	Live load - H30S24	Gumbel	1.00 (1.05-1.02) for one lane	0.165
			0.78 (0.79-0.76) for two lanes	
	Live Load- HL93	Gumbel	1.12 (1.23-1.03) for one lane	0.165
			0.86 (0.92-0.75) for two lanes	
IM	Impact factor	Normal	0.30 (mean=0.10)	0.800
GDF	Girder distribution factor	Normal	0.93	0.120

CHAPTER 4

STATISTICS OF RESISTANCE

In reliability analysis, precast prestressed concrete girders are designed to express nominal values of resistance parameters for both strength and service limit states. The following chapter introduces design expressions and procedures according to AASHTO LRFD bridge design specification [1]. In addition, the statistical parameters of resistance that are required to calculate the reliability index are assessed by the available local statistical data, as well as relevant results reported by other studies are also presented.

4.1 NOMINAL FLEXURAL RESISTANCE CAPACITY ACCORDING TO AASHTO LRFD DESIGN SPECIFICATION

The AASHTO LRFD Design Specifications introduce unified design provisions, which are applicable to a variety of structures including concrete members that are reinforced with a combination of rebars and prestressing strands. These are called partially prestressed members. The design equations can also be applicable when reinforcement bars or prestressing strands are not present. [4]

Nominal flexural resistance capacity equations can be found in AASHTO LRFD 5.7.3.1.1. [1] for bonded tendons. In prestressed concrete girders, the tendon, which is a strand or a group of strands, is fully bonded to concrete. If

tendons are bonded, the change in strain of the prestressing steel is equal to the change in strain of the concrete when the member is subjected to loads. [4]
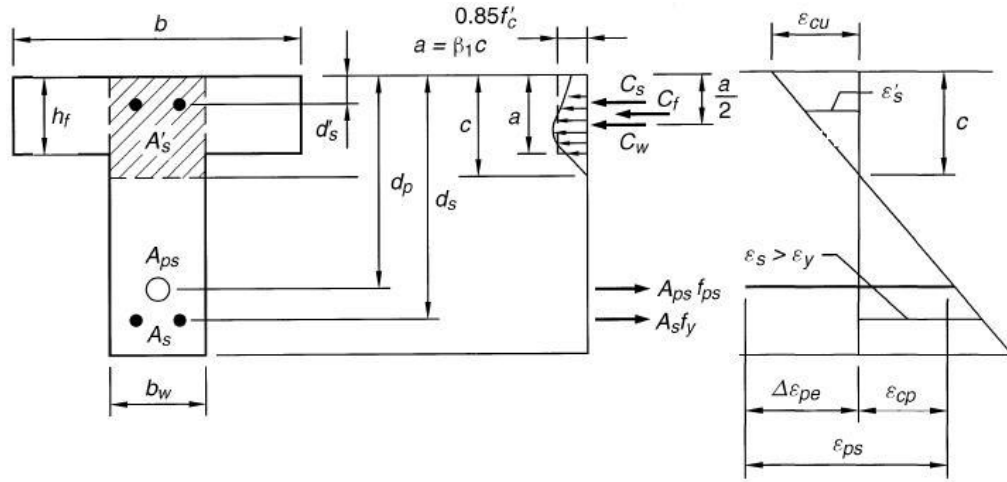
Figure 4-1 Forces on Reinforced Concrete Beam [4]

The forces on a reinforced concrete beam are shown at a given cross-section in Figure 4-1. Depth of neutral axis, c, will be calculated from the equilibrium equation of these forces. C_s is the compressive force due to non-prestressed steel. C_w is the concrete compressive force in the web, which is equal to $0.85 \cdot \beta_1 \cdot f_c' \cdot c \cdot b_w$, and C_f is the concrete compressive force in the flange, which is equal to $0.85 \cdot \beta_1 \cdot f_c' \cdot (b - b_w) \cdot h_f$. f_{ps} is the average stress in prestressing steel, which is (AASHTO LRFD 5.7.3.1.1-1)

$$f_{ps} = f_{pu}\left(1 - k\frac{c}{d_p}\right)$$

(4-1)

where, f_{pu} is the specified tensile strength of prestressing steel, d_b is the distance from extreme compression fiber to the centroid of the prestressing strands, k is equal to (AASHTO LRFD 5.7.3.1.1-2)

$$k = 2\left(1.04 - \frac{f_{py}}{f_{pu}}\right) \tag{4-2}$$

for low relaxation strands k is taken as 0.28 (AASHTO LRFD Table C5.7.3.1.1-1).

The equilibrium equation can be expressed as $T_n = C_n$

$$T_n = A_{ps} f_{pu}(1 - k\frac{c}{d_p}) + A_s f_s \tag{4-3}$$

$$C_n = 0.85\beta_1 f_c' c b_w + 0.85\beta_1 f_c'(b - b_w)h_f + A_s' f_s' \tag{4-4}$$

Solving the equilibrium equation for c by utilizing Equation 4-3 and 4-4 will yield to the following: (AASHTO LRFD 5.7.3.1.1-3),

$$c = \frac{A_{ps} f_{pu} + A_s f_s - A_s' f_s' - 0.85 f_c'(b - b_w)h_f}{0.85 f_c' \beta_1 b + kA_{ps}\dfrac{f_{pu}}{dp}} \tag{4-5}$$

where, A_{ps} is the area of prestressing steel, A_s is the area of mild steel tension reinforcement, A_s' is area of compression reinforcement, f_c' is the compressive stress of deck concrete, f_s is the yield strength of tension reinforcement, f_s' is stress in mild steel compression reinforcement at nominal flexural resistance, b

76

is the width of compression flange, b_w is the width of web, h_f is the depth of compression flange, β_1 is the stress factor of compression block (AASHTO LRFD 5.7.2.2), which is expressed as follows:

$$\beta_1 : \begin{cases} 0.28 & for \quad f'_c \leq 28MPa \\ 0.85 - 0.05(f'_c - 28Mpa)/7Mpa \geq 0.65 \ for & f'_c > 28MPa \end{cases} \tag{4-6}$$

Equation 4.5 is developed for T section compression block. For rectangular compression block, b is equal to b_w. Therefore, c becomes (AASHTO LRFD 5.7.3.1.1-4),

$$c = \frac{A_{ps} f_{pu} + A_s f_s - A'_s f'_s}{0.85 f'_c \beta_1 b + k A_{ps} \dfrac{f_{pu}}{dp}} \tag{4-7}$$

The nominal moment capacity, M_n, can be calculated at C_w application point (AASHTO LRFD 5.7.3.2.2-1)

$$M_n = A_{ps} f_{ps}(d_p - \frac{a}{2}) + A_s f_s(d_s - \frac{a}{2}) - A'_s f'_s(d'_s - \frac{a}{2})$$
$$+ 0.85 f'_c(b - b_w) h_f(\frac{a}{2} - \frac{h_f}{2}) \tag{4-8}$$

where, d_s: distance from extreme compression fiber to the centroid of non prestressed tensile reinforcement, d'_s: distance from extreme compression fiber to the centroid of non prestressed compression reinforcement, a: $\beta_1 c$, depth of equivalent stress block.

Under the circumstances of a rectangular section behavior and no compression reinforcement or mild tension reinforcement, the flexural nominal moment capacity can be computed from the equation given below

$$M_n = A_{ps} f_{ps} (d_p - \frac{a}{2}) \qquad (4\text{-}9)$$

4.2 TENSILE STRESS CHECK ACCORDING TO SERVICE III LIMIT STATE

The required number of strands is usually estimated by limiting concrete tensile stresses at the bottom fiber using Service III requirements of AASHTO LRFD design specifications (see Section 3.1). It is due to the need to control the cracking of concrete under 80% of service loads. Bottom fiber tensile stress estimated for the load combination of Service III can be computed from basics of elastic stress theory.

$$f_b = \frac{P_{pe}}{A} + \frac{P_{pe} e_c}{S_b} - \frac{M_g + M_s}{S_b} - \frac{M_b + M_{ws} + 0.8(M_{LT} + M_{LL})}{S_{bc}} \qquad (4\text{-}10)$$

where, f_b is the bottom fiber tensile stress, M_g is the unfactored bending moment due to beam self-weight, M_s is the unfactored bending moment due to slab and haunch weights, M_{ws} is the unfactored bending moment due to barrier weights, M_{LT} is the unfactored bending moment due to truck load, M_{LL} is the unfactored bending moment due to lane load, S_b is the section modulus for the extreme bottom fiber of the non-composite precast beam, S_{bc} is the composite section modulus for the extreme bottom fiber of the non-composite precast beam, P_{pe} is the total prestressing force, and e_c is the strand eccentricity.

The tensile stress in the bottom fiber of beam, f_b, should be smaller in magnitude than the concrete limiting tensile stress, of either $0.50\sqrt{f_c'}$ representing not worse than moderate corrosion conditions or $0.25\sqrt{f_c'}$ representing severe corrosive conditions (AASHTO LRFD Table 5.9.4.2.2-1). In this relationship, f_c' is the specified 28-day concrete strength of precast beam (MPa).

The total prestressing force, P_{pe}, is estimated by subtracting the prestressing losses from the tensile stress capacity and multiplying it with the number of prestressing steels. Total prestress loss (AASHTO LRFD 5.9.5.1-1) can be computed from the equation below:

$$\Delta f_{pT} = \Delta f_{pES} + \Delta f_{pLT} \qquad (4\text{-}11)$$

where, Δf_{pES} is the sum of all losses or gains due to elastic shortening or extension at the time of application of prestress, Δf_{pLT} describes the losses due to long term shrinkage and creep of concrete, and relaxation of the steel.

The change in prestressing steel stress due to the elastic deformations of the section may occur at any stage of loading. The loss due to elastic shortening can be computed from the following relationship (AASHTO LRFD 5.9.5.2.3a-1)

$$\Delta f_{pES} = \frac{E_p}{E_{ct}} f_{cgp} \qquad (4\text{-}12)$$

where, f_{cgp} is the concrete stress at the center of gravity of prestressing tendons due to the prestressing force immediately after transfer and the self-weight of the member at the section of maximum moment, and E_p is the modulus of elasticity of prestressing steel, and E_{ct} is the modulus of elasticity of concrete at transfer or time of load application.

The time dependent losses Δ_{fpLT} can be estimated approximately from the equation given below (AASHTO LRFD 5.9.5.3-1):

$$\Delta_{pLT} = 10.0 \frac{f_{ps}A_{ps}}{A_g} \gamma_h \gamma_{st} + 12.0 \gamma_h \gamma_{st} + \Delta f_{pR} \qquad (4\text{-}13)$$

where,

$$\gamma_h = 1.7 - 0.01H \quad \text{(AASHTO LRFD 5.9.5.3-2)} \qquad (4\text{-}14)$$

$$\gamma_{st} = \frac{5}{(1 + f_{ci}')} \quad \text{(AASHTO LRFD 5.9.5.3-3)} \qquad (4\text{-}15)$$

In the above equation, f_{pi} is the prestressing steel stress immediately prior to transfer, H is the average annual ambient relative humidity (%) (it is taken as 70% in this research, which is a very typical application in engineering practice), γ_h is the correction factor for relative humidity of the ambient air, γ_{st} is the correction factor for specified concrete strength at time of prestress transfer to the concrete member, and Δf_{pR} is an estimate of relaxation loss taken as 17 MPa (2.4 ksi) for low relaxation strands.

80

4.3 ASSESSMENT OF THE STATISTICAL PARAMETERS OF THE RESISTANCE VARIABLES

4.3.1 Concrete

In many countries which have no well-developed steel industry, concrete is the most preferred building material. It can be shaped and conformed to almost any alignment and profile. The raw materials, cement, aggregate and water, can be found easily in most areas of the world. Moreover, it is very economical as to both material and application. For this reason, concrete can be the most preferred and commonly used material in bridge construction.[4]

Cast-in-place (CIP) reinforced concrete deck-girder bridges can span up to the length of 25 m. Generally, between 25 m to 40 m, precast prestressed concrete girders with cast in place concrete decks are preferred.

Compressive strength, creep and shrinkage and durability against physical and chemical effects are mechanical properties of concrete. Most crucial of them is compressive strength of concrete. Tensile strength, elastic modulus and shear strength are determined by using compressive strength of concrete. In bridge construction, high quality and high compressive strength concretes are used.

The quality of compressive strength of concrete depends on several factors. One of these factors is the quality and ratio of raw materials such as cement, aggregates, and water. Water-cement ratio has an important effect on the strength of concrete. Lowering the water-cement ratio can yield high compressive strength in concrete. Without increasing the water ratio, the chemical additives are used to increase workability. The chemical additives are also used to accelerate the hardening time of concrete to reduce the duration of manufacturing. In precast prestressed concrete beams, generally prestressing force is transferred to concrete in a day after placement.

In this section, the statistical parameters, namely mean, standard deviation, and coefficient of variation of compressive strength of concrete used in the construction of bridges in Turkey, are estimated. Grades of concrete used in deck and in precast prestressed beam are different and therefore are separately investigated.

4.3.1.1 Statistical Parameters of Compressive Strength of Concrete Used in the Deck of Bridges

The deck of bridge is usually made of cast-in-place concrete. Generally, the distance between the precast girders are so tight (2-2.5 cm) that the flanges of girders can be used as formwork for the upper deck.

Design concrete strength shall not be used above 10.0 ksi (70 MPa) and below 2.4 ksi (16 MPa) per AASHTO LRFD 5.4.2.1. The specified compression strength for prestressed concrete and decks shall not be less than 4 ksi (28 MPa). In Turkey, generally C30 class concrete is used in designing bridge decks. Therefore, in this research, C30 class concrete is investigated in the design of bridge decks.

Fatih et al. [5] aimed to shed some light upon the quality of concrete production in Turkey. In that study, the quality of concrete was investigated statistically by considering the compressive strength of concrete and its variations according to years and regions.

Table 4-1 Statistical Parameters of Compressive Strength Data According to Years for Turkey [5]

Years	Number of Samples	Mean (N/mm^2)	Coefficient of Variation	Number of Values Under the Limit	Percentage of Values Under the Limit (%)
94/95	417	20.60	---	58	13.00
2000	732	26.97	0.142	40	5.46
2001	535	30.97	0.107	23	4.30
2002	465	31.21	0.104	10	2.15
2003	644	30.78	0.131	36	5.59
2004	1283	28.87	0.123	30	2.34
2005	615	29.97	0.120	24	3.90

150mmx150mmx150 mm cube specimens obtained from various laboratories located in different cities of Turkey were investigated. Table 4-1 shows the variation of compressive strength according to each year. Results indicate that mean compressive strength has increased considerably between the years 2000-2005 in Turkey compared to the period between 1994-1995 [5].

The statistical parameters of C30 class concrete are taken from this research. As indicated in Table 4-2, the mean compressive strength of C30 class concrete is 40.07 N/mm^2 and coefficient of variation (the aleatory uncertainty) is 0.079. In this table, the mean values are presented in terms of the cubic concrete compressive strength (fck,cub). Therefore, mean value is divided by 1.23 to obtain cylinder compressive strength of concrete (fck,cyl). Mean value of C30 class concrete becomes 40.07/1.23=32.5 N/mm^2. Mean bias factor which is the ratio between mean compressive strength to nominal compressive strength is determined to be 32.5/30=1.08. Compressive strength shows a normal distribution according to this research.

Table 4-2 Statistical Parameters of 28 day Compressive Strength Data
According to Concrete Class for Turkey [5]

Concrete Class	Number of Samples	fck,cyl (fck,cub) (N/mm^2)	Mean (N/mm^2)	Coefficient of Variation	Number of Values Under the Limit	Percentage of Values Under the Limit (%)
C14	137	14 (18)	20.04	0.143	1	0.83
C16	755	16 (20)	25.11	0.144	13	1.73
C18	739	18 (22)	25.82	0.12	23	3.11
C20	5817	20 (25)	28.46	0.104	118	2.7
C25	2767	25 (30)	32.48	0.1	53	2.81
C30	870	30 (37)	40.07	0.079	14	2.47
overall	11085		29.87	0.105	222	2.65

4.3.1.2 Statistical Parameters of Compressive Strength of Concrete Used in Precast Prestressed Girders

In Turkey, prestressed girders have been generally constructed with C40 class of concrete. In order to estimate the statistical parameters of C40 class concrete for Turkey, the laboratory test results were obtained from the bridge construction companies. Compressive strength limits that are the same for bridge decks are valid for girders.

In statistical calculations, two types of analyses were carried out. In the first one, the overall data is used to estimate the mean and standard deviation of compressive strength. In the second one, in-batch variability is utilized. In practice, three specimens are taken from the same concrete mix. The results of these grouped specimens are averaged, and the statistical parameters are calculated from the overall averaged test results. A similar mean value is obtained from both analytical methods. In the second method, in-batch variability is determined to be less than the one obtained in the first method.

The twenty-seven standard 150x150x150 mm cube specimens were obtained from firm 1. All test results of cubic compressive strength were converted to cylinder compressive strength by dividing cubic strengths by 1.25. The results are tabulated in Table 4-3. This construction technique is almost standard in precast concrete industry

According to data from firm 1, 7-day and 28-day mean compressive strengths are observed to be 39.58 MPa and 47.57 MPa, respectively. In-batch coefficient of variations for 7-day and 28-day are computed to be 0.043 and 0.026, respectively.

Firm 2 provided with 462 standard 150x300 mm cylinder specimens. The results are tabulated in Table 4-4. According to data taken from firm 2, 7-day and 28-day mean compressive strength are computed to be 37.24 MPa and 47.84 MPa, respectively. In-batch coefficient of variations for 7-day and 28-day are obtained to be 0.084 and 0.066, respectively. Almost the same mean compressive strength is estimated from tested specimens obtained from firms 1 and 2. Due to a larger sample size, the standard deviation is higher in the investigated data obtained from firm 2. The seven day concrete compressive strength is observed to reach to 80% of 28 day strength due to the addition of chemical additives. This construction technique is almost standard in precast concrete industry.

Table 4-3 Statistical Parameters of 7 and 28 day Laboratory (Cylinder) Compressive Strength Data of Firm 1 According to C40 Concrete Class

Statistical Parameters	7-Day		28-Day	
	Overall	In-Batch	Overall	In-Batch
Max Value (MPa)	43.30	42.62	50.15	49.17
Min Value (MPa)	35.96	37.59	44.44	45.59
μ, Mean (MPa)	39.58		47.57	
σ, Standard Deviation (MPa)	1.86	1.70	1.39	1.26
COV, Coefficient of Variation	0.047	0.043	0.029	0.026
Bias Factor (mean/nominal)	-		1.189	

Table 4-4 Statistical Parameters of 7 and 28 day Laboratory (Cylinder) Compressive Strength Data of Firm 2 According to C40 Concrete Class

Statistical Parameters	7. Days		28. Days	
	Overall	In-Batch	Overall	In-Batch
Max Value (MPa)	47.52	44.68	60.2	57.78
Min Value (MPa)	30.85	31.9	40.87	42.72
μ, Mean (MPa)	37.24		47.84	
σ, Standard Deviation (MPa)	3.37	3.13	3.66	3.16
COV, Coefficient of Variation	0.090	0.084	0.077	0.066
Bias Factor (mean/nominal)	-		1.196	

All compressive strength test results obtained from both companies are combined to estimate the statistical parameters of C40 class concrete. Combined histograms for 7-day and 28-day compressive strength of C40 are presented in Figure 4-2 and Figure 4-3 using overall (first method) and in Figure 4-4 and Figure 4-5 using in-batch analysis (second method). The in-batch statistical parameters are used in this research, because the concrete mix used in precast girders is generally supplied only one manufacturer. As depicted in Table 4-5, the 28 day mean compressive strength is computed to be 47.82 MPa, and in-batch coefficient of variation is 0.064. Mean bias factor for

C40 class concrete is 47.82 MPa / 40 MPa = 1.2. In order to assign an appropriate probability distribution to the compressive strength of C40 class concrete, a statistical analysis is conducted, based on the available data. For this purpose, the Chi-square goodness of fit test is used. According to the Chi-square goodness of fit test, the lognormal distribution is found to be acceptable at a significance level of 1%.

Table 4-5 Statistical Parameters of 7 and 28 day Laboratory (Cylinder) Compressive Strength Data of Firm 1 and Firm 2 for C40 Concrete Class

Statistical Parameters	7. Days		28. Days	
	Overall	In-Batch	Overall	In-Batch
Max Value (MPa)	47.52	44.68	60.20	57.78
Min Value (MPa)	30.85	31.90	40.87	42.72
μ, Mean (MPa)	37.37		47.82	
σ, Standard Deviation (MPa)	3.34	3.11	3.57	3.08
COV, Coefficient of Variation	0.089	0.083	0.075	0.064
Bias factor (mean/nominal)	-		1.2	
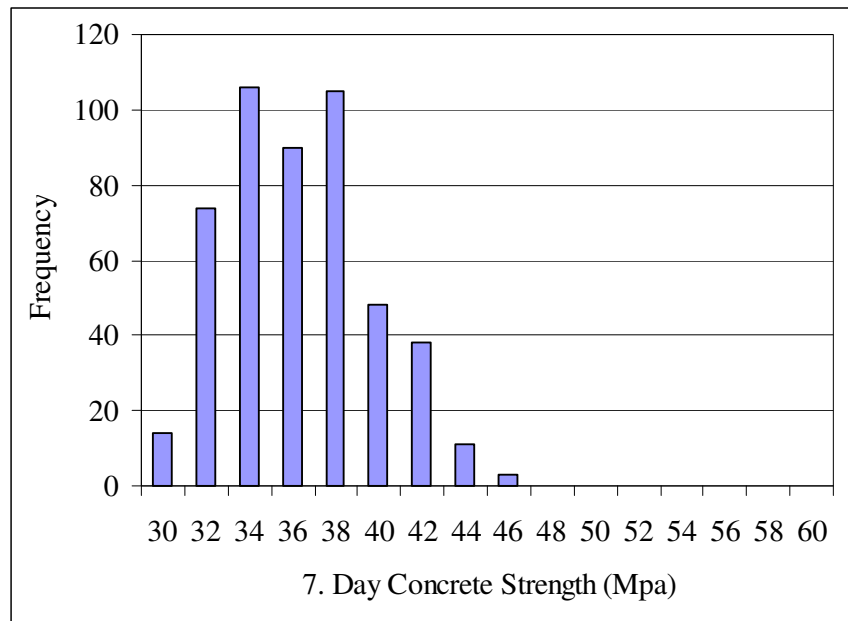
Figure 4-2 Combined Histogram of 7 Day Laboratory (Cylinder) Compressive
Strength Data (Overall) for C40 Concrete Class
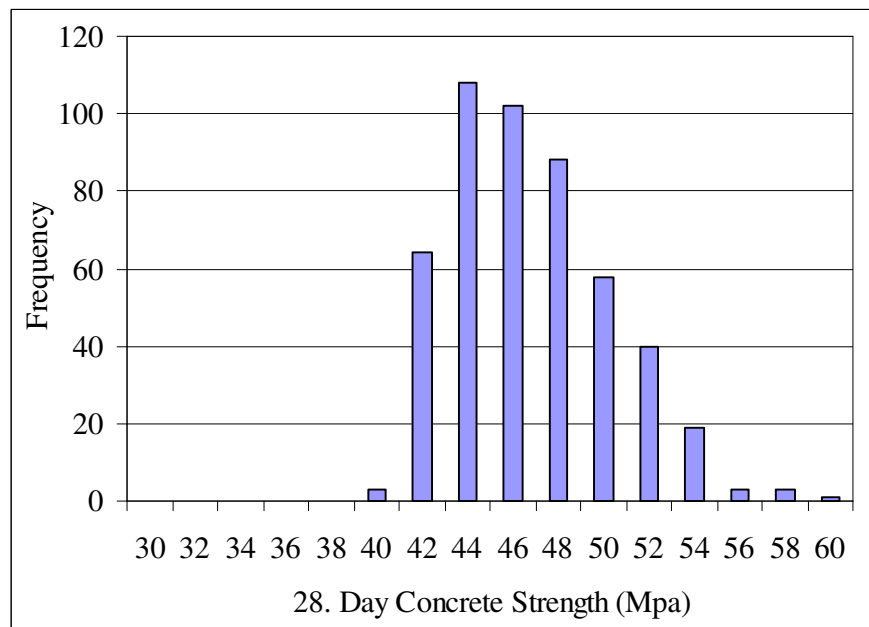
Figure 4-3 Combined Histogram of 28 Day Laboratory (Cylinder)
Compressive Strength Data (Overall) for C40 Concrete Class
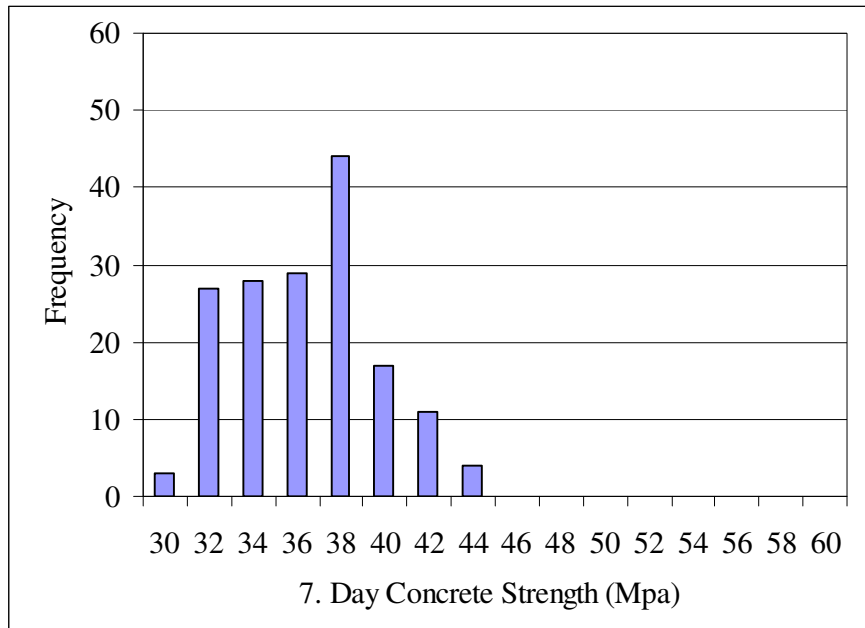
Figure 4-4 Combined Histogram of 7 Day Laboratory (Cylinder) Compressive
Strength Data (In-batch) for C40 Concrete Class
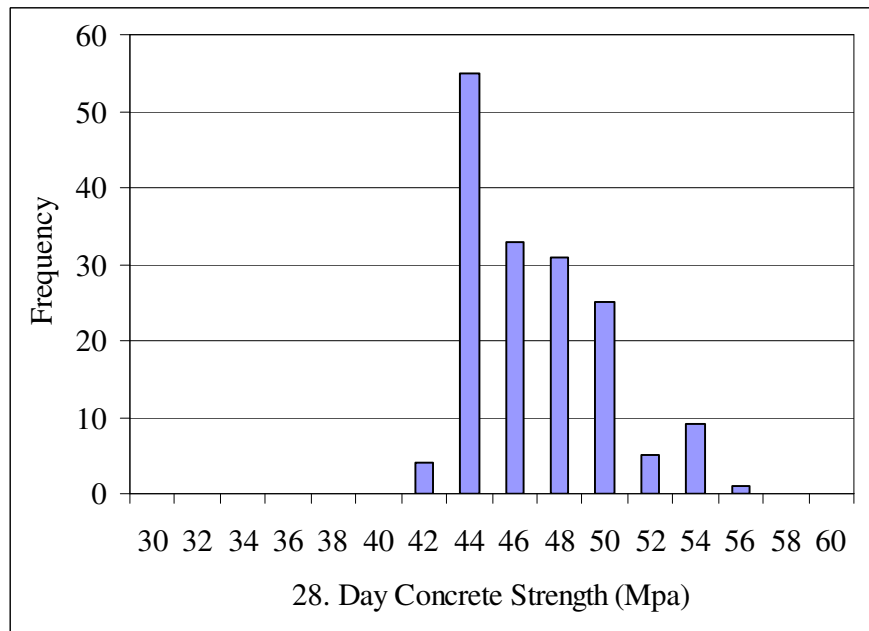
Figure 4-5 Combined Histogram of 28 Day Laboratory (Cylinder)
Compressive Strength Data (In-batch) for C40 Concrete Class

4.3.1.3 Uncertainty Analysis for the Compressive Strength of Concrete

Earlier in this study, the inherent variability (aleatory uncertainty) of compressive strength of concrete used in bridge decks and precast prestressed girders are estimated. Besides the inherent variability, additional epistemic uncertainties can result from the following effects: [5]

- Discrepancies between the laboratory test conditions and in-situ (actual) conditions,
- Rate of loading,
- Specimens not exactly belonging to actual mix and human errors.

The compressive strength of a cube or a cylinder specimen measured under laboratory conditions can be higher than the strength of concrete placed in a member of structure. Different curing and placing processes, the segregation of concrete, different sizes and shapes and different stress conditions result in difference in the actual (in-situ) strength and laboratory strength of concrete. Mirza et al. [6] stated that the average ratio of core strength to actual strength varies within the range of 0.74 and 0.96 with the prediction (epistemic) uncertainty of 0.1 expressed in terms of coefficient of variation. [5]

In engineering, information can be expressed in terms of the lower and upper limits of an uncertain variable in order to convey judgmental information. The mean value of a variable and the associated uncertainty in terms of coefficient of variation can be estimated by prescribing a suitable distribution between these two limits. [8]

The quality control in a bridge construction is usually high compared to the one in standard building construction. Plant manufactured concrete components can increase the quality of construction. Therefore, the distribution of the

correction factor, N_1, for the difference between laboratory and in-situ strength can be taken as an upper triangular distribution as shown in Figure 4-6.
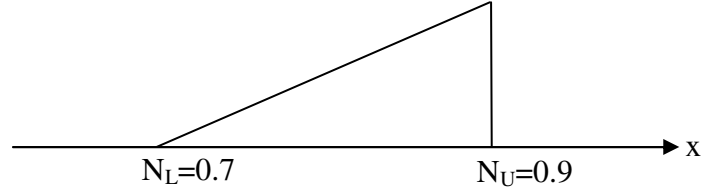
Figure 4-6 Upper Triangle Probability Density Function between N_L (lower limit) and N_U (upper limit) for N_1

The mean value and coefficient of variation can be estimated by the following expressions [8],

$$\overline{N} = \frac{1}{3}(N_L + 2 \cdot N_U)$$ (4-16)

$$\Delta = \frac{1}{\sqrt{2}}\left(\frac{N_U - N_L}{2N_U + N_L}\right)$$ (4-17)

where, N_L is the lower limit and N_U is the upper limit of the correction factor. Mean correction factor, $\overline{N}_1$, is calculated as 0.89 and epistemic uncertainty, Δ_1 as 0.06, but it is taken as 0.1 as given in [5].

An additional uncertainty is due to the rate of loading in performing the laboratory tests. If the rate of loading increases, the compressive strength of concrete will reach higher values than the actual strength. Mirza et al. [6] accounted for this effect through the correction factor, N_2. The mean value, $\overline{N}_2$, is expressed by the following empirical formula.

91

$$\overline{N}_2 = 0.89(1 + 0.08\log(R))\qquad\qquad(4\text{-}18)$$

where, R is the rate of loading and $\overline{N}_2$ is the mean correction factor for this effect. Fırat et al. [5] took $\overline{N}_2$ as 0.89 and ignored the epistemic uncertainty associated with N_2. The same values are taken in this study to account for the uncertainty due to the rate of loading.

One other source of uncertainty is the human error. The specimens can be taken from a special concrete batch instead of random picks. Moreover, standard testing procedures may not be conducted. Kömürcü et al. [9] introduced a prediction error, $\Delta_3 = 0.05$ and a mean correction factor, $\overline{N}_3 = 0.95$ for human induced errors. In this study, the mean correction factor is taken as $\overline{N}_3 = 1.0$ due to higher quality control in bridge construction.[5]

After evaluating additional uncertainties, the in-situ value of compression strength of concrete can be modeled by

$$f_c = \overline{N}_{f_c} \cdot \bar{f}_c\qquad\qquad(4\text{-}19)$$

where, f_c is the in-situ value of compressive strength of concrete, $\bar{f}_c$ is the compressive strength of cylindrical specimens tested at the laboratory, and $\overline{N}_{f_c}$ is the overall bias in f_c. The mean value, $\overline{N}_{f_c}$ is computed based on the first-order second moment approximation as:

$$\overline{N}_{fc} = \overline{N}_1 \cdot \overline{N}_2 \cdot \overline{N}_3 = 0.89 \cdot 0.89 \cdot 1.00 = 0.8\qquad\qquad(4\text{-}20)$$

Therefore, in-situ compressive strength for C30 class concrete is equal to 32.5x0.8=26 MPa and for C40 class concrete to 47.82x0.8= 38.3 MPa.

The total uncertainty, Ω_{fc} in f_c in terms of coefficient of variation can expressed as:

$$\Omega_{f_c} = \sqrt{(\delta_{fc})^2 + (\Delta_{fc})^2} \tag{4-21}$$

where, δ_{fc} is the inherent (aleatory) uncertainty (calculated in the previous sections) and Δ_{fc} is the total prediction (epistemic) uncertainty, which is evaluated as

$$\Delta_{fc} = \sqrt{\Delta_1^2 + \Delta_2^2 + \Delta_3^2} = \sqrt{0.1^2 + 0 + 0.05^2} = 0.11 \tag{4-22}$$

Total uncertainty for C30 class concrete is equal to $\sqrt{0.079^2 + 0.11^2} = 0.135$ with the inherent uncertainty, δ_{fc} of 0.079 and for C40 class concrete, it is equal to $\sqrt{0.064^2 + 0.11^2} = 0.127$. Summary of the statistical parameters of 28 day in-situ compressive strength concrete is presented in Table 4-6. The mean values of the bias factor, which is the ratio of mean to nominal compressive strength, for C30 and C40 class concretes, are determined to be 0.87 and 0.96, respectively.

In the literature, Mirza et al. [18] determined the bias factors as 0.85 and 0.81 and the coefficients of variation as 0.18 and 0.15 for the compressive strength of 28 MPa and 34.5 MPa class concrete, respectively. In addition, normal distribution was assumed for the compressive strength of concrete, in that study. The closest bias factors are calculated if C30 class concrete is compared

with C28 class concrete and C40 class concrete is compared with C34.5 class concrete. The coefficients of variation that calculated in this work are lower than that found by Mirza.

Table 4-6 Statistical Parameters of (Cylinder) Compressive Strength of C30 and C40 Concrete Class

Statistical Parameters	Concrete Class	
	C30	C40
Laboratory Measured Mean (MPa)	32.5	47.8
In-situ Mean (MPa)	26.0	38.3
Standard Deviation (MPa)	3.5	4.9
Coefficient of Variation	0.135	0.127
Nominal (MPa)	30.0	40.0
Bias Factor (mean/nominal)	0.87	0.96

4.3.2   Prestressing Strand

Seven-wire strand is the most common prestressing type used in the construction of bridge girders. There are two types of seven-wire strands based on the manufacturing process they go through; stress-relieved and low-relaxation strand. Seven-wire strand is produced by wrapping six wires around one central wire in a helical manner. The residual stress is formed in untreated strands due to cooling and twisting of wires during the process, and this causes a decrease in yield stress. The strands are heated to 350°C, and as they are allowed to cool slowly in order to eliminate the residual stresses and increase the yield strength of strand, this process is called stress relieving. In another type of manufacturing process, the strands are put into tension during the heating and cooling process in order to reduce the relaxation of the strands. The strand produced by this method is called low-relaxation strand. [4]

The stress-strain response of seven-wire strand manufactured by different processes is shown in Figure 4-7. The low relaxation strands having the highest yield strength have been used in designing girders presented in this study.
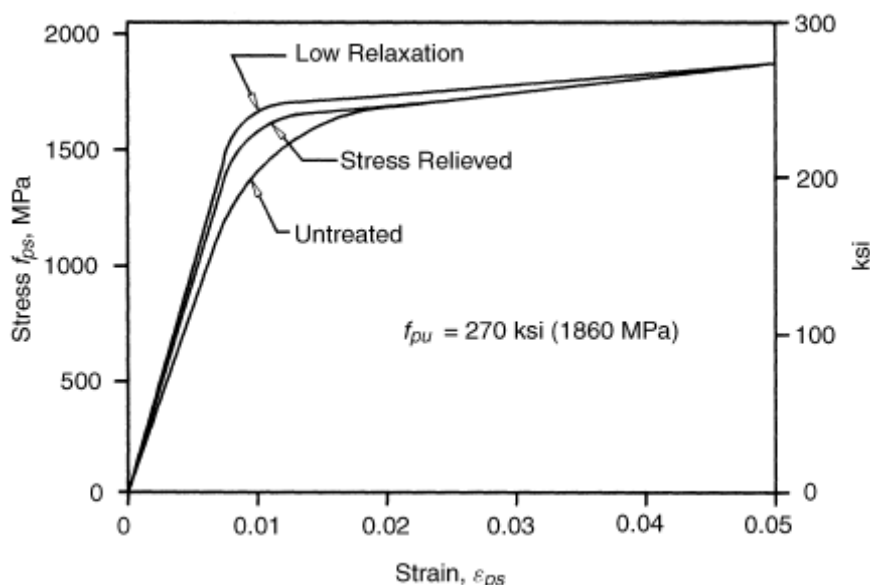
Figure 4-7 Stress-strain Response of Seven-wire Strand Manufactured by Different Processes [4]

In AASHTO LRFD Bridge Design Specifications [1], the ultimate tensile strength of low relaxation strand is taken as 1860 MPa (270 ksi). Yield strength of strand is the 90 percent of ultimate tensile strength, which is equal to 0.9x1860=1674 MPa.

4.3.2.1 Statistical Parameters of Prestressing Strands

One hundred forty six tensile strength test results obtained for the strands from the manufacturers are evaluated. The histogram of yield strengths is plotted as shown in Figure 4-8, and the statistical parameters are presented in Table 4-7.

The mean of yield strength of prestressing strands is computed as 1740 MPa and coefficient of variation as 0.021. The mean bias factor is 1740/1674=1.04.
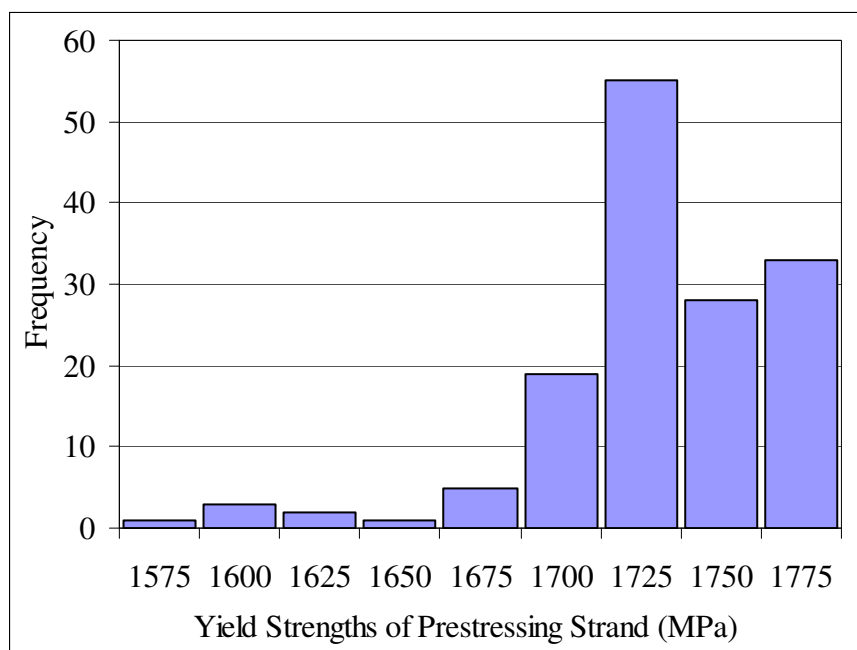
Figure 4-8 Histogram of Laboratory Yield Strength of Strands

Table 4-7 Statistical Parameters of Laboratory Yield Strength of Strand

Statistical Parameters	Values
Max Value (MPa)	1781
Min Value (MPa)	1599
μ, Mean (MPa)	1740
σ, Standard Deviation (MPa)	36.29
COV, Coefficient of Variation	0.021
Bias Factor (mean/nominal)	1.04

Mirza et al. [19] evaluated the statistical parameters of yield strength of prestressing strands by using 200 test records of the manufacturers. In his

research, the mean bias factor of yield strength of prestressing strands was found to be 1.04, and the corresponding coefficient of variation was estimated as 0.025. In addition, probability distribution of yield strength of prestressing strands was assumed to be normal. Most studies on the reliability analysis of prestressed concrete girders utilize these findings. It is important to note that the mean bias factor and the coefficient of variation of prestressing strands estimated in this study are found to be in agreement with these results. Consequently, in this study, the mean bias factor and coefficient of variation is rounded to 1.00 and 0.03, respectively, to be on the safe side.

Cross sectional area of prestressing strands also involve uncertainties. Al-Harty and Frangopol et al. [10] used 1.01 for the mean bias factor and 0.0125 for the coefficient of variation due to uncertainty resulting from the cross-sectional area of prestressing strands in their research on the reliability analysis of prestressed concrete beams. In this study, the same coefficient of variation is taken, but the bias factor is set to 1.00 to be on the conservative side. The statistical parameters of prestressing strands are tabulated in Table 4-8.

Table 4-8 Statistical Parameters of Prestressing Strand

Statistical Parameters	Prestressing Strand	
	Yield strength	Cross sectional area
COV, Coefficient of Variation	0.03	0.0125
Bias Factor	1	1

4.3.3 Dimensions

The aim of this section is to evaluate the variability and the resulting uncertainty in the girder width and effective depth for bottom prestressing. Mirza et al. [7] proposed expressions for the statistical parameters of dimensions of in-situ and precast reinforced concrete beams as shown in Table 4-9. By using the values given in this table, the mean, μ_b, and coefficient of variation, δ_b, of beam width can be expressed by

$$\mu_b = b_n + 3.96mm. \quad \text{or} \quad b_n + 5/32in.. \quad\quad (4\text{-}23)$$

$$\delta_b = (6.35)mm./(b_n + 3.96mm.) \quad \text{or} \quad (1/4)in./(b_n + 5/32in.) \quad (4\text{-}24)$$

Table 4-9 Recommended Ranges and Values of the Statistical Parameters of Beam Dimensions [7]

Dimension description		In-Situ beam			Precast Beam		
		Nominal range	Mean deviation from nominal	Standard deviation	Nominal range	Mean deviation from nominal	Standard deviation
Width	Rib	11-12	+3/32	3/16	14	0	3/16
	Flange	-	-	-	19-24	+5/32	1/4
Overall Depth		18-27	-1/8	1/4	21-39	+1/8	5/32
Effective Depth	Top Rein.	1-1/2	+1/8	5/8	2-2 1/2	0	5/16
			-1/4	11/16		+1/8	11/32
	Bottom Rein.	3/4-1	+1/16	7/16	3/4	0	5/16
			-3/16	1/2		+1/8	11/32
Beam Spacing and Span		-	0	11/16		0	11/32
- Dimensions are in inches.							

where, b_n is the nominal precast (flange) beam width.

The mean, μ_{dp}, and coefficient of variation, δ_{dp}, of the effective depth of bottom prestressing strands can be estimated by using the following relationships,

$$\mu_{dp} = d_{pn} + 3.18mm \quad \text{or} \quad d_{pn} + (1/8)in \qquad (4\text{-}25)$$

$$\delta_{dp} = 8.73mm/(d_{pn} + 3.18mm) \quad \text{or} \quad (11/32)in./(d_{pn} + 1/8in.) \quad (4\text{-}26)$$

where, d_{pn} is the nominal effective depth.

For instance, if b_n is assumed as 1000 mm, then the mean is calculated as 1003.96 mm, and coefficient of variation is 0.0063. Moreover, if d_{pn} is assumed to be 1200 mm, the corresponding mean and coefficient of variation are 1203.18 mm and 0.0072, respectively. These results indicate that variation in dimensions is quite small. Therefore, in this study, the true mean value of both dimensions is assumed to be equal to the corresponding nominal values; that is, the mean bias factor for these dimensions is taken as 1.00, and coefficient of variation is assumed to be 0.01.

4.4 SUMMARY OF THE STATISTICAL PARAMETERS OF RESISTANCE

The probability distributions, coefficients of variation and mean bias factor values of the resistance parameters that are assessed in the previous sections are summarized in Table 4-10. k and β1 are assumed to be deterministic quantities. PF denotes the professional factor that describes the uncertainty resulting from the use of approximate resistance and idealized stress and strain models [12].

Table 4-10 Summary of Statistical Parameters of Resistance

Parameter	Description	Probability Distribution	Bias Factor	Coefficient of Variation
Aps	Area of prestressing strand	Normal	1.0	0.0125
fpu	Ultimate tensile strength of prestressing steel	Normal	1.0	0.03
fc,C30	Compression strength of deck concrete	Normal	0.87	0.135
fc,C40	Compression strength of precast beam	Lognormal	0.96	0.127
dp	Distance from extreme compression fiber to the centroid of prestressing steel	Normal	1.0	0.010
b	Width of compression flange	Normal	1.0	0.010
k	0.28 for low relaxation strands	-	-	-
β1	Stress factor for compression block	-	-	-
PF	Professional factor	Normal	1.01	0.06

CHAPTER 5

TURKISH TYPE PRECAST PRESTRESSED CONCRETE BRIDGE GIRDERS

5.1 TYPICAL CROSS-SECTIONS OF PRECAST PRESTRESSED CONCRETE GIRDERS

The prestressed concrete girders are precast members that are produced in plants. The formworks of girders are made of steel plates. They are welded to each other to form the geometry of cross-section of a girder. The formworks have an important role in the cost of the girder. Hence, the typical girder cross sections are used in order to decrease the cost. The formworks have been reused in different projects until the end of their economic life span.

The typical cross-sections of prestressed concrete girders are known by the bridge designers in Turkey. Bridges girders are generally tried to be designed by the typical girders to avoid additional cost in construction. In this study, four typical cross-sections of the bridge girders mostly used in Turkey are selected for each span length. The cross-sections are shown in Figure 5-1. In addition, the cross-sectional dimensions of prestressed precast concrete girders are shown on these figures:
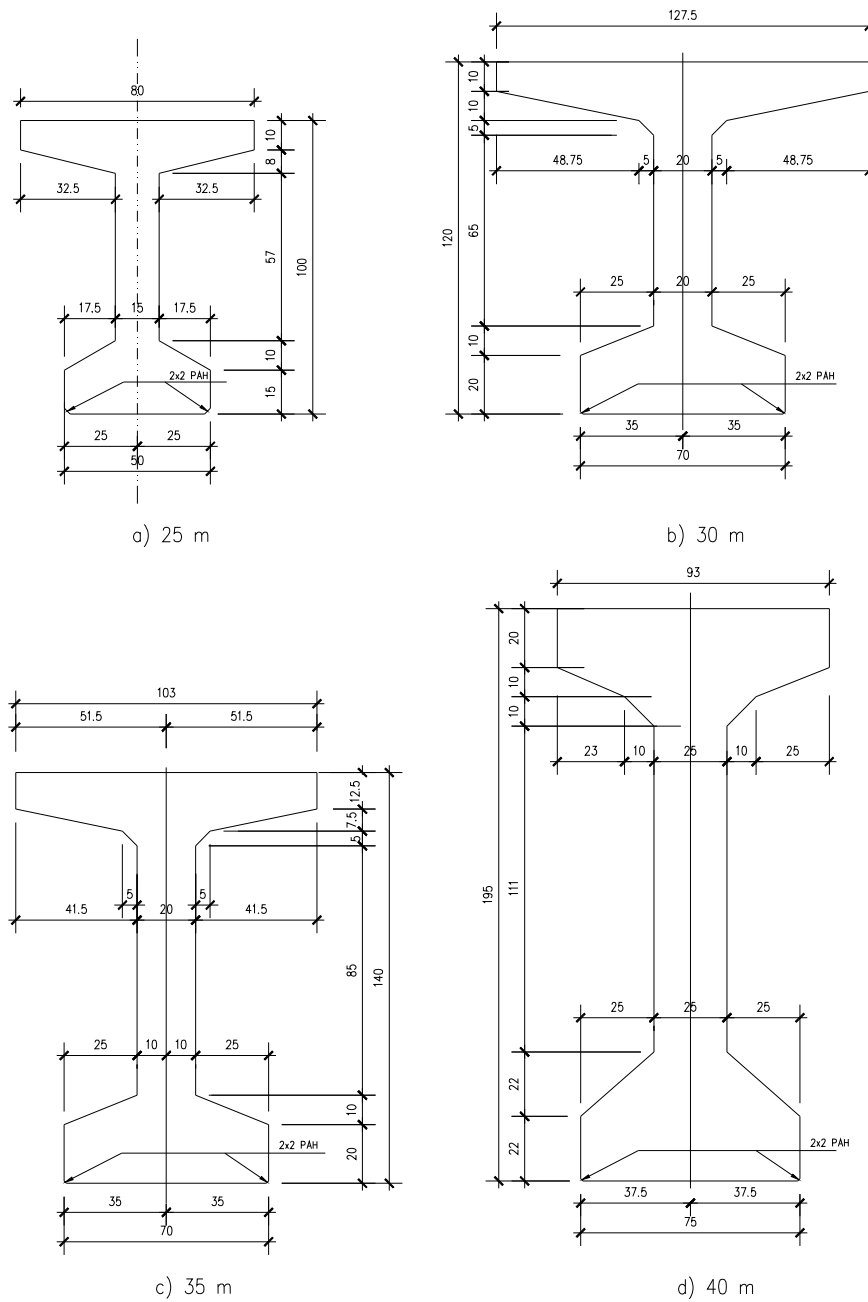
Figure 5-1 Cross-Sections of the Typical Prestressed Precast Concrete Girders
Conducted in Turkey (dimensions are in cm.)

5.2 TYPICAL BRIDGE CROSS-SECTIONS

The bridge cross-sections used in this study are shown in Figure 5-2 to Figure 5-5. In this section, the general properties of typical cross sections are introduced. Reliability analysis is carried out for the given bridge cross-sections.

Total width of bridges is 12.25 m. Spaces of 75 cm and 150 cm are left on each side for pedestrian walk ways, barriers, and drainage pipes. Clear roadway width is 10 m. The number of design lanes estimated by taking the integer part of the ratio of clear roadway width to 3.6 m. (AASHTO LRFD 3.6.1.1.1) is equal to two. The spacing between girders and the number of girders are shown in Table 5-1. The prestressed precast concrete girders are generally placed with 2-2.5 cm spacing. Due to the small spacing, the girders can work as a formwork for the deck. Thickness of cast-in-place concrete deck is taken as 25 cm for all spans. C30 class concrete for deck and C40 class concrete for prestressed precast beams are considered.

Unit weights are taken from AASHTO LRFD Table 3.5.1-1 [1]. The unit weight of both concrete classes is taken as 2400 kg/m^3. An asphalt layer of 6 cm is placed on bridge deck, and unit weight is taken as 2240 kg/m^3. The barrier weight is taken as 4.4 kN/m.

Table 5-1 Selected Precast Prestressed Concrete Girder Bridges

Bridge No.	Span (m)	Girder Spacing (cm)	Girder Type	Number of Girders
1	25	82	H100	14
2	30	130	H120	9
3	35	105	H140	11
4	40	95	H195	12

Figure 5-2 Bridge Cross-Section for Span Length of 25 m

Figure 5-3 Bridge Cross-Section for Span Length of 30 m
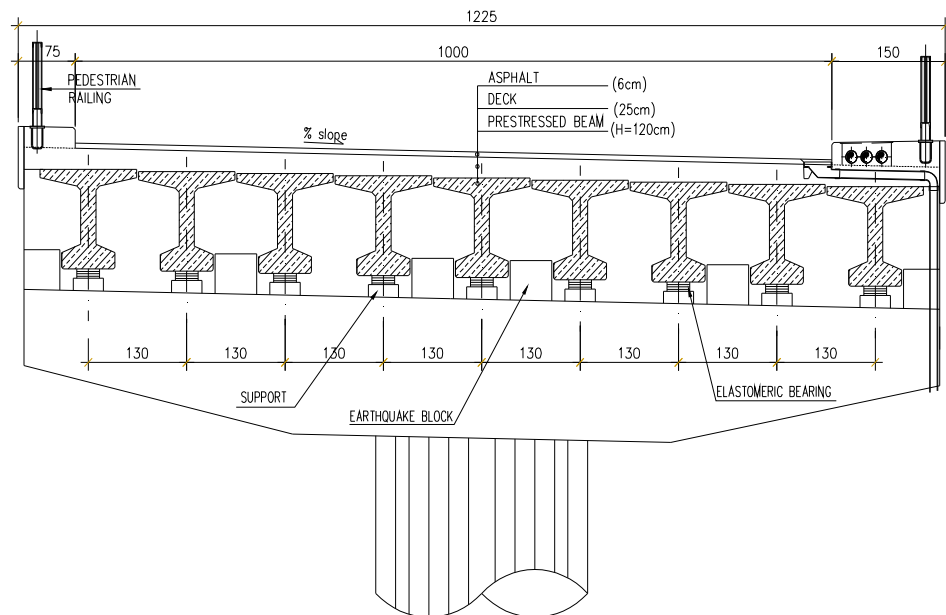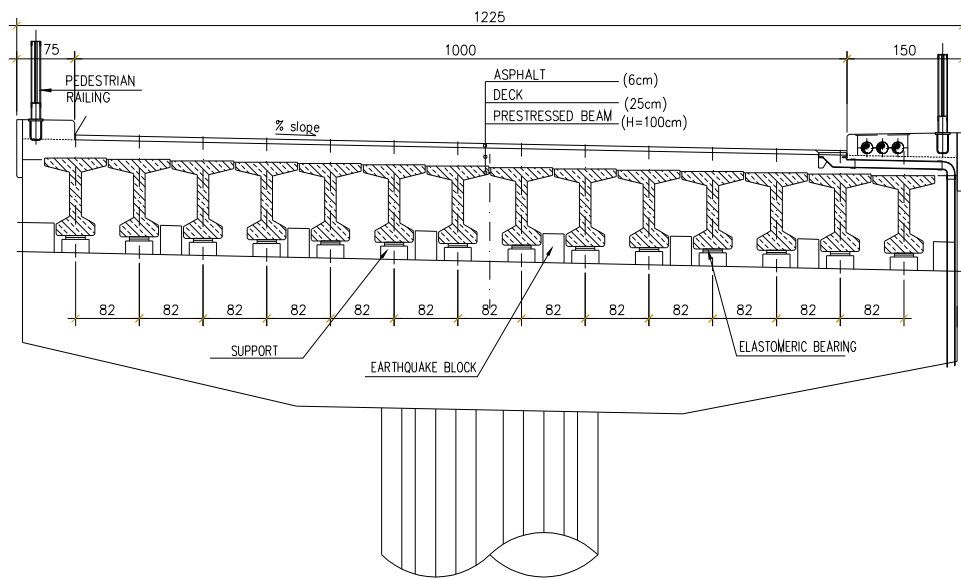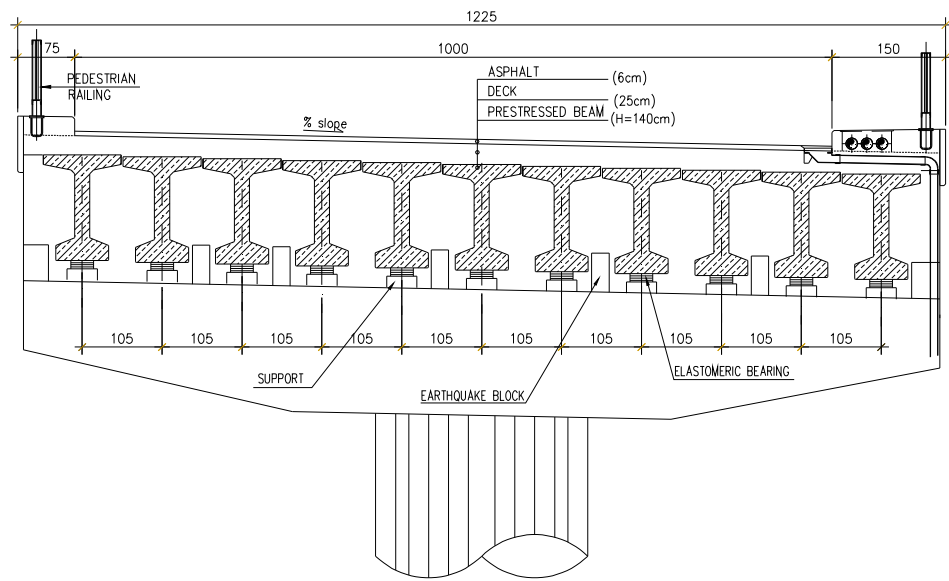
Figure 5-4 Bridge Cross-Section for Span Length of 35 m
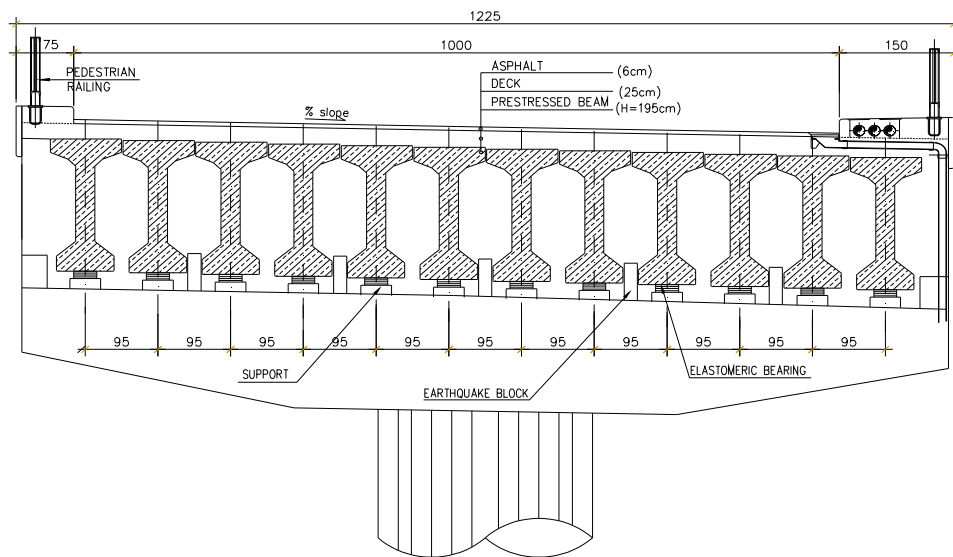
Figure 5-5 Bridge Cross-Section for Span Length of 40 m

5.3 DESIGN OF BRIDGES

In C++ programming language, the algorithm is developed to design prestressed concrete girders according to both strength and service limit states of AASHTO LRFD Specifications [1]. Maximum span moments due to dead and live loads and girder distribution factors are tabulated for each considered span lengths in Table 5-2 according to AASHTO LRFD Specifications. In this table, D1 is the maximum moment due to weight of precast prestressed girder, D2 is the maximum moment due to weight of haunch and bridge deck, D3 is the maximum moment due to weight of asphalt, D4 is the maximum moment due to weight of barrier, LL is the maximum moment due to live load that includes impact factor and girder distribution factor for both H30S24 and HL93 design loading. It should be noted that all calculated moments are per girder.

Table 5-2 Calculated Moments due to Dead and Live Loads per Girder

Load Type	Span Length			
	25 m	30 m	35 m	40 m
D1 (kN.m)	572	1413.7	1968.9	3967.2
D2 (kN.m)	389.9	879.4	971.6	1151.3
D3 (kN.m)	84.5	192.8	212	250.5
D4 (kN.m)	49.1	110	122.5	146.7
LL (H30S24) (kN.m)	1074.4	1823.2	1886.5	2165.3
LL (HL93) (kN.m)	858.5	1514.1	1626.7	1936.2
GDF, Girder Distr. Func.	0.29	0.4	0.35	0.34

The aim of the design is to determine the minimum required number of prestressing strands for the identified cross-section, material property and span length. The required number of prestressing strands for strength I limit state shall satisfy the minimum required resistance corresponding to the factored flexural moment demand at the investigated section. Flexural resistance capacity (R) is calculated as explained in Section 4.1, and minimum required resistance (Rmin) is calculated by multiplying the moment due to dead and live load effects by each corresponding load factors of strength I limit state by Eq. 4.1. The number of prestressing strands required for service III limit state shall prevent cracking at the bottom fiber (see chapter 4.2). The design of prestressed concrete girders is done by the program developed as a part of this research. The results are shown for both design loadings and the considered span lengths and for both strength and service limit states in Table 5-3 to Table 5-6.

Table 5-3 Results of Design According to Strength I Limit State for H30S24

Parameters	Span Length			
	25 m	30 m	35 m	40 m
Rmin (kN.m)	3283.1	6511.3	7478.7	10783.1
R (kN.m)	3416.4	6691.9	7627.3	10861
Max Tensile Stress Limit (MPa)	3.162	3.162	3.162	3.162
Tensile Stress at Bottom (MPa)	3.771	4.842	5.177	4.54
Number of Strands	18	30	30	31

Table 5-4 Results of Design According to Strength I and Service III Limit
States for H30S24

Parameters	Span Length			
	25 m	30 m	35 m	40 m
Rmin (kN.m)	3283.1	6511.3	7478.7	10783.1
R(kN.m)	3572	7407.1	8672.1	12352.8
Max Tensile Stress Limit (MPa)	3.162	3.162	3.162	3.162
Tensile Stress at Bottom (MPa)	3.025	3.12	3.004	2.836
Number of Strands	19	34	35	36

Table 5-5 Results of Design According to Strength I Limit State for HL93

Parameters	Span Length			
	25 m	30 m	35 m	40 m
Rmin (kN.m)	2905.2	5970.4	7024	10382
R (kN.m)	2927.5	6113.6	7190.3	10551
Max Tensile Stress Limit (MPa)	3.162	3.162	3.162	3.162
Tensile Stress at Bottom Fiber (MPa)	4.596	5.131	5.294	4.521
Number of Strands	15	27	28	30

Table 5-6 Results of Design According to Strength I and Service III Limit
States for HL93

Parameters	HL93			
	25 m	30 m	35 m	40 m
Rmin (kN.m)	2905.2	5970.4	7024	10382
R (kN.m)	3258.7	7052.2	8270.1	11769
Max Tensile Stress Limit (MPa)	3.162	3.162	3.162	3.162
Tensile Stress at Bottom Fiber (MPa)	2.961	2.822	3.021	3.122
Number of Strands	17	32	33	34

The required number of prestressing strands is plotted in Figure 5-6. H30S24 design truck model results in a higher number of prestressing strands in both limit states compared to the HL-93 truck model. In addition, the number of prestressing strands required by service III limit state is typically more than the minimum number of strands required by the strength I limit state. Strand ratio, calculated by dividing the minimum required number of strands determined in service III limit state to the ones determined in strength I limit state, is adopted for comparison. If strand ratio is greater than 1, it means that there is an additional factor of safety the prestressed concrete bridge girders possess beyond the minimum value required by the strength limit state [17] as depicted in Figure 5-7. The average additional safety is around %15 and %13 for HL93 and H30S24, respectively.
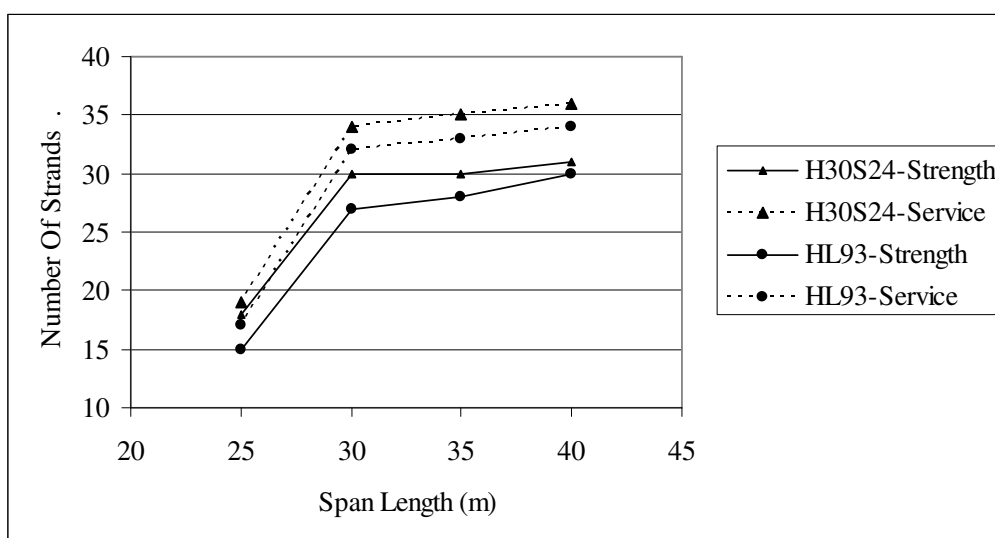
Figure 5-6 Number of Strands per Girder for Strength I and Service III Limit States
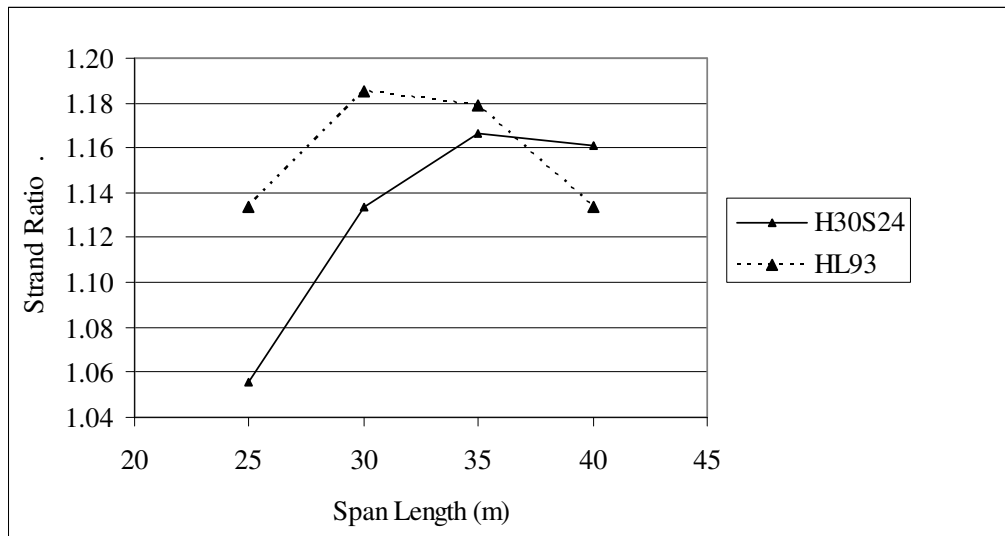
Figure 5-7 Comparison of Calculated Strand Ratios with Respect to Each Span
Lengths and Loadings

CHAPTER 6

RELIABILITY-BASED SAFETY LEVEL EVALUATION

6.1 LIMIT STATE FUNCTION

There are many ways and modes of failure of bridges. These are cracking, corrosion, excessive deformations, exceeding the carrying capacity for shear or bending moment, local or overall buckling. A traditional notion of the safety limit is associated with the ultimate limit states which is the ultimate bending (flexural) moment capacity.[12]

Let R be the resistance (moment carrying capacity in this case) and Q represents the load effect (total moment applied to considered beam) then, the limit state function, g, can be expressed by

$$g = R - Q \qquad (6\text{-}1)$$

If $g > 0$, the structure is safe; otherwise it fails. The probability of failure, P_F is defined as,

$$P_F = P(R - Q < 0) = P(g < 0) \qquad (6\text{-}2)$$

In this study, total load effect is expressed by

$$Q = D1 + D2 + D3 + D4 + LL \cdot (1 + IM) \cdot GDF \qquad (6\text{-}3)$$

and bending resistance is expressed by

$$R = A_{ps} f_{pu} \left(1 - k \frac{\left(\dfrac{A_{ps} f_{pu}}{0.85 f_c' \beta_1 b + k A_{ps} \dfrac{f_{pu}}{dp}} \right)}{d_p} \right) \left(d_p - \frac{\beta_1 \left(\dfrac{A_{ps} f_{pu}}{0.85 f_c' \beta_1 b + k A_{ps} \dfrac{f_{pu}}{dp}} \right)}{2} \right) \cdot PF$$

$$(6\text{-}4)$$

For the symbols used in Equation 6-3 and 6-4 please refer to Chapters 3 and 4. As the expressions indicate, the limit state is a function of many random variables such as load components, resistance parameters, material properties, dimensions, and analysis factors. Full description of the joint probability distribution function of these random variables and evaluation of multiple integrals is quite difficult. Therefore, it is convenient to utilize the First-Order-Second-Moment reliability models and to measure structural safety in terms of the reliability index.

The reliability index, β can be expressed as a function of P_F, if all variables are normally distributed and the failure function is linear.

$$\beta = -\Phi^{-1}(P_F) \qquad (6\text{-}5)$$

where, Φ^{-1} is the inverse standard normal distribution function. Reliability index and corresponding failure probability assuming normal distribution are presented in Table 6-1.

There are various methods available for the calculation of the reliability index. The required accuracy, available input data and computational difficulties are the main criteria for selecting the proper calculation methods. Nowak et al. [12] computed the reliability index based on the Mean-Value-First-Order-Second-Moment (MVFOSM) Method. In the present study, reliability index is calculated not only by MVFOSM method but also First-Order-Second-Moment (FOSM) analysis, First Order Reliability Method (FORM) and Second-Order-Reliability Method (SORM).

Table 6-1 Reliability Index and the Corresponding Failure Probability Assuming Normal Distribution

Reliability Index, β	Probability of Failure, P_f
0	0.5
1	0.159
2	0.0228
3	0.00135
4	0.0000317
5	0.000000287
6	0.000000000987

The MVFOSM method is based on a first-order Taylor series approximation of the performance (failure) function linearized at the mean values of the random basic variables, and it uses only second moment statistics of the random variables. There are deficiencies of MVFOSM method. If the limit state (failure) function is nonlinear, significant errors may be introduced by neglecting higher order terms. Also, the MVFOSM method fails to be invariant to different mechanically equivalent formulations of the same problem. This means that reliability index depends on how the limit state is formulated. Due

113

to these shortcomings of the MVFOSM method, Hasofer and Lind [26] proposed a new reliability index, β_2. The process of calculating β_2 is generally referred as the advanced first-order second moment method (FOSM). Reliability index β_2 is defined as the shortest distance from the origin to the failure surface in the z-coordinate system, and the design point is defined as the point having the shortest distance to the origin on the failure surface (see Figure 6-1). When the failure surface is nonlinear, the search for the design point and the calculation of the reliability index is carried out by an iterative algorithm.[5]
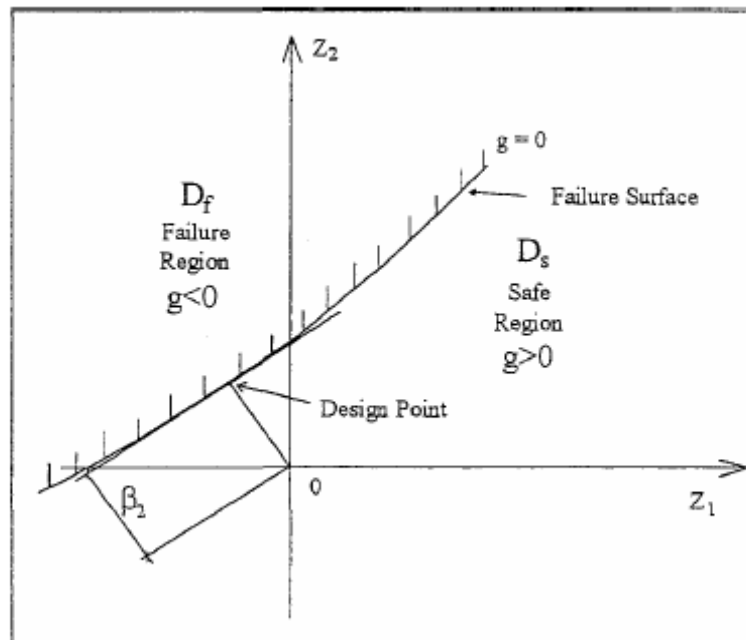
Figure 6-1 Description of Reliability Index β_2 [5]

FORM is an analytical approximation in which the reliability index is interpreted as the minimum distance from the origin to the limit state surface in standardized normal space (z-space). The performance function is approximated by a linear function in the z-space at the design point, accuracy problems occur when the performance function is strongly nonlinear. The

second-order reliability method (SORM) has been established as an attempt to improve the accuracy of FORM. SORM is obtained by approximating the limit state surface in the z-space at the design point by a second-order surface. In SORM, the difficult, time consuming portion is the computation of the matrix of second-order derivatives. [25]

Since the exact computation of the failure probability is quite complicated, numerous studies have contributed to develop some approximations that have closed forms, the accuracy of which is generally dependent on the three parameters of the limit state surface, i.e. the curvature radius R at the design point, the number of random variables n and the first-order reliability index. Breitung [27] has derived an asymptotic formula which approaches the exact failure probability as $\beta_F \to \infty$ with $\beta_F k_i$, where k_i is a principal curvature at the design point, fixed. [25] However, such methods are not considered in this study and reliability index is computed by using MVFOSM, FOSM, FORM and SORM.

6.2 RELIABILITY LEVEL ACCORDING TO AASHTO LRFD BASED ON LOCAL CONDITIONS

The reliability indexes are calculated according to AASHTO LRFD [1] by using statistical parameters of load and resistance variables that were assessed in the previous sections (see Table 4-10 and Table 3-26) reflecting the conditions of Turkey. In these computations four different reliability analysis methods, namely MVFOSM, FOSM, FORM and SORM are used. Both service and strength limit states are considered. The results are tabulated in Table 6-2. As the results demonstrate, the calculated reliability indexes vary according to the chosen–method. In this study, minimum reliability index is chosen among the reliability indexes calculated by different methods for each case. In general,

the reliability indexes calculated by the Second-Order-Reliability Method (SORM) are observed to be lower than these obtained from the others.

Reliability indexes calculated based on the statistical parameters reflecting the local conditions for service and strength limit states are plotted in Figure 6-2. The reliability indexes based on the requirements of strength limit state are observed to vary between 4.48-4.21 for girders designed according to H30S24 loading and between 3.92-3.67 for girders designed according to HL93 loading. Moreover, the reliability indexes calculated based on the requirements of service limit state lie between 4.91-5.33 for girders designed according to H30S24 loading and 4.59-4.73 for girders designed according to HL93 loading. The results indicate that reliability indexes of girders designed by H30S24 loading result in a higher reliability index than the ones designed by HL93 for strength and service limit states. Designs according to service limit state result in higher reliability indexes due to providing extra safety in design in this limit state.

The reliability indexes are calculated according to AASHTO LRFD [1] by using statistical parameters of load and resistance variables that were taken from calibration report [12] reflecting the conditions of USA. The results are shown in Figure 6-3. It is concluded that the reliability indexes reflecting the conditions of USA are observed to be lower in comparison with that reflecting the conditions of Turkey.

Table 6-2 Reliability Indexes Calculated by Alternative Reliability Methods for Different Loading and Limit States Based on Local Conditions of Turkey

| Case	Reliability Method	Span Length			
		25 m	30 m	35 m	40 m
Strength-H30S24	MVFOSM	5.44	5.11	4.84	4.32
	FOSM	5.28	5.08	4.87	4.41
	FORM	4.51	4.53	4.49	4.32
	SORM	4.48	4.49	4.43	4.21
Service-H30S24	MVFOSM	6.07	6.11	6.01	5.49
	FOSM	5.92	6.14	6.13	5.68
	FORM	4.94	5.29	5.44	5.42
	SORM	4.91	5.28	5.35	5.33
Strength-HL93	MVFOSM	4.61	4.37	4.17	3.8
	FOSM	4.47	4.32	4.17	3.85
	FORM	3.96	3.96	3.92	3.79
	SORM	3.93	3.92	3.85	3.67
Service-HL93	MVFOSM	5.54	5.74	5.53	4.91
	FOSM	5.4	5.74	5.59	5.03
	FORM	4.61	5	5.01	4.81
	SORM	4.59	4.99	4.96	4.73
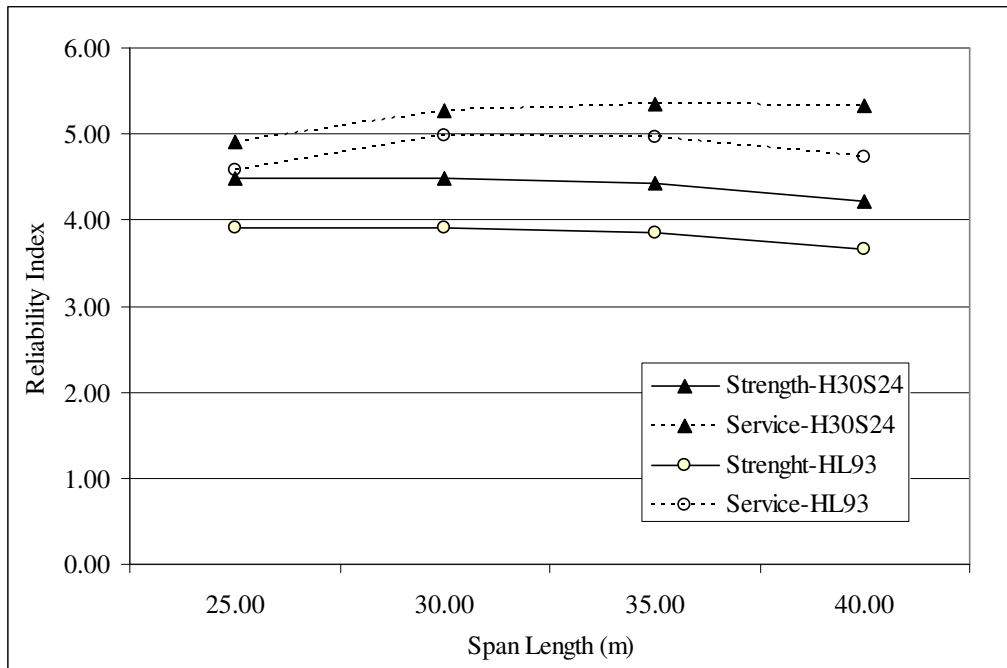
Figure 6-2 Variation of Reliability Indexes with Span Lengths Considering the Local Conditions in Turkey
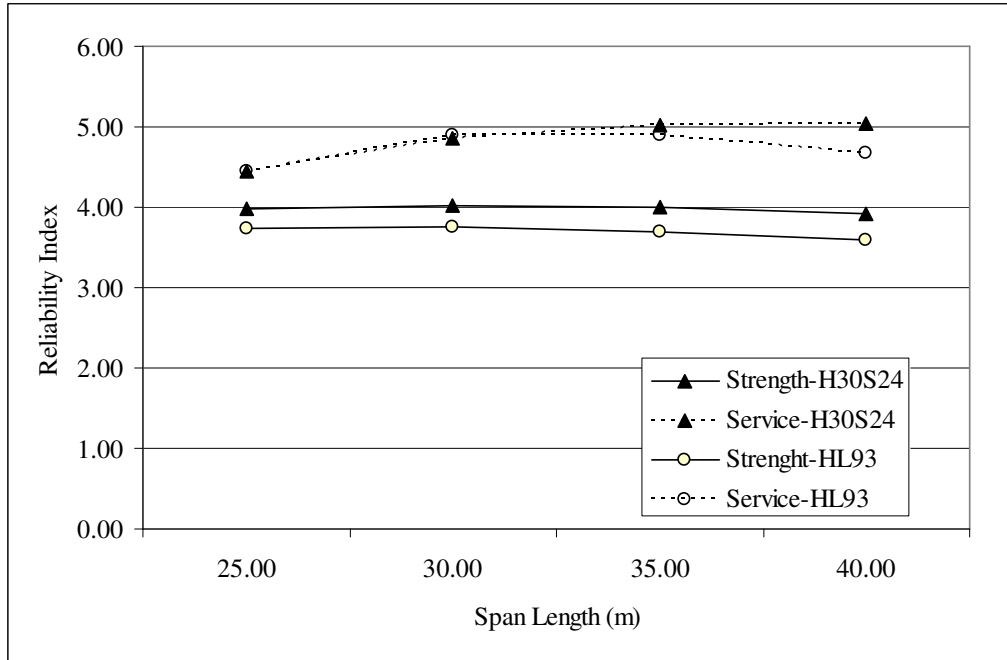
Figure 6-3 Variation of Reliability Indexes with Span Lengths Considering the Local Conditions in USA

118

6.3 COMPARISON WITH OTHER DESING CODES AND COUNTRIES

Similar studies have been carried out for different design codes consistent with the uncertainties existing in the design practice of different countries. The countries considered in this section are Spain [3] and China [17]. Reliability indexes taken from such studies are summarized in Table 6-3, and the results are plotted in Figure 6-5. Note that, in this table and figure, the first entry is the country name that the statistical parameters of load and resistance variables are based on, and the second entry is the design code used.

Reliability index is highly dependent on the statistical parameters of load and resistance variables, assumptions and method of analysis. Before comparison of the reliability indexes of girders designed by other specifications and corresponding to other local conditions, the difference between the studies from which reliability indexes are taken should be determined. For this purpose, the reliability indexes reflecting the designs by AASHTO LRFD and local conditions of USA that are determined from each study are compared and the values are plotted in Figure 6-4. Note that, in this figure, the word in parenthesis refers to the county that the study is carried out. It is expected that the reliability indexes are close to each other because of using same design code and same statistical parameters of load and resistance components. However, the Spanish and Chinese researchers found higher reliability indexes than that estimated in the calibration report. So, the reliability levels calculated in these researches may be higher than actual level due to taking into different statistical parameters and assumptions.

As Figure 6-5 indicates, the reliability levels of girders of Turkey for both loadings are higher than that of girders designed by AASHTO LRFD and HONG KONG CODE [17] using the statistical parameters of load and

resistance variables reflecting the local conditions of US. The most conservative code is the one having the reliability index calculated according to Eurocode by statistical parameters reflecting the local conditions of Spain.

Table 6-3 Reliability Indexes Corresponding to Bridge Designs of Various Countries and Design Codes

| Country / Specification	Reference	Span Length			
		25 m	35 m	35 m	40 m
Spain/AASHTO LRFD	[3]	4.80	4.70	4.70	4.70
Spain/EUROCODE	[3]	7.20	7.70	8.00	7.70
Spain/SPANISH NORMA IAP	[3]	5.80	6.10	6.70	6.50
US/CHINESE CODE	[17]	5.30	5.20	5.25	5.50
US/HONG KONG CODE	[17]	3.40	3.50	3.50	3.40
Turkey/AASHTO LRFD-HL93	This study	3.92	3.92	3.85	3.67
Turkey/AASHTO LRFD-H30S24	This study	4.48	4.49	4.43	4.21
US/AASHTO LRFD	[13]	3.80	3.77	3.73	3.67
US/AASHTO LRFD (SPAIN)	[3]	4.50	4.30	4.30	4.20
US/AASHTO LRFD (CHINESE)	[17]	4.40	4.30	4.00	3.90
US/AASHTO LRFD (TURKEY)	This study	3.73	3.75	3.69	3.60
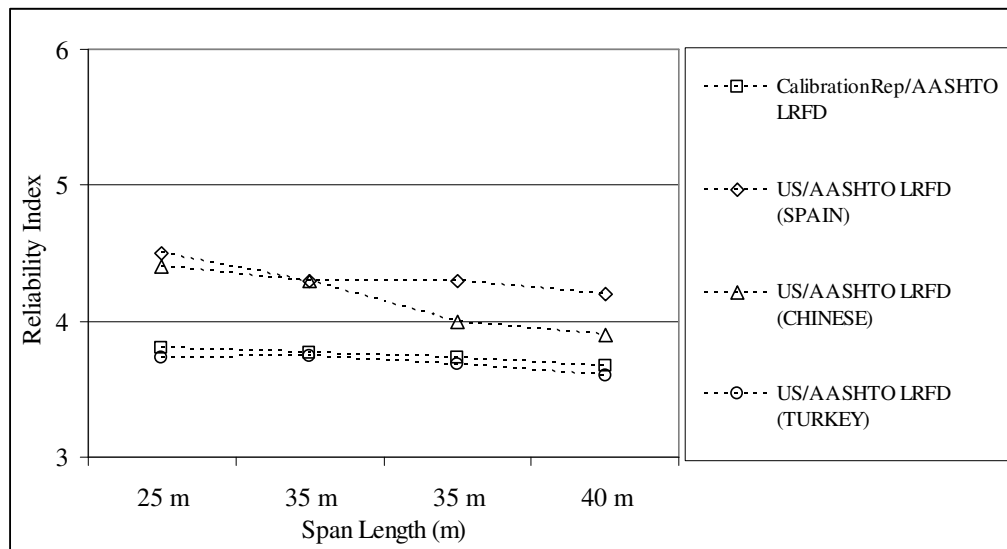
Figure 6-4 Comparison of Reliability Indexes Based on Calibration Report of
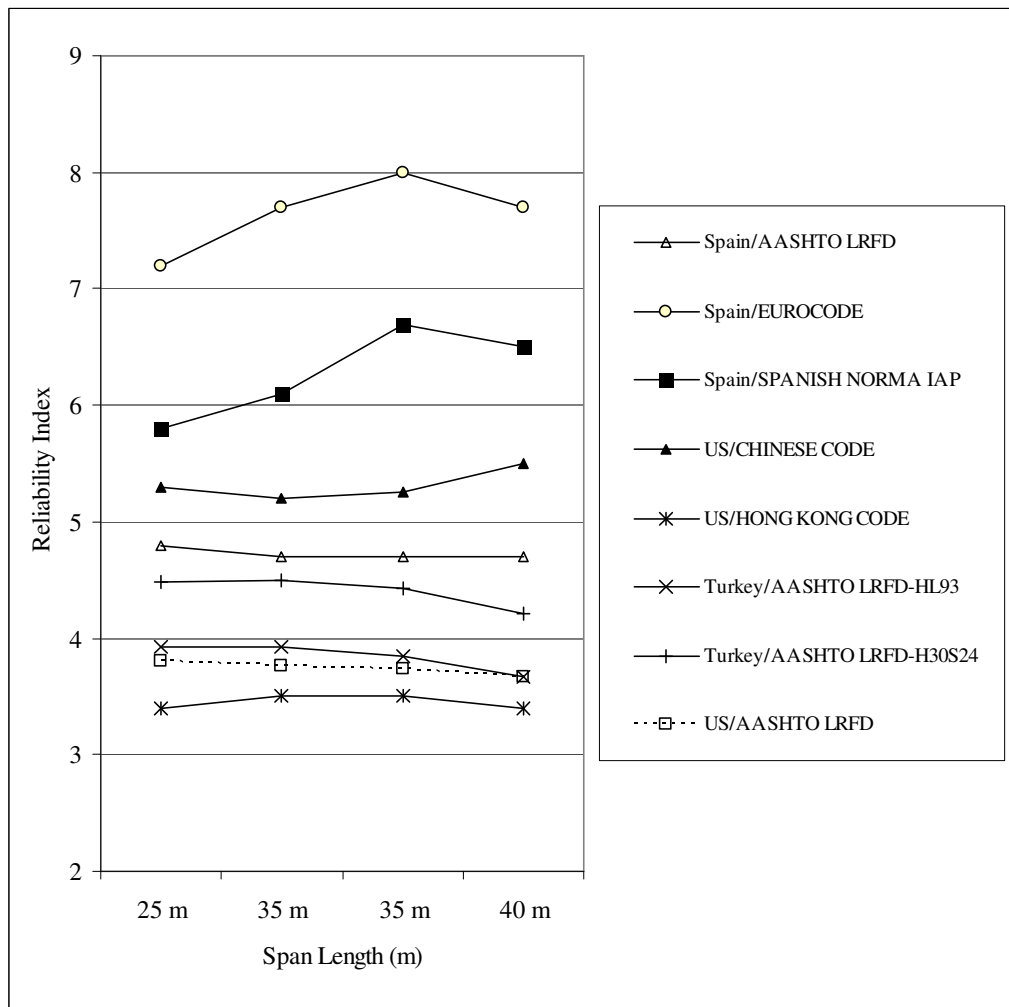AASHTO LRFD as Calculated by Different Studies

Figure 6-5 Comparison of Reliability Indexes of Various Countries and Different Design Codes

6.4 CODE CALIBRATION AND TARGET RELIABILITY LEVEL

Code-writing groups evaluating reliability indexes recommend appropriate load and resistance factors for structural design specifications. The main aim of code calibration is that each type of structure should have uniform or consistent reliability levels over the full range of application. It means that similar reliability indexes should be calculated for bridges of different span lengths, numbers of lanes, spans, and roadway categories by using the load and resistance factors. This is achieved by defining a single target reliability level for all applications.[20]

There are two parameters that determine the optimum value of the target reliability index, β_T. These are consequences of failure and incremental cost of safety. Generally, the higher the expected cost of failure is, the higher the target reliability is. However, financial concerns also affect the optimum target reliability level. For instance, if additional safety can be achieved by little additional cost, target reliability level can be set slightly higher than the acceptable minimum level. On the other hand, if it is rather costly to supply additional safety, then target reliability can be taken lower than the acceptable minimum level. [21] Therefore, higher reliability levels cause higher construction costs; the justification should be based on a cost/benefit analysis whereby target reliability levels are chosen considering balance between cost and risk [20].

In many code calibration efforts, the target reliability level is estimated based on performance of existing bridge designs. It means that if the safety performance of bridges designed according to the current design practice and codes is satisfactory, then the reliability index calculated for these can be selected as the target reliability level for the bridges to be constructed in the future.

123

In AASHTO LRFD Bridge Design Specification, the target reliability level is taken as 3.5 (AASHTO LRFD C3.4.1) based on the study of Nowak et al.[12] in the assessment of load and resistance factors for the strength limit states.

In Eurocode, the target reliability index of ultimate limit state for standard bridges is 4.7 and 3.8 for periods of one year and 50 years, respectively. In order to estimate the target reliability level for different periods, the following expression can be used: [22]

$$\Phi(\beta_n) = \left[\Phi(\beta_1)\right]^n \qquad (6\text{-}6)$$

where, β_n is the reliability index for a reference period of n years, and β_1 is the reliability index for one year. Therefore, target reliability index for 75 year duration is calculated as 3.72 by this expression by taking β_1 as 4.7 and n as 75.

Load and resistance factors and nominal design loads are chosen by trial and error to satisfy the target reliability level as closely as possible for the whole range of applications in order to develop a new set of load and resistance factors. The reliability indexes are calculated for various sets of load and resistance factors to achieve the selected target reliability level.

6.5 LOAD AND RESISTANCE FACTORS

Load and resistance factors are investigated by an iterative method to achieve the target reliability level. Reliability indexes are calculated for each load and resistance factor and each considered span length for corresponding bridge cross sections. Load factors of dead load components are taken as constant throughout the analysis as defined in AASHTO LRFD. Load factors for the

factory made elements and cast-in-place concrete components (DC) are taken as 1.25, and wearing surface and miscellaneous (DW) are set equal to 1.5.

Fifteen different combinations of load and resistance factors are taken into consideration. To create these combinations, 1.50, 1.75, 1.90, 2.0 and 2.2 are taken as the live load factors and 1.0, 0.95 and 0.9 are assigned to the resistance factors. Consistent with the traditional approach of taking resistance factors less than 1.0, we choose 1.0, 0.95 and 0.9 as alternative values for the resistance factor. For each combination, the design is carried out individually for every considered span length and the corresponding bridge cross-section. The reliability indexes of each case are determined by using the design results for five analysis methods, and minimum reliability index is taken. Generally, minimum one corresponded to SORM. The calculated reliability indexes are plotted in Figure 6-6 and Figure 6-7 , and tabulated in Table 6-4 and Table 6-5 for H30S24 and HL93 loading, respectively. By using these graphs, the load and resistance factors can be chosen for different target reliability levels.

Table 6-4 Reliability Index Values Corresponding to Different Load and
Resistance Factor Combinations for H30S24 Loading

Live Load (L) and Resistance Factors (R)	Span Length (m)				Ave. Rel. Index
	25	30	35	40	
L:1.5 ; R:1	3.99	4.00	3.96	3.77	3.93
L:1.5 ; R:0.95	4.29	4.35	4.33	4.21	4.29
L:1.5 ; R:0.9	4.60	4.70	4.70	4.68	4.67
L:1.75 ; R:1	4.48	4.49	4.43	4.22	4.40
L:1.75 ; R:0.95	4.77	4.80	4.79	4.66	4.76
L:1.75 ; R:0.9	5.00	5.13	5.14	5.10	5.09
L:1.9 ; R:1	4.74	4.74	4.68	4.47	4.66
L:1.9 ; R:0.95	5.01	5.05	5.03	4.91	5.00
L:1.9 ; R:0.9	5.28	5.38	5.35	5.32	5.33
L:2 ; R:1	4.91	4.90	4.85	4.64	4.83
L:2 ; R:0.95	5.09	5.21	5.18	5.07	5.14
L:2; R:0.9	5.45	5.47	5.53	5.47	5.48
L:2.2 ; R:1	5.23	5.21	5.13	4.95	5.13
L:2.2 ; R:0.95	5.47	5.53	5.45	5.36	5.45
L:2.2 R:0.9	5.77	5.81	5.84	5.76	5.79

Table 6-5 Reliability Index Values Corresponding to Different Load and Resistance Factor Combinations for HL93 Loading

Live Load (L) and Resistance Factors (R)	Span Length (m)				Ave. Rel. Index
	25	30	35	40	
L:1.5 ; R:1	3.45	3.45	3.39	3.24	3.38
L:1.5 ; R:0.95	3.78	3.81	3.78	3.71	3.77
L:1.5 ; R:0.9	4.11	4.18	4.17	4.18	4.16
L:1.75 ; R:1	3.92	3.92	3.85	3.67	3.84
L:1.75 ; R:0.95	4.24	4.25	4.21	4.13	4.21
L:1.75 ; R:0.9	4.54	4.60	4.58	4.58	4.58
L:1.9 ; R:1	4.19	4.17	4.10	3.92	4.09
L:1.9 ; R:0.95	4.48	4.50	4.46	4.36	4.45
L:1.9 ; R:0.9	4.79	4.84	4.82	4.80	4.81
L:2 ; R:1	4.35	4.33	4.26	4.08	4.26
L:2 ; R:0.95	4.64	4.65	4.60	4.50	4.60
L:2 ; R:0.9	4.96	4.99	4.94	4.94	4.96
L:2.2 ; R:1	4.66	4.63	4.54	4.38	4.55
L:2.2 ; R:0.95	4.93	4.92	4.89	4.79	4.88
L:2.2 ; R:0.9	5.24	5.25	5.24	5.20	5.23
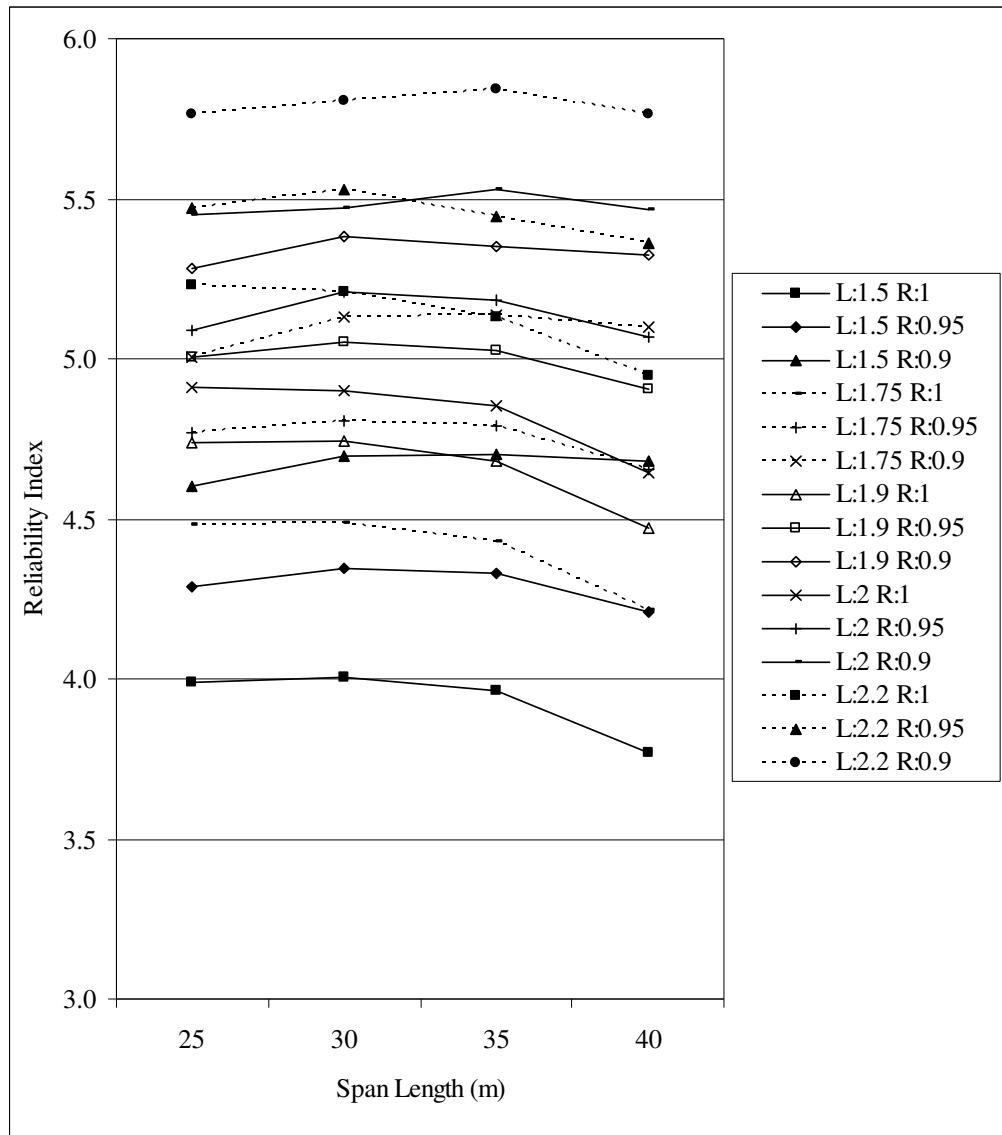
Figure 6-6 Variation of Reliability Index Corresponding to Different Load and
Resistance Factor Combinations with Span Length (H30S24 Loading)
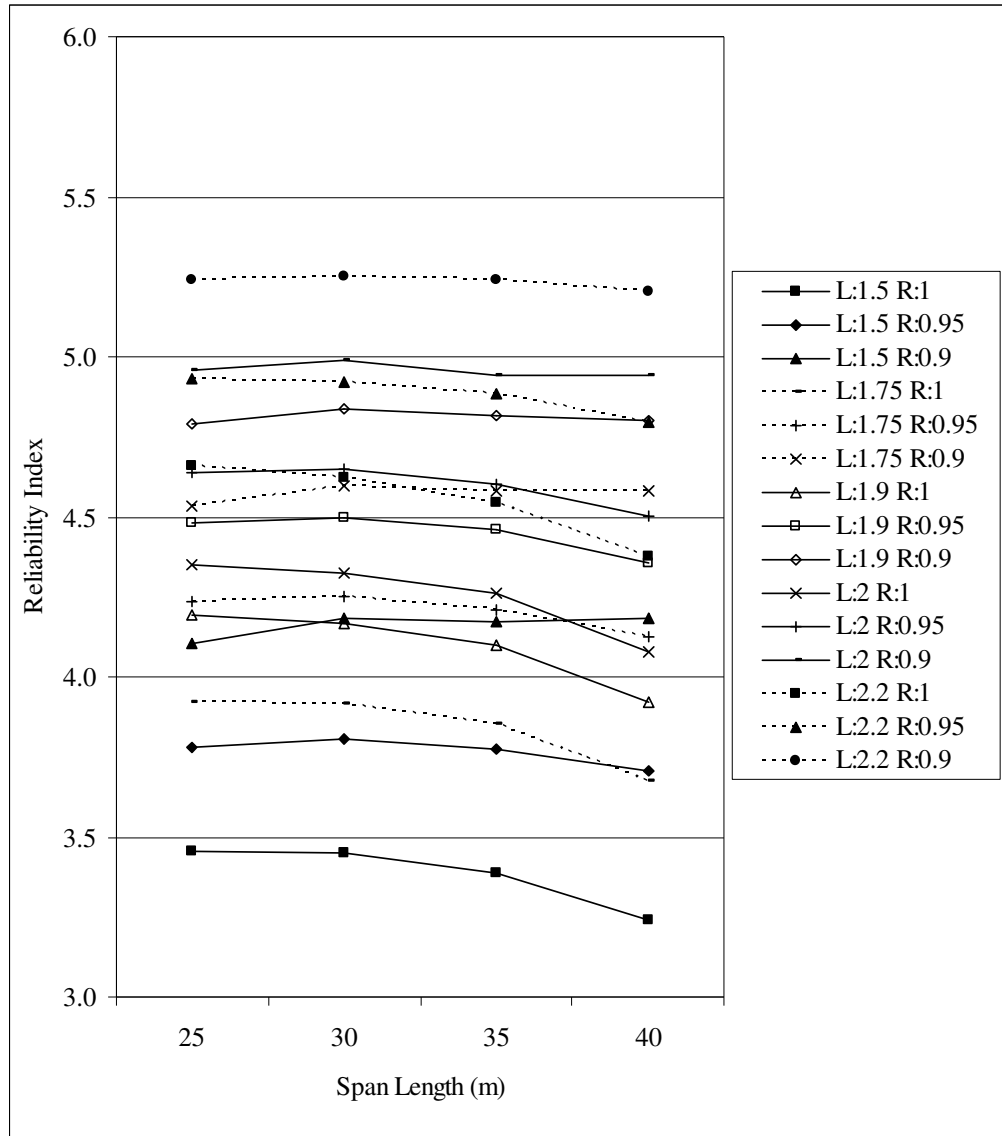
Figure 6-7 Variation of Reliability Index Corresponding to Different Load and
Resistance Factor Combinations with Span Length (HL93 Loading)

If the target reliability index is chosen as 4.5 considering the maximum current
reliability level of Turkish type prestressed precast concrete bridge girders
using H30S24 load effect with L:1.75 and R:1.0, the following load and
resistance factors may be suggested: L:1.9 and R: 1.0 for designs using
H30S24 loading, and L:1.75 and R:0.9 for designs using HL93 loading.

129

CHAPTER 7

CONCLUSION

7.1 CONCLUDING COMMENTS

The new shift in international bridge design applications is to utilize load and resistance factor design (LRFD) method that targets a minimum uniform safety among a variety of bridge designs. LRFD method is calibrated based on study of series of statistical parameters related to both resistance and load components. The same reliability theory used in calibration of AASHTO LRFD is adopted in this research to evaluate the safety levels for Turkish type precast prestressed bridge girders. These girders are designed to satisfy minimum requirements of AASHTO LRFD service and strength limit states for the two truck models, H30S24 and HL93. In this research, different multiple-girder bridge configurations with variation in span length, type of girders and number of prestressing strands are studied to investigate the moment due to loads and flexural resistance at the mid-span. Statistical parameters (probability distribution, bias factor and coefficient of variation) related to live load, compressive strength of concrete and tensile strength of prestressing strands are assessed using the Turkish data. The statistical parameters of other load and resistance components are taken from the calibration report of AASHTO LRFD and international research.

Based on the results of this research, several conclusions can be drawn:

1.   The H30S24 truck model case yields to a conservative design compared to the HL93 truck model case in terms of safety level evaluation of Turkish type prestressed precast concrete girders designed in accordance with AASHTO LRFD. In strength limit state evaluations, the H30S24 loading case yields to 14% more in terms of reliability index compared to the HL93 loading case on average. The similar observation is made for the service limit state with a 10% difference.

2.   Reliability indexes determined for the two truck models at service limit state evaluations are about 20% higher than the ones computed at strength limit state.

3.   For the two truck loadings investigated at strength limit state, reliability indexes yield to higher values than the target reliability level of 3.5 set in the AASHTO LRFD. Therefore, the current load and resistance factors (L:1.75 and R:1.0) need not to be modified for design cases in Turkey. If a higher level of reliability index is targeted in design, design aids provided in this research can be used. For instance; if the target reliability index is set to be higher than 4.5 considering maximum current reliability level of Turkish type precast concrete bridge girders, the load and resistance factors may be suggested as; L:1.9 and R: 1.0 for designs with H30S24 loading, and L:1.75 and R:0.9 for designs with HL93 loading.

4.   Three extrapolation cases described in this research being *overall, upper tail* and *extreme* are used to assess statistical parameters of the live load effect for an extended period of time using extreme value theory. Out of all these cases, *extreme* case is selected to be used in the assessment of time-dependent live load effects since *extreme* case is more representative of extreme truck

load effects in the survey. This case also results in lowest coefficient of variation and highest bias factor compared to the others.

5.   Statistical parameters related to live load, compressive strength of concrete and tensile strength of prestressing strands are listed below for the Turkish data reflecting the local conditions.

Table 7-1 Summary of Statistical Parameters Assessed Using Turkish Data

Parameter	Description	Probability Distribution	Bias Factor	Coef. of Variation
LL	Live load - H30S24	Gumbel	1.00 (1.05-1.02) for one lane	0.165
			0.78 (0.79-0.76) for two lanes	
	Live load-HL93	Gumbel	1.12 (1.23-1.03) for one lane	0.165
			0.86 (0.92-0.75) for two lanes	
Fpu	Ultimate tensile strength of prestressing steel	Normal	1.00	0.030
fc,C30	Compression strength of deck concrete	Normal	0.87	0.135
fc,C40	Compression strength of precast beam	Lognormal	0.96	0.127

7.2 RECOMMENDATIONS FOR FUTURE STUDIES

The work presented in this study can be replicated to evaluate the safety levels for other types of bridges such as steel, post tensioned and reinforced concrete. The future study can also be carried out to evaluate not only mid-span moments but also the shear force and negative moments.

In the current study, only bridge girder members are considered. The reliability level of other components of bridges like piers, supports, abutments and foundation can be assessed considering the conditions peculiar to Turkey.

In this study, truck catalogs are used to determine the axle spacing of the surveyed trucks. The distance between each truck axle can be measured to be reported in the surveys to determine the truck axle load patterns. The General Directorate of Highways can also classify the trucks during the surveys as light, medium and heavy weight based on their tonnages.

Other limit states such as extreme event limit state and fatigue limit state described in the AASHTO LRFD can also be investigated in terms of safety level evaluations.

REFERENCES

[1]   AASHTO LRFD Bridge Design Specifications. Washington, DC: Association of State Highway and Transportation Officials; 2007 4th Edition.

[2]   PCI (2003) Bridge Design Manual, Design Example, Chapter 9, Section 9-4, Bulb-Tee Single Span, Composite Deck, LRFD Specifications. MANUAL Chapter 7. http://www.pci.org/publications/bridge/

[3]   Nowak AS, Park CH, Casas JR. Reliability Analysis of Prestressed Concrete Bridge Girders; Comparison of Eurocode, Spanish Norma IAP and AASHTO LRFD. Struct Safety 2001;23:331-44.

[4]   Barker R. M., Puckett J.A. Design of Highway Bridges An LRFD Approach. Second Edition. John Wiley and Sons Inc. 2007

[5]   Fırat, F.K., Development of Load and Resistance Factors for Reinforced Concrete Structures in Turkey, Phd.Thesis, Department of Civil Engineering, METU, Ankara, 2007.

[6]   Mirza, S.A.,Hatzinikolas, M. and MacGregor J.G., Statistical Description of the Strenght of Concrete, Journal of the Structural Division. ASCE, Vol. 105, No. ST6, pp.1021 – 1037, 1979.

[7]   Mirza, S. A. and MacGregor, J.G. Variations in Dimensions of Reinforced Concrete Members, Journal of Structural Divisions, ASCE Vol. 105, No. ST4, pp. 921-937, 1979

[8]   Ang, A. H.S and Tang, W.H., Probability Concepts in Engineering Planning and Desing, Volume II, John Wiley and Sons Inc, New York, 1984.

[9]   Kömürcü, A.M., A Probabilistic Assessment of Load and Resistance Factors for Reinforce Concrete Structures Considering the Design Practice in Turkey, M.Sc.Thesis, Department of Civil Engineering, METU, Ankara, 1995.

[10] Al-Harty AS, Frangopol DM. Reliability Assessment of Prestressed Concrete Beam. J Struct Eng 1994; 120(1):180-99.

[11] Tabsh SW, Nowak AS, Reliability of Highway Girder Bridges. J Struct Eng 1991; 117(8):2372-88.

[12] Nowak, A.S., Calibration of LRFD Bridge Design Code, NCHRP Report 368, TRB, 1999.

[13] Nowak, A.S., Updating the Calibration Report For AASHTO LRFD Code, Final Report, NCHRP 20-7/186, TRB, 2007.

[14] Technical Provision for Highway Bridges, T.C. Republic of Turkey, Ministry of Transport, General Directorate of Highways Ankara, 1982.

[15] Castillo, E. Extreme Value Theory in Engineering, Academic Press Inc., 1988.

[16] Hwang, E.S., and Nowak, A.S., Simulation of Dynamic Load for Bridges. ASCE Journal of Structural Engineering, Vol.117, No.5, (1991), pp. 1413-1434.

[17] J.S. Du , F.T.K. Au. Deterministic and Reliability Analysis of Prestressed Concrete Bridge Girders: Comparison of the Chinese, Hong Kong and AASHTO LRFD Codes. Struct Safety Vol. 23, pp 331–344, 2001.

[18] MacGregor, J.G., Mirza, S. A., Ellingwood B. Statistical Analysis of Resistance of Reinforced and Prestressed Concrete Members. ACI Journal, No. 80-16, pp. 167-176, 1983.

[19] Mirza SA, Kikuchi DK, MacGregor JG. Flexural Strength Reduction Factor for Bonded Prestressed Concrete Beams. J ACI 1980;77(4):237–46.

[20] Ghosn M. and Moses F., Design of Highway Bridges for Extreme Events, NCHRP Report 489, TRB, 2003.

[21] Szerszen M. M. and Nowak A. S., Calibration of Design Code For Buildings (ACI 318): Part2-Reliability Analysis and Resistance Factors. ACI Structural Journal, V100, No.3, May-June 2003.

[22] Eurocode EN 1990, Basis of Structural Design, April 2002.

[23] AASHTO LFD Bridge Design Specifications. Washington, DC: Association of State highway and Transportation Officials; 1971.

[24] Axle Weight Measurements Data Recorded by the General Directorate of Highways between 1997 and 2006 Years.

[25] Yan-Gang Zhao, Tetsura Ono, A General procedure for first/Second Order Reliability Method (FORM/SORM), Structural Safety 21 (1999) 95-112.

[26] Hasofer, A. and Lind, N.C., Exact and Invariant Second-Moment Code Format, Journal of Engineering Mechanics Division, ASCE, Vol. 100, No. EM. 1, pp. 111-121, 1974.

[27] Breitung, K., Asymptotic Approximation for Multi-normal Integrals, Journal of Engineering Mechanics Division, ASCE, Vol. 66, No. EM. 3, pp. 110, 1984.